INFRARED FINE STRUCTURE LINES: RISING

~~C+~~: The ~~New~~ Workhorse for Submm studies of Galaxy Evolution

Presented by Drew Brisbin
ALMA postdoctoral fellow

August 7, 2014

Image: Katsushika City Museum


galaxies
CII
high
formation
ALMA
emission
micron
FIR
luminosity
gas
dust
star
line
lines
redshift
redshifts
density
heating
ISM
SFR
normal
physical
conditions
Herschel
kinematics
infrared
observations
star-formation
star-forming
temperature
mode
early
mergers
sample
survey
systems
rate
range
studies
important
results
data
low
also
potential
resolution
observed
work
surface
using
constrain
detected
ratios
IR
CI
high-z
fine-structure
sources
source
color
well
luminous
regions
highly
wide
show
forming
archival
dominant
Galaxies
result
Universe
neutral
instruments

[CII]

- Very bright, up to ~1% FIR
- *Associated* with SF

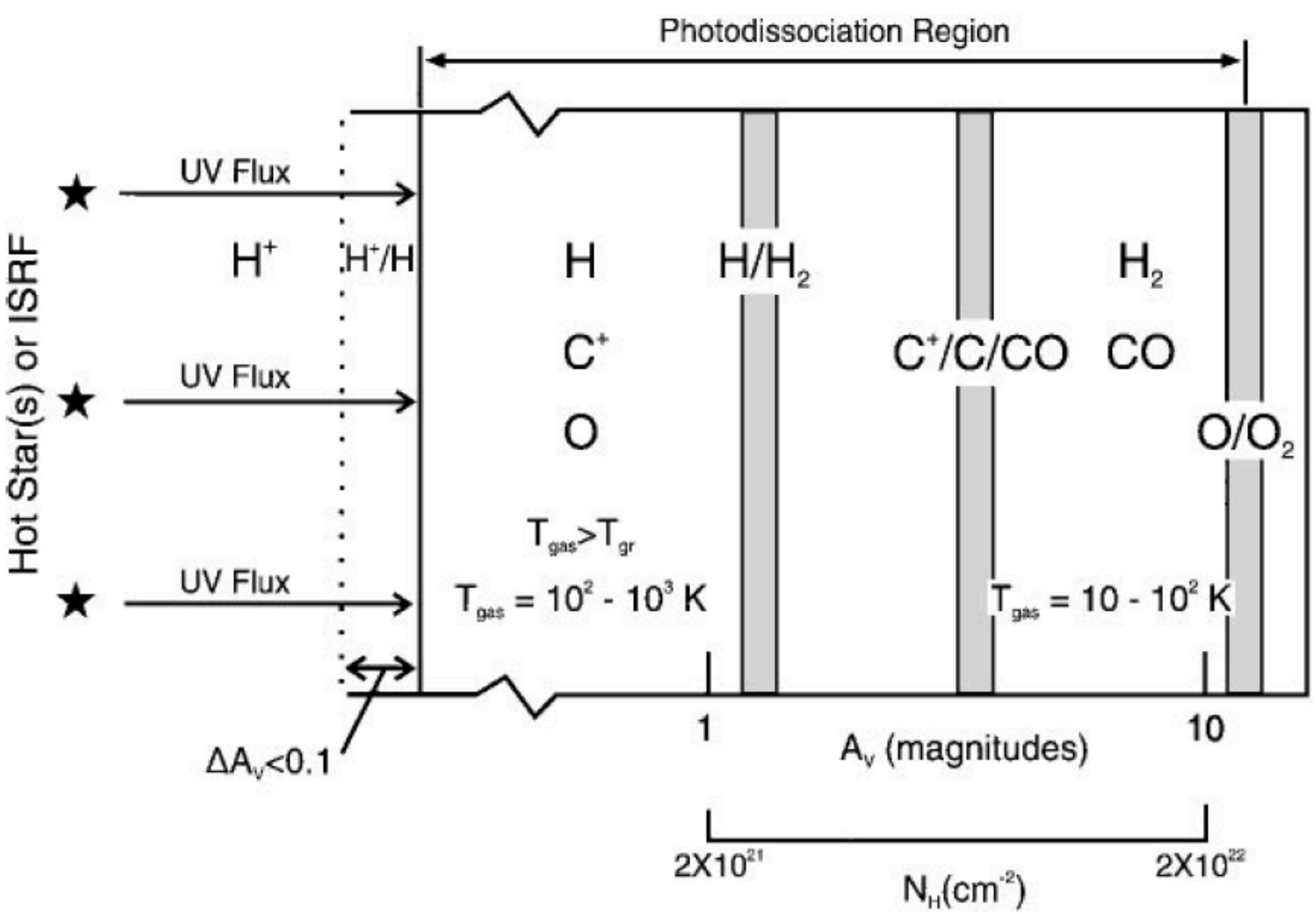

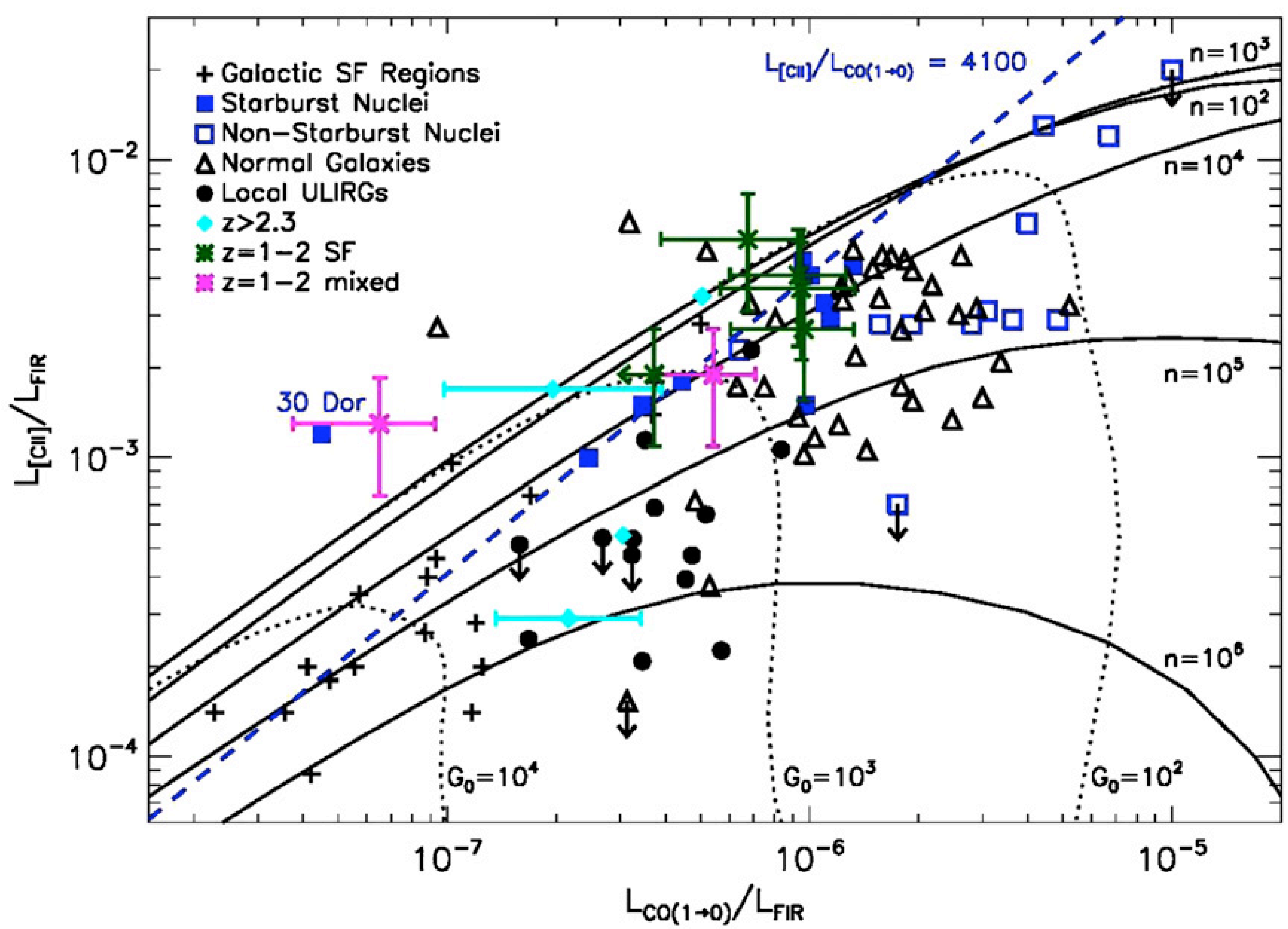

[CII]

- Optically thin
- Very little extinction

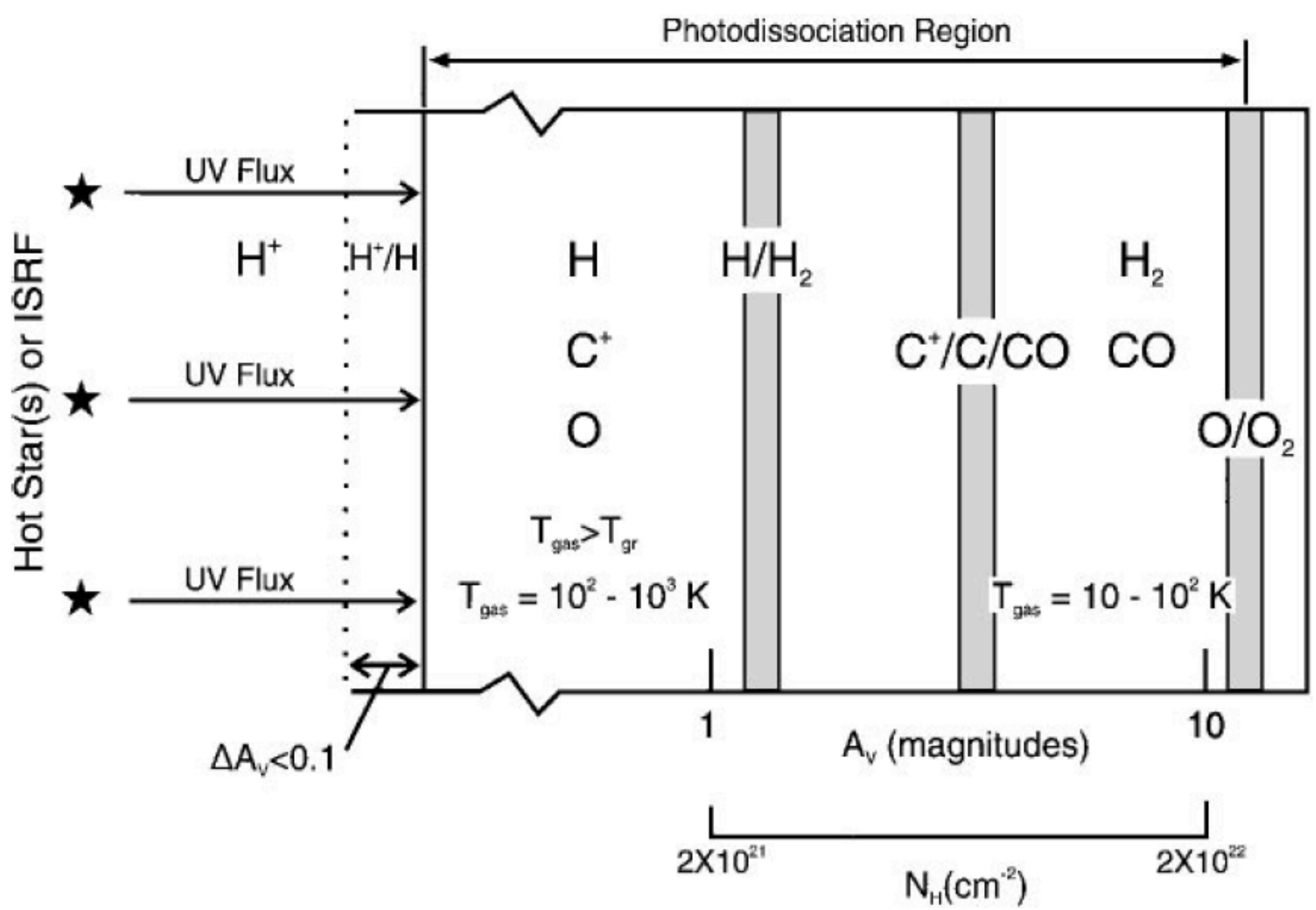

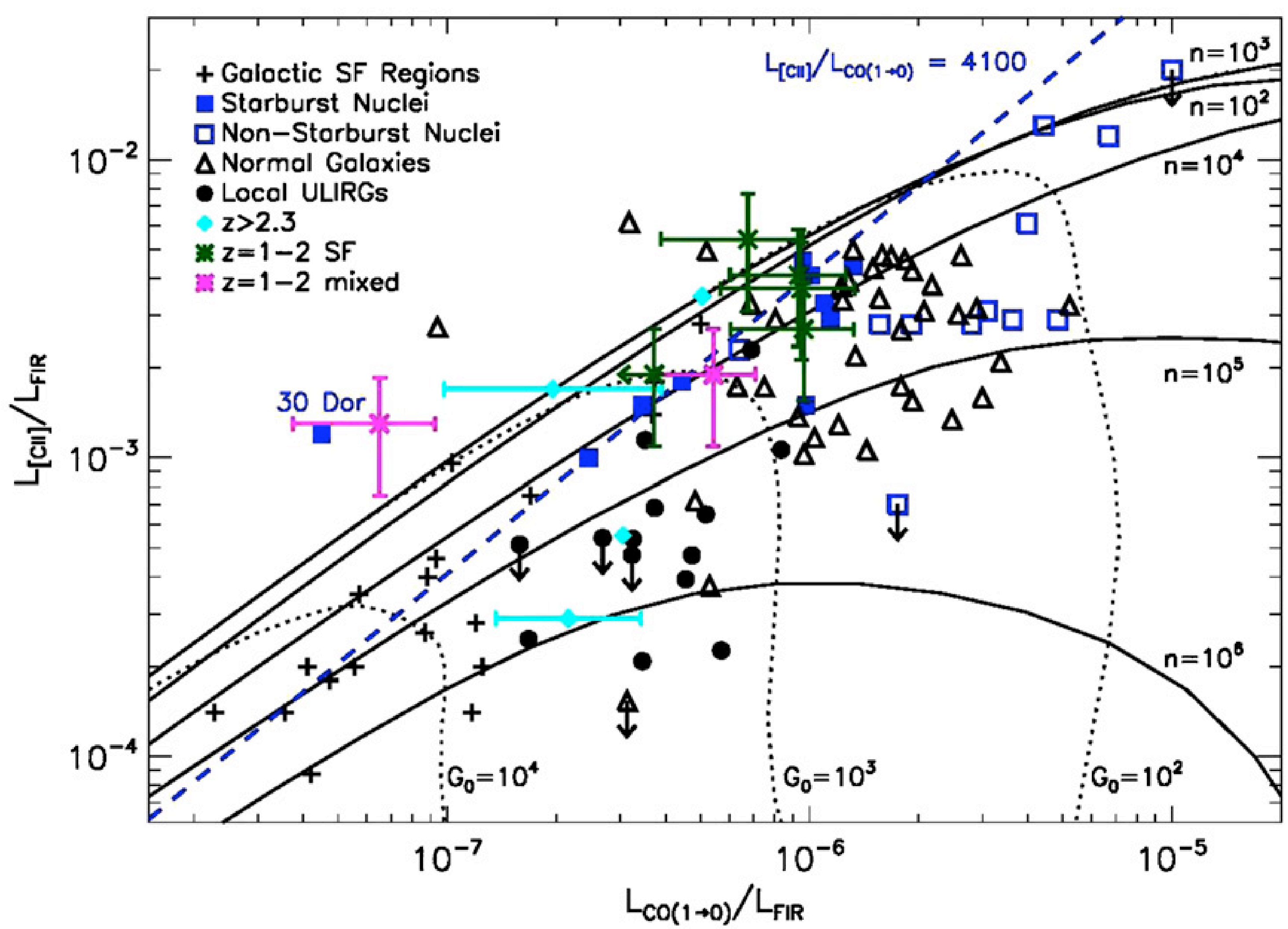

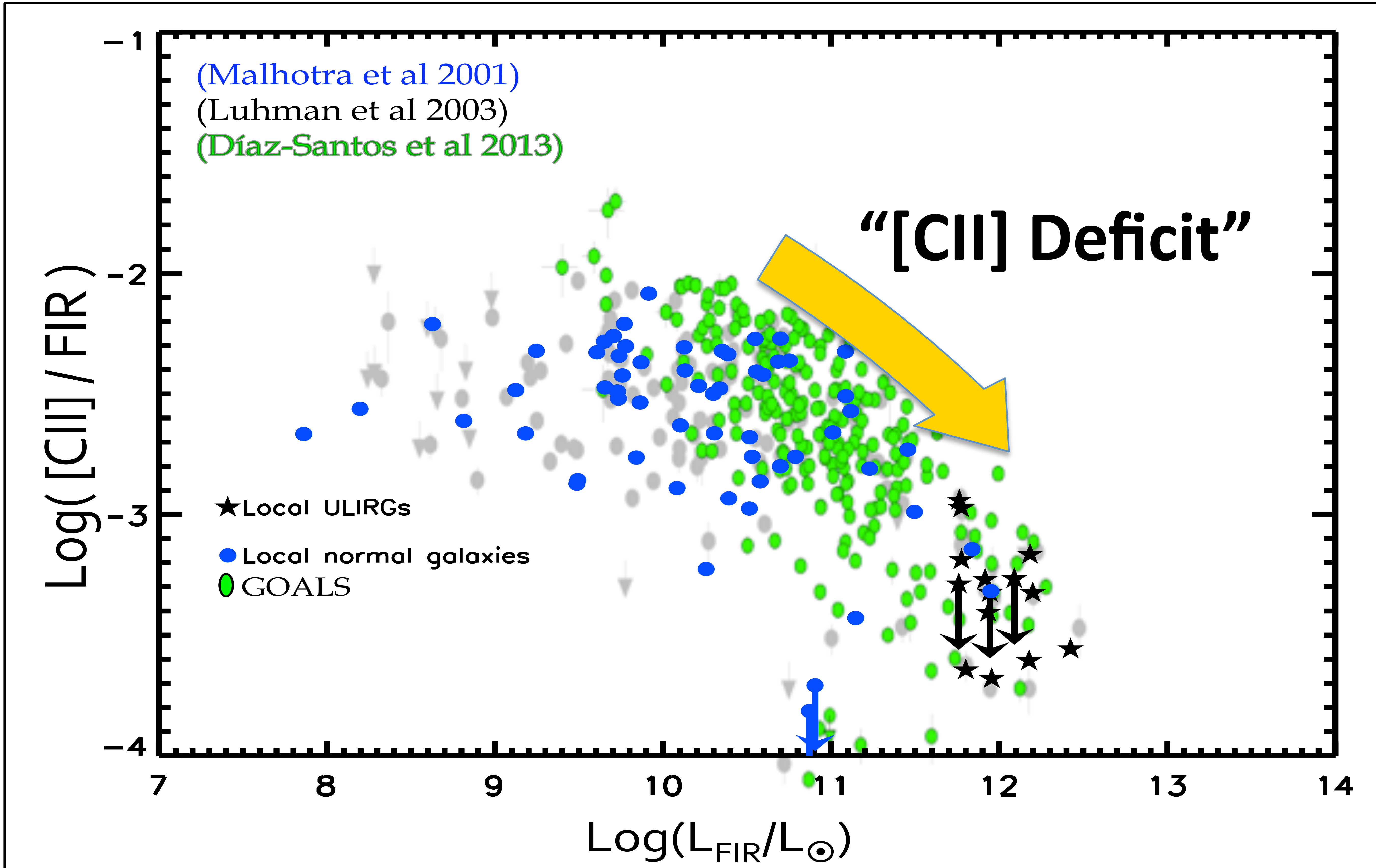

(Malhotra et al 2001)
(Luhman et al 2003)
(Díaz-Santos et al 2013)
"[CII] Deficit"
Local ULIRGs
Local normal galaxies
GOALS
Log([CII] / FIR)
Log(L_FIR/L_⊙)
−1
−2
−3
−4
7
8
9
10
11
12
13
14

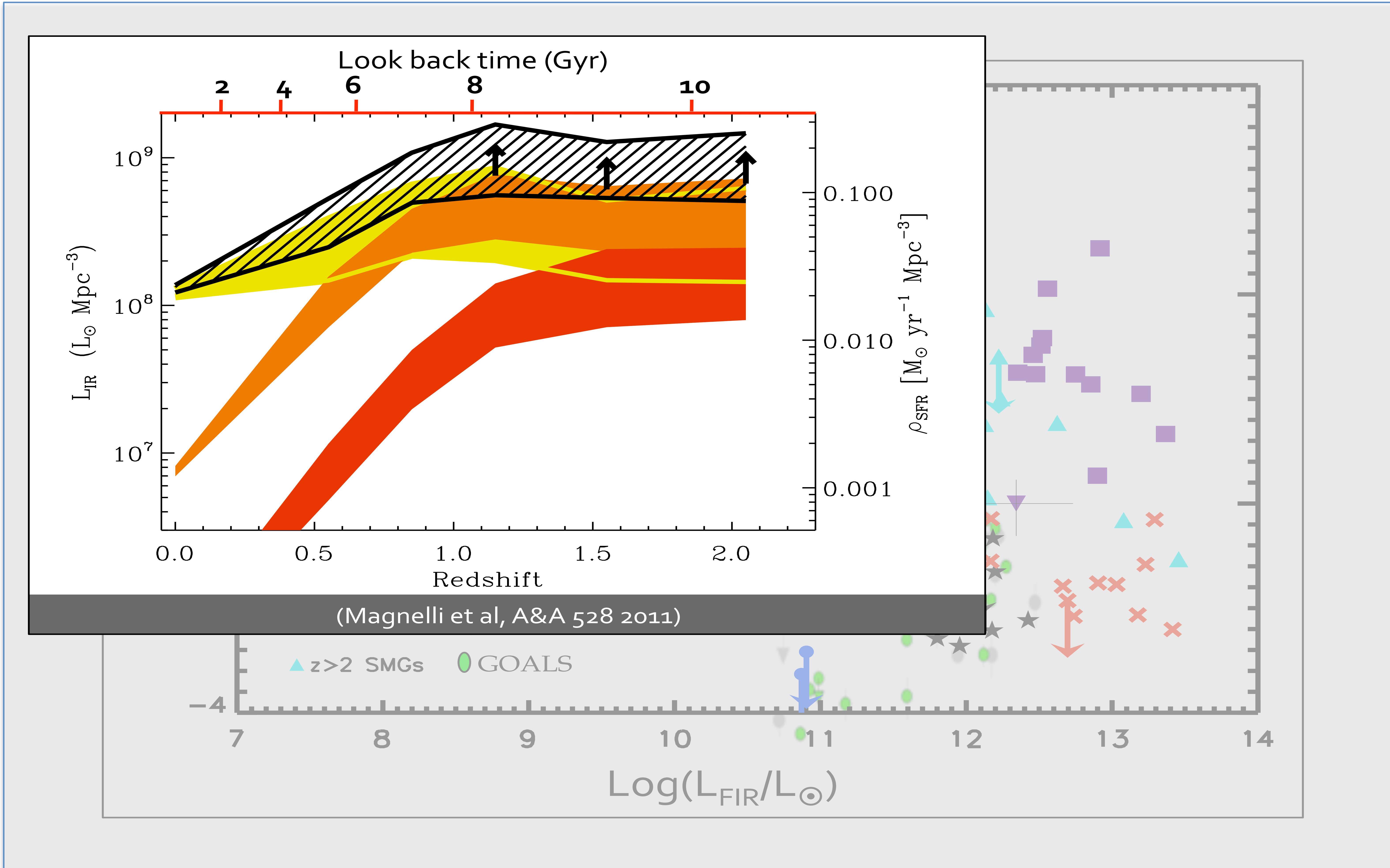
Look back time (Gyr)
2
4
6
8
10
10^9
10^8
10^7
L_{IR} ($L_\odot$ Mpc^{-3})
0.100
0.010
0.001
ρ_{SFR} [$M_\odot$ yr^{-1} Mpc^{-3}]
0.0
0.5
1.0
1.5
2.0
Redshift
(Magnelli et al, A&A 528 2011)
z>2 SMGs
GOALS
−4
7
8
9
10
11
12
13
14
Log($L_{FIR}/L_\odot$)

Line diagnostics

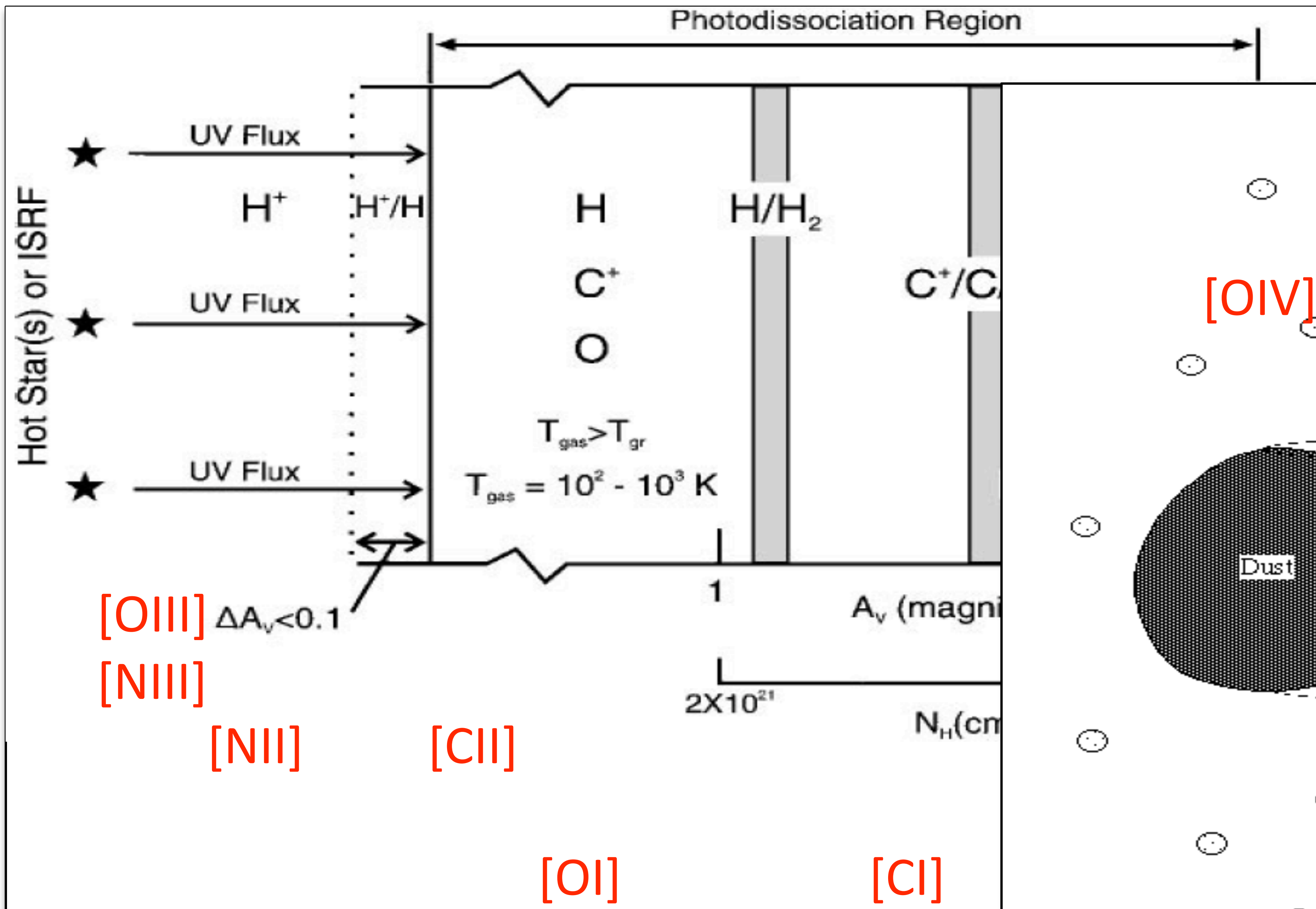

Hollenbach and Tielens 1997, ARAA 35, 179

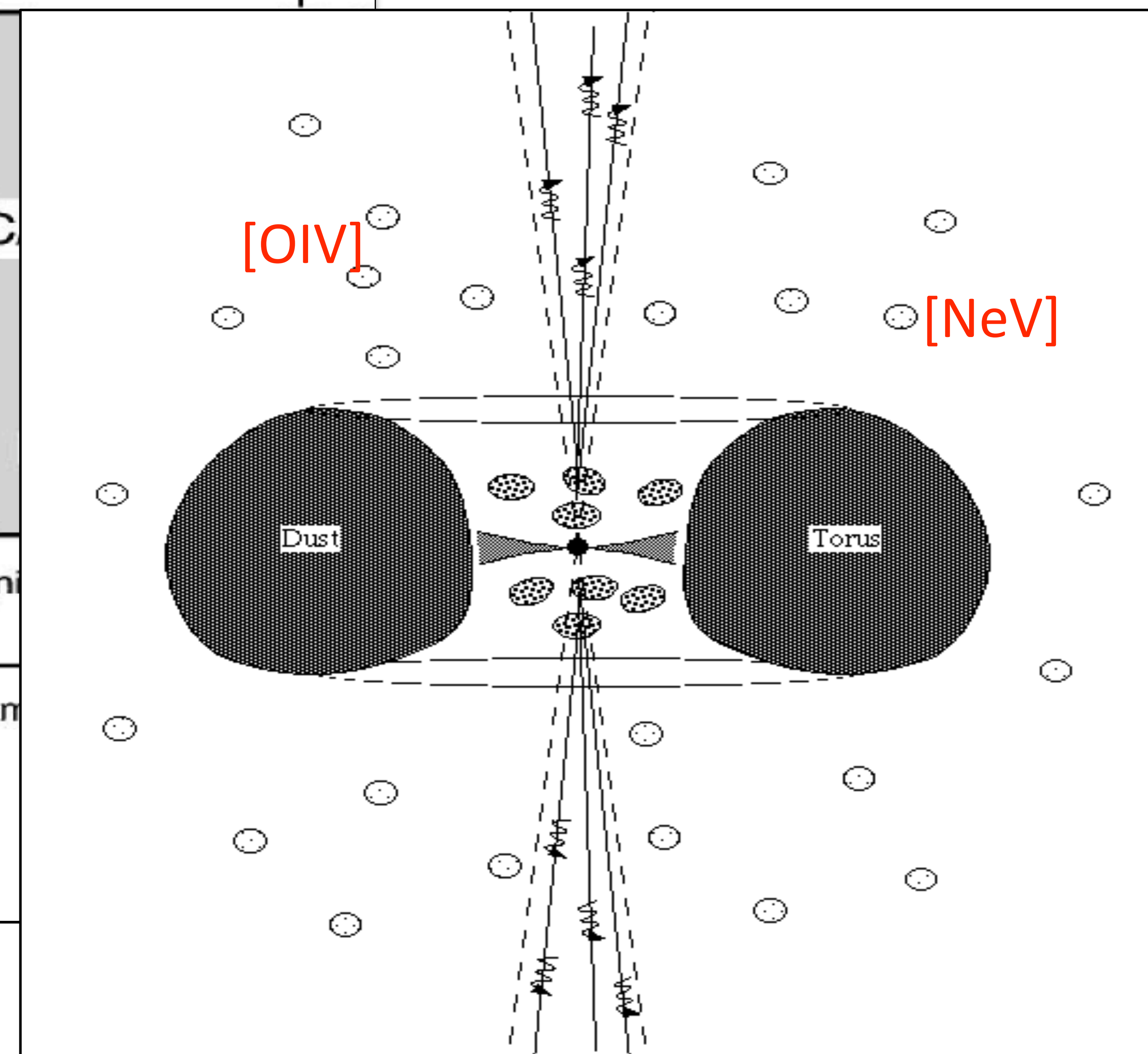

Line diagnostics

- Radiation field:

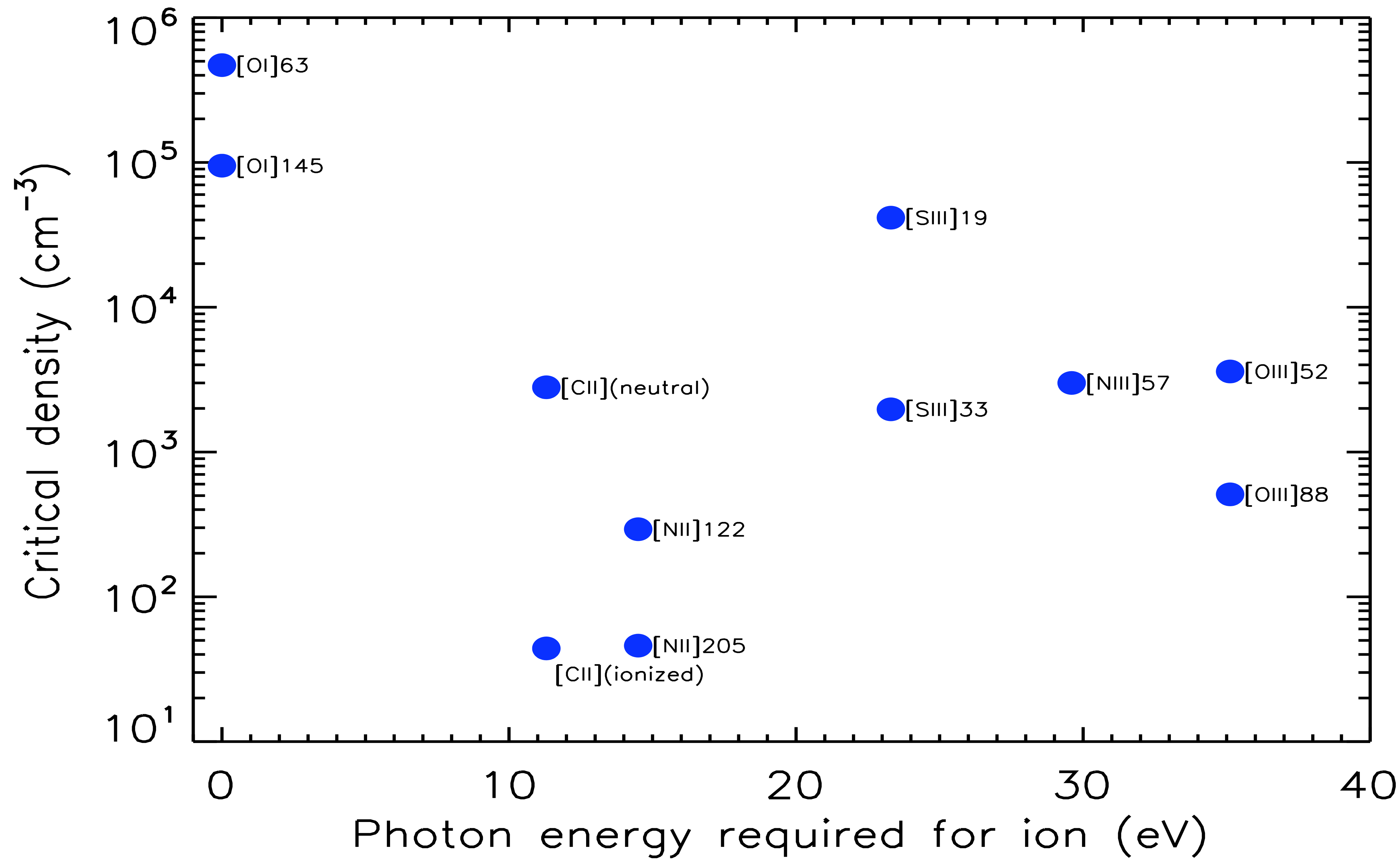

Line diagnostics

- Radiation field
  - [OIII]/[SIII]

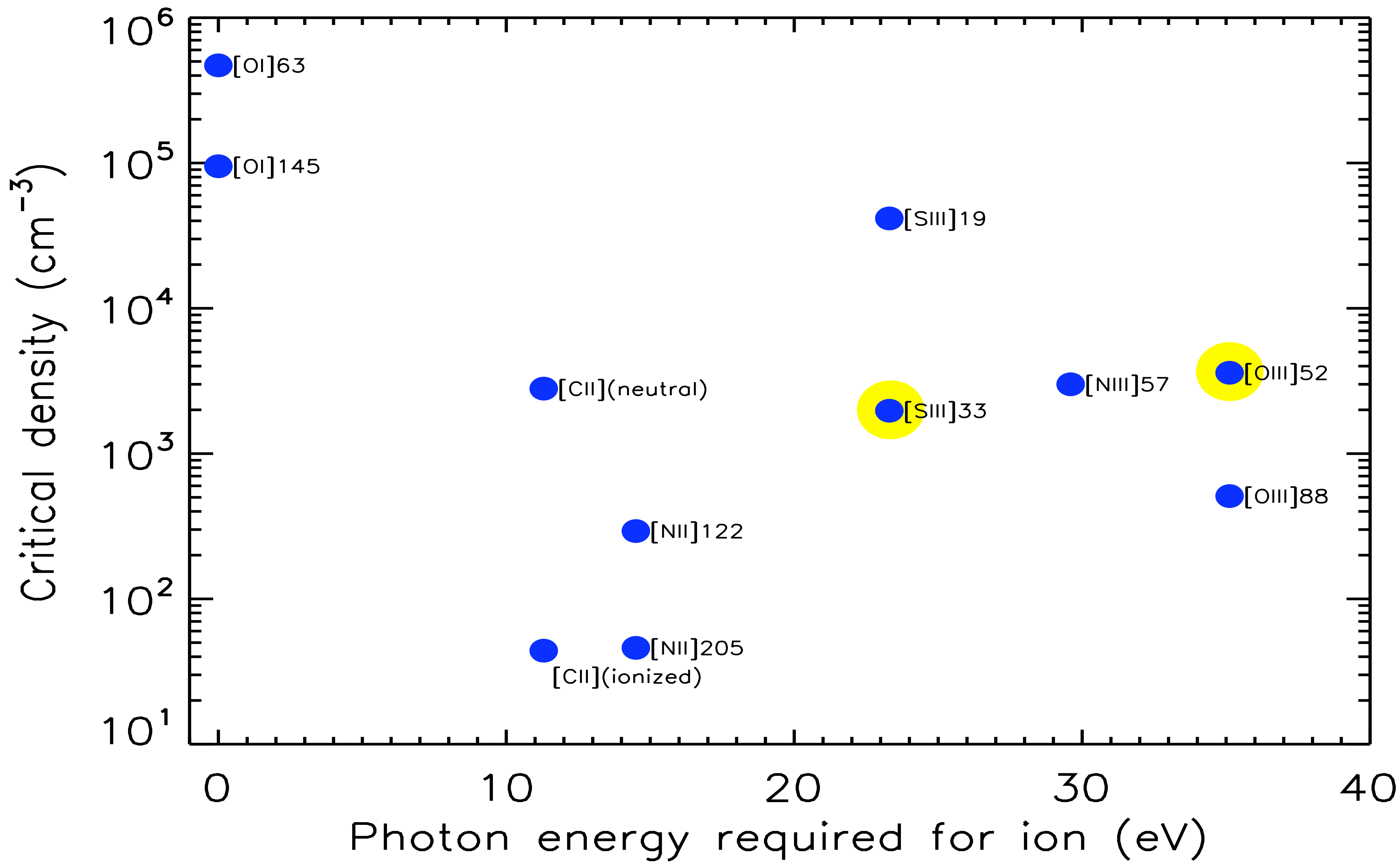

Line diagnostics

- Radiation field :
  - [OIII]/[SIII]
  - [NII]/[OIII]
    (Ferkinhoff 2011)

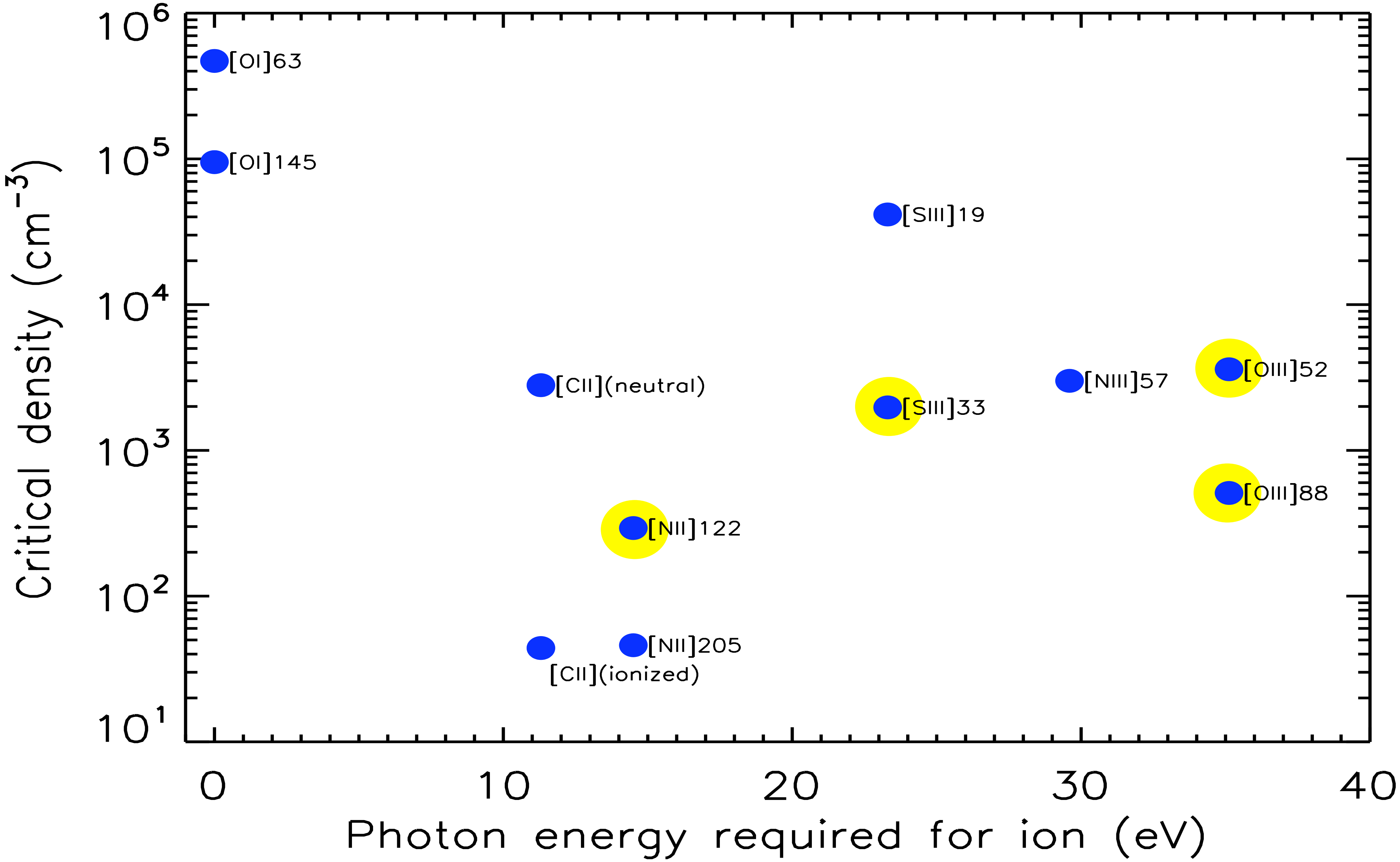

Line diagnostics

- Radiation field:
  - [OIII]/[SIII]
  - [NII]/[NIII]
- Densities
  - [NII], [OIII], [SIII] pairs

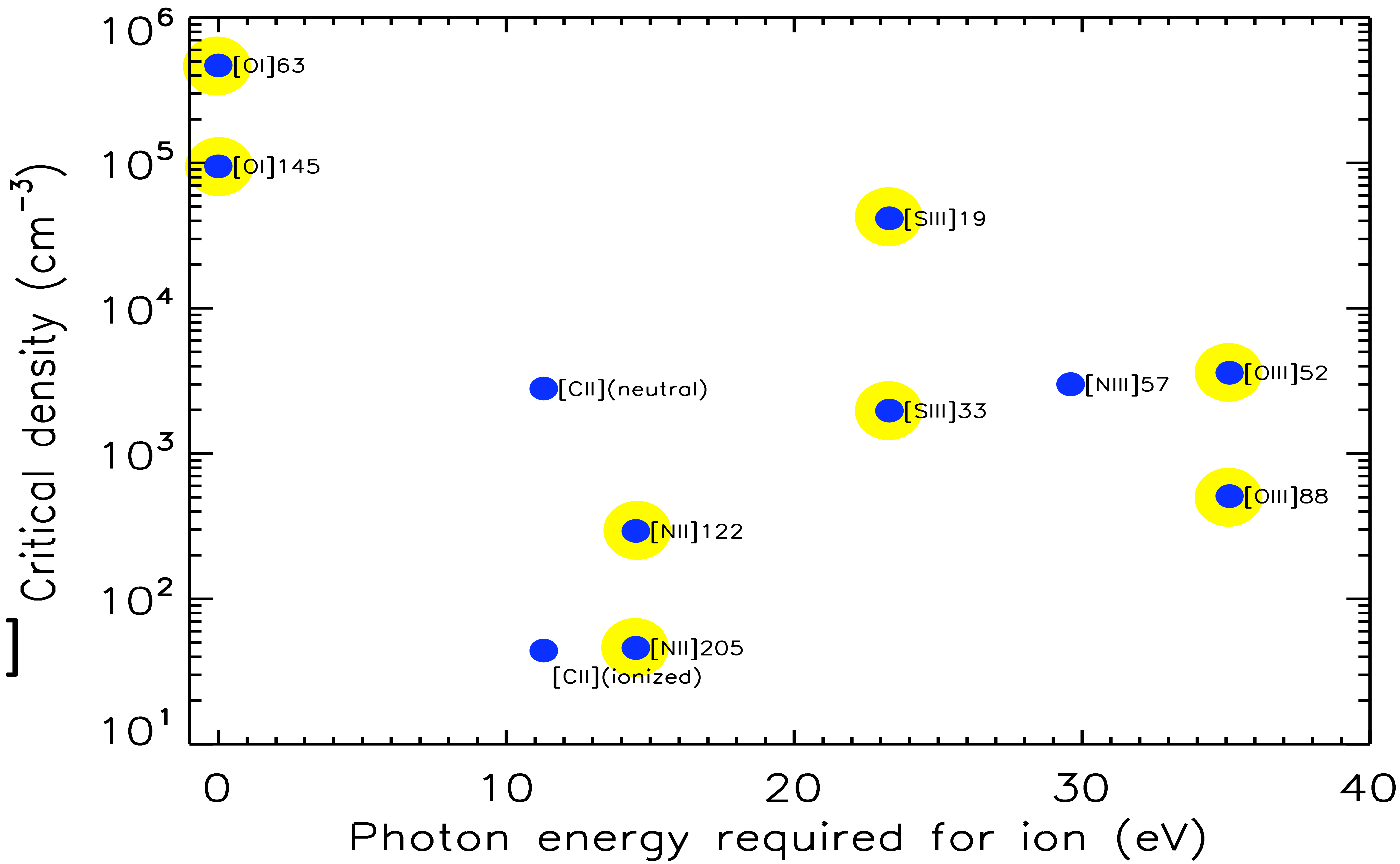

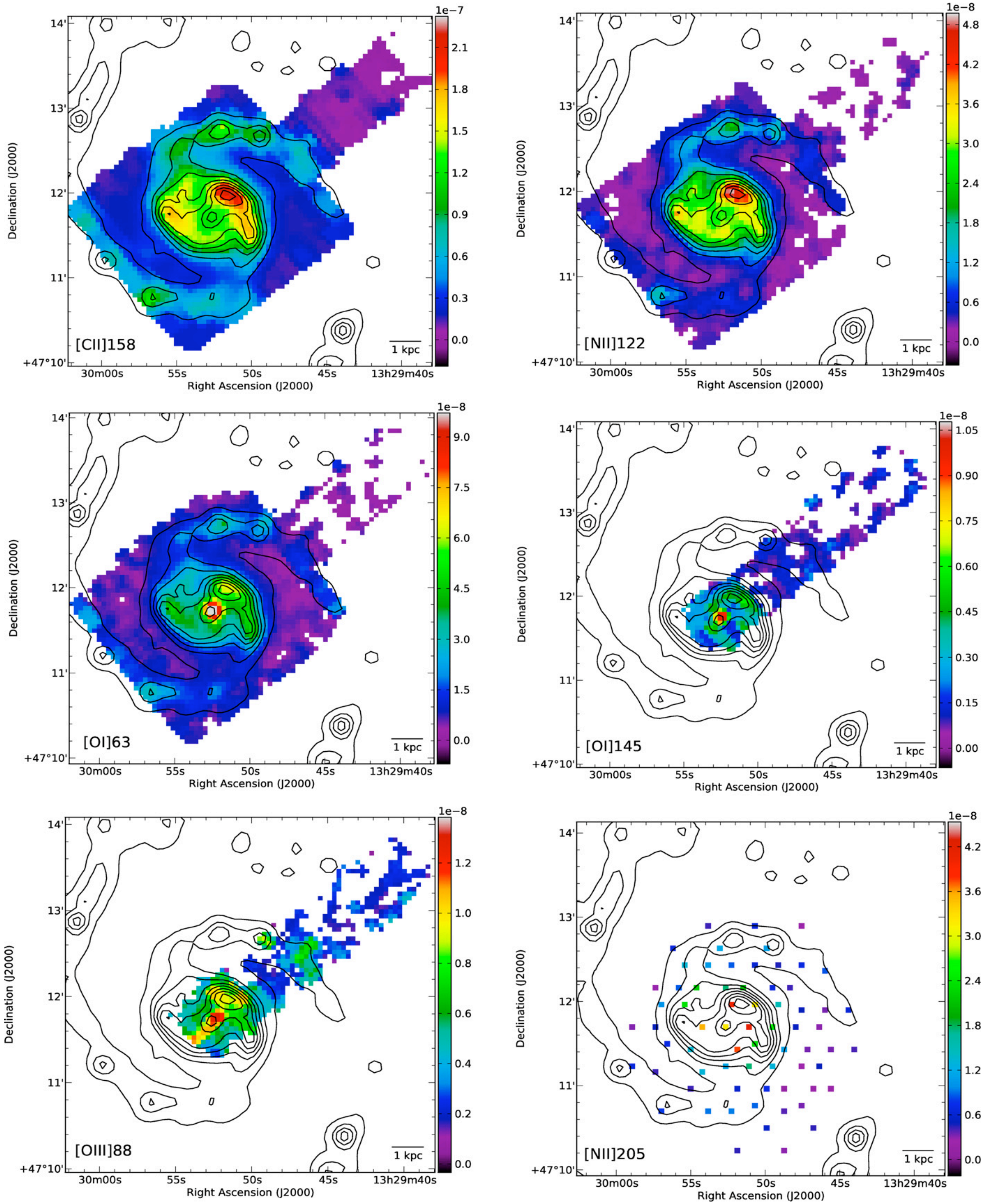

Resolved line emission

M51:

[CII] [NII] 122

[OI] 63 [OI] 145

[OIII] 88 [NII] 205

(Parkin et al. ApJ 776, 2013)

Resolved line emission

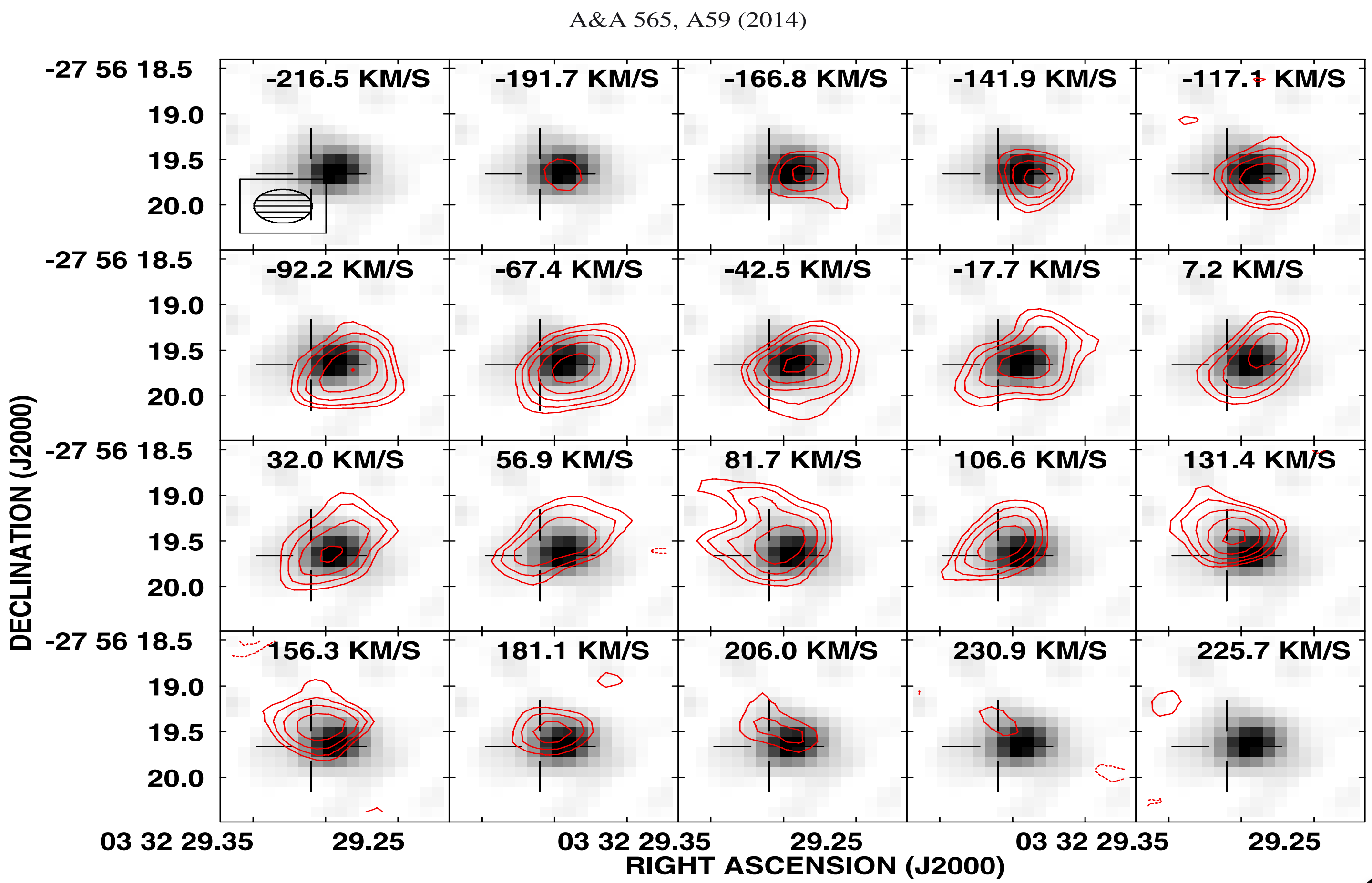

(De Breuck et al. A&A 565 2014)
Resolved [CII]
ALESS 73.1, z=4.76

(Neri et al. A&A 562 2014)
Resolved [CII]
HDF 850.1, z=5.185

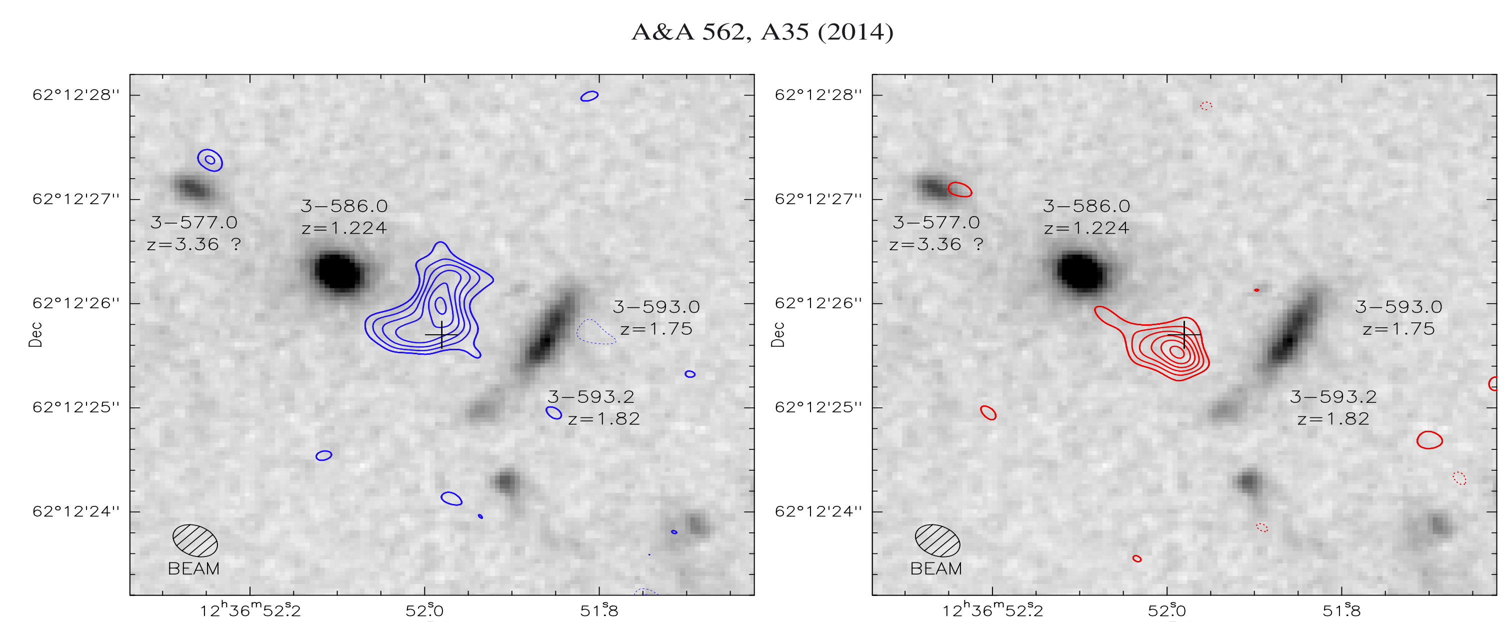

Fig. 1. Maps of blueshifted (*left*) and redshifted (*right*) C^+ emission in HDF 850.1, with the 0.98 mm continuum subtracted. These two channels are each 470 km s^{-1} wide, centered on −205 km s^{-1} and +265 km s^{-1}, with integration ranges of −440 km s^{-1} to +30 km s^{-1} (*left*) and +30 km s^{-1} to +500 km s^{-1} (*right*). These velocities are relative to 307.267 GHz (C^+ 158 μm at z = 5.1853). Contours are -3σ (dashed), $+3\sigma$, and then go up in steps of 1σ = 0.20 Jy $beam^{-1}$ km s^{-1}. The blueshifted, C^+ north peak (*left*) is 1.6 Jy $beam^{-1}$ km s^{-1}, and its spatially integrated flux is 6.9 Jy km s^{-1}. The redshifted, C^+ south peak (*right*) is 1.4 Jy $beam^{-1}$ km s^{-1}, and its spatially integrated flux is 3.0 Jy km s^{-1}. The beam (lower left, in each panel), is $0.38'' \times 0.29''$ at PA = 59° (FWHM), with T_b'/S = 118 K Jy^{-1}. The cross marks the phase reference position, at 12:36:51.980, +62:12:25.70 (J2000). The C^+-line contours are superimposed on a greyscale version (Downes et al. 1999) of the *BVI* image from the *Hubble* Deep Field.

Line diagnostics

- Difficult to observe
- Low atmospheric transmission
- High atmospheric emission

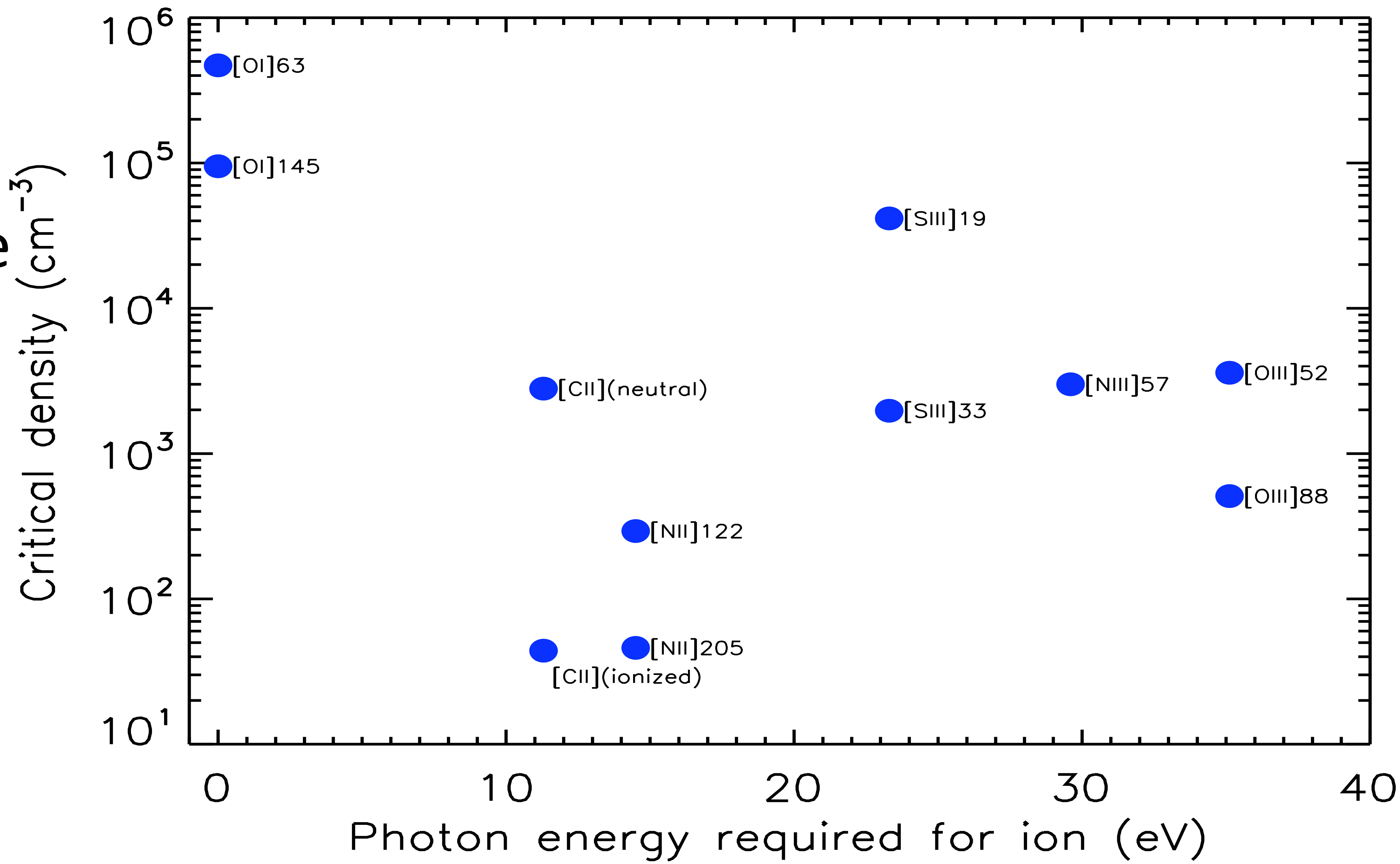

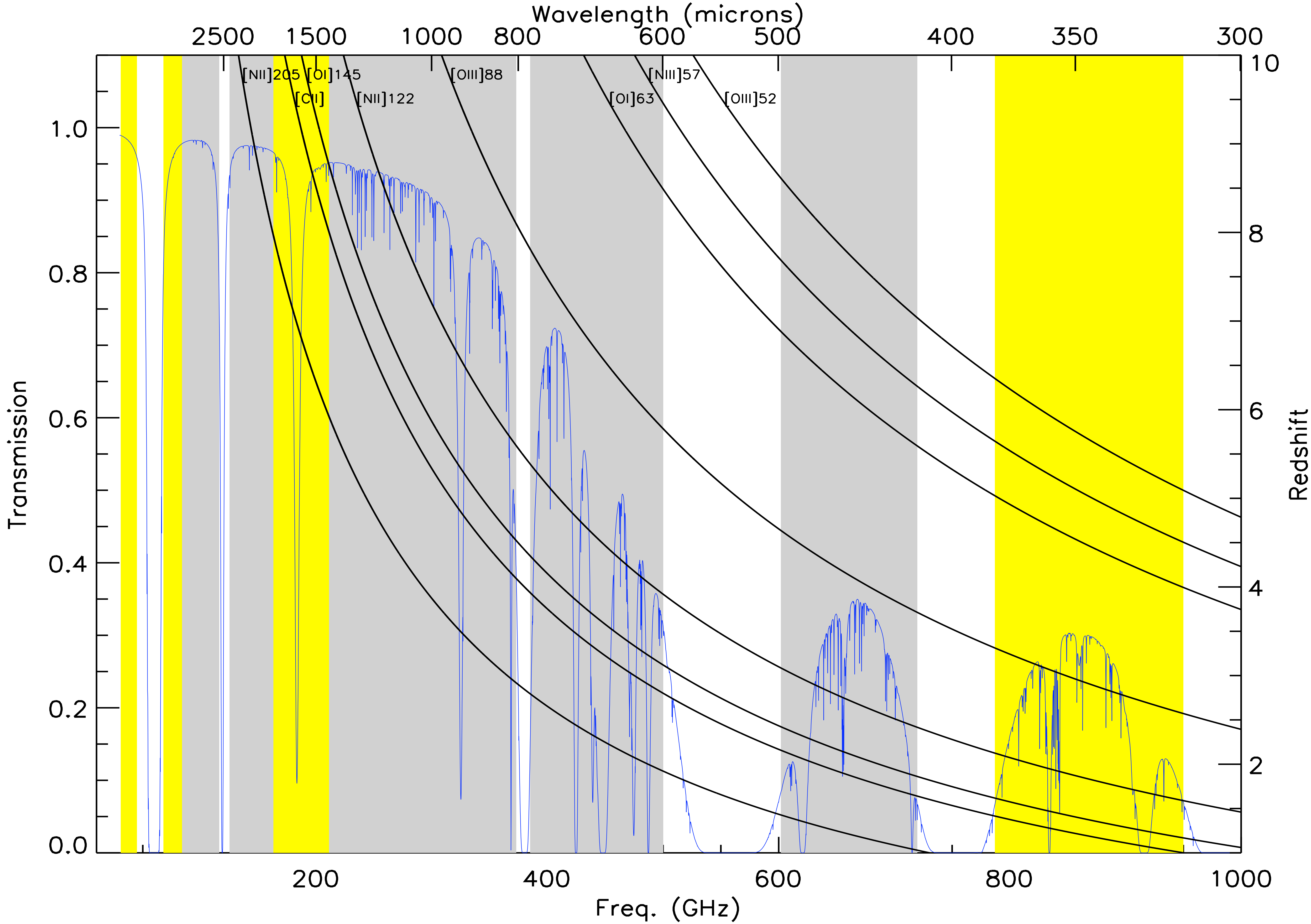

Wavelength (microns)
2500
1500
1000
800
600
500
400
350
300
[NII]205
[OI]145
[CII]
[NII]122
[OIII]88
[OI]63
[NIII]57
[OIII]52
Transmission
1.0
0.8
0.6
0.4
0.2
0.0
Redshift
10
8
6
4
2
200
400
600
800
1000
Freq. (GHz)

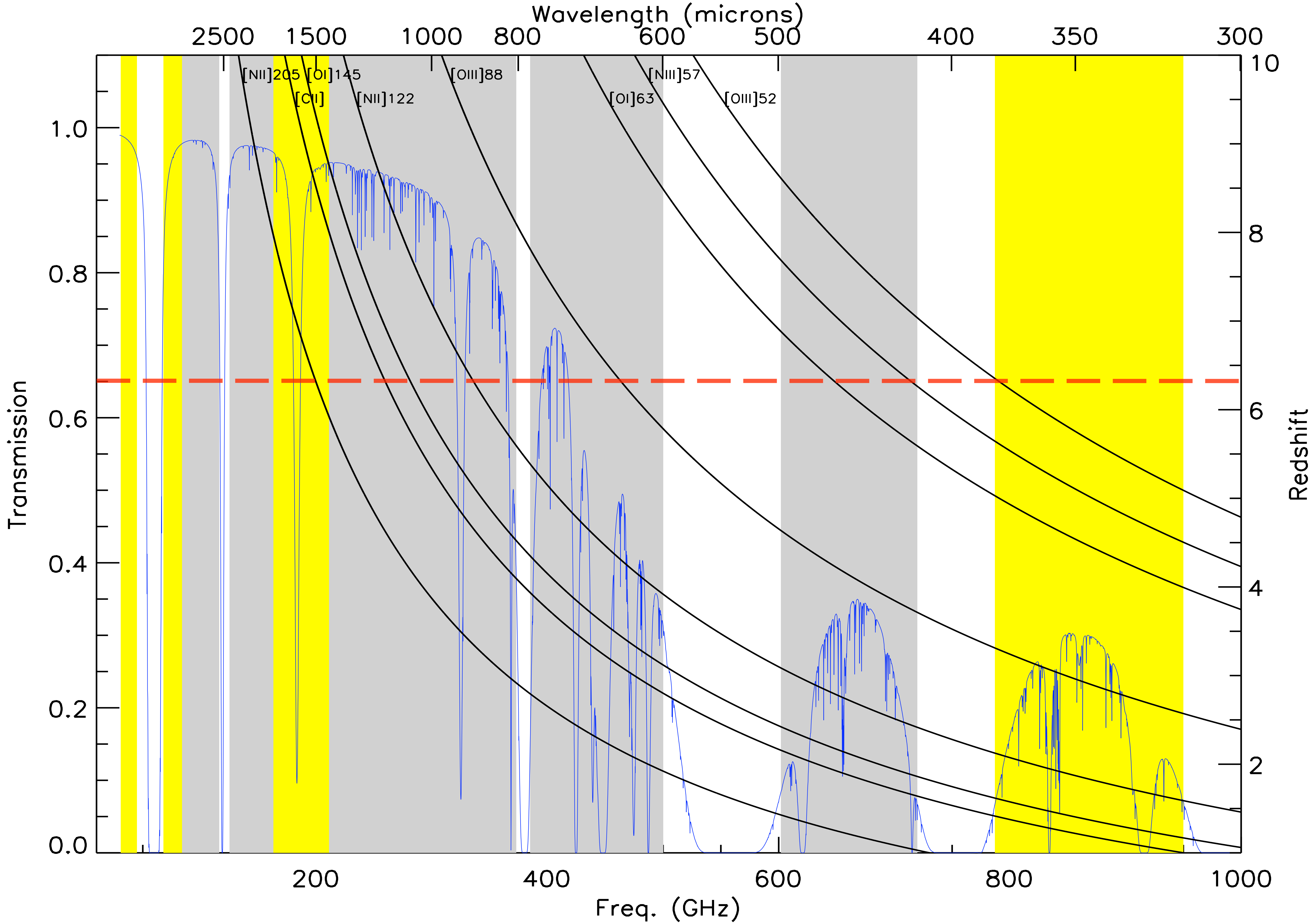

Wavelength (microns)
2500
1500
1000
800
600
500
400
350
300
[NII]205
[OI]145
[CII]
[NII]122
[OIII]88
[OI]63
[NIII]57
[OIII]52
Transmission
1.0
0.8
0.6
0.4
0.2
0.0
Redshift
10
8
6
4
2
200
400
600
800
1000
Freq. (GHz)

[CII] from ionized gas?

- (Decarli et al. ApJL 782, 2014)
- [CII] and [NII] 205 in BR1202-0725
- Z=4.7

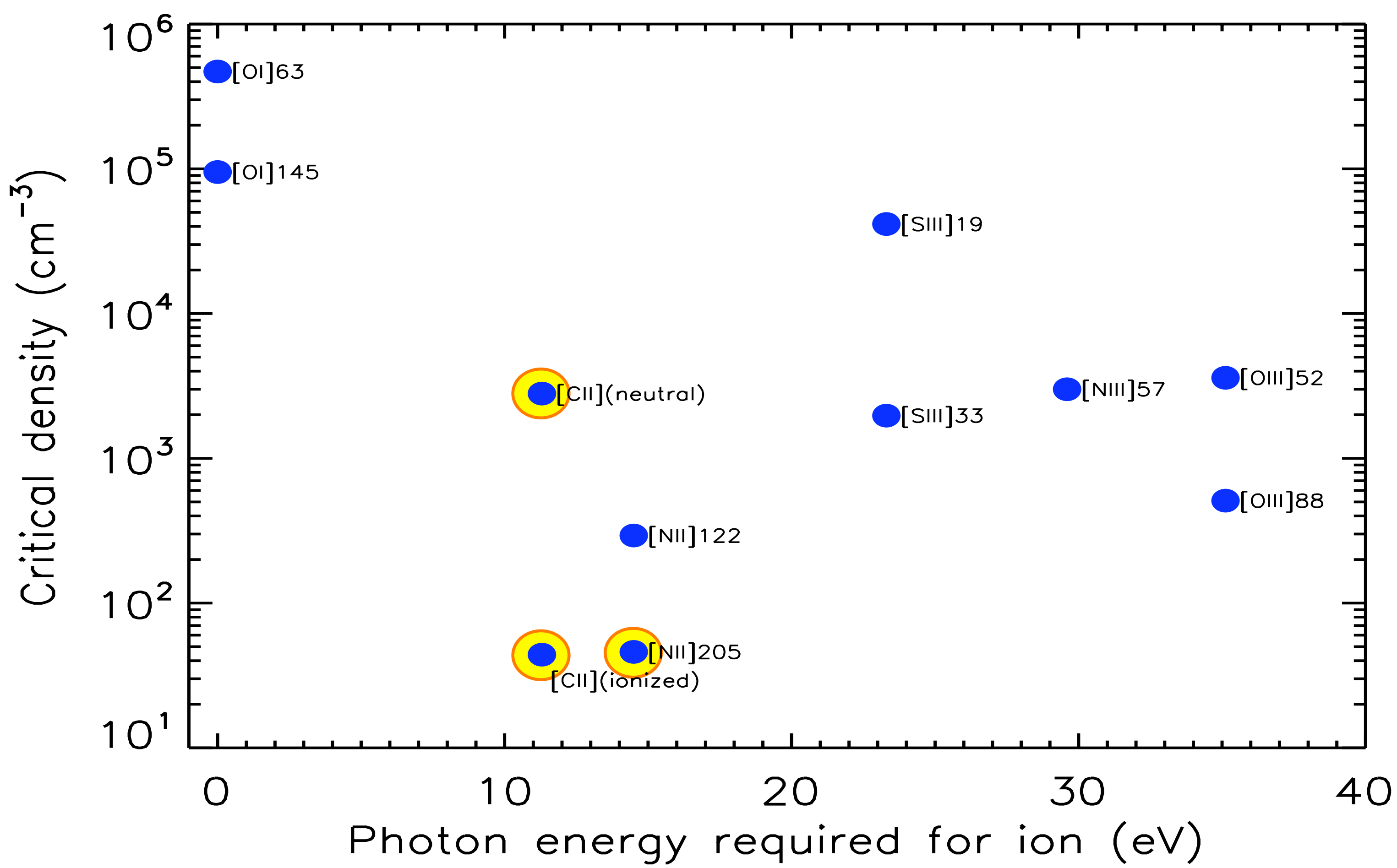

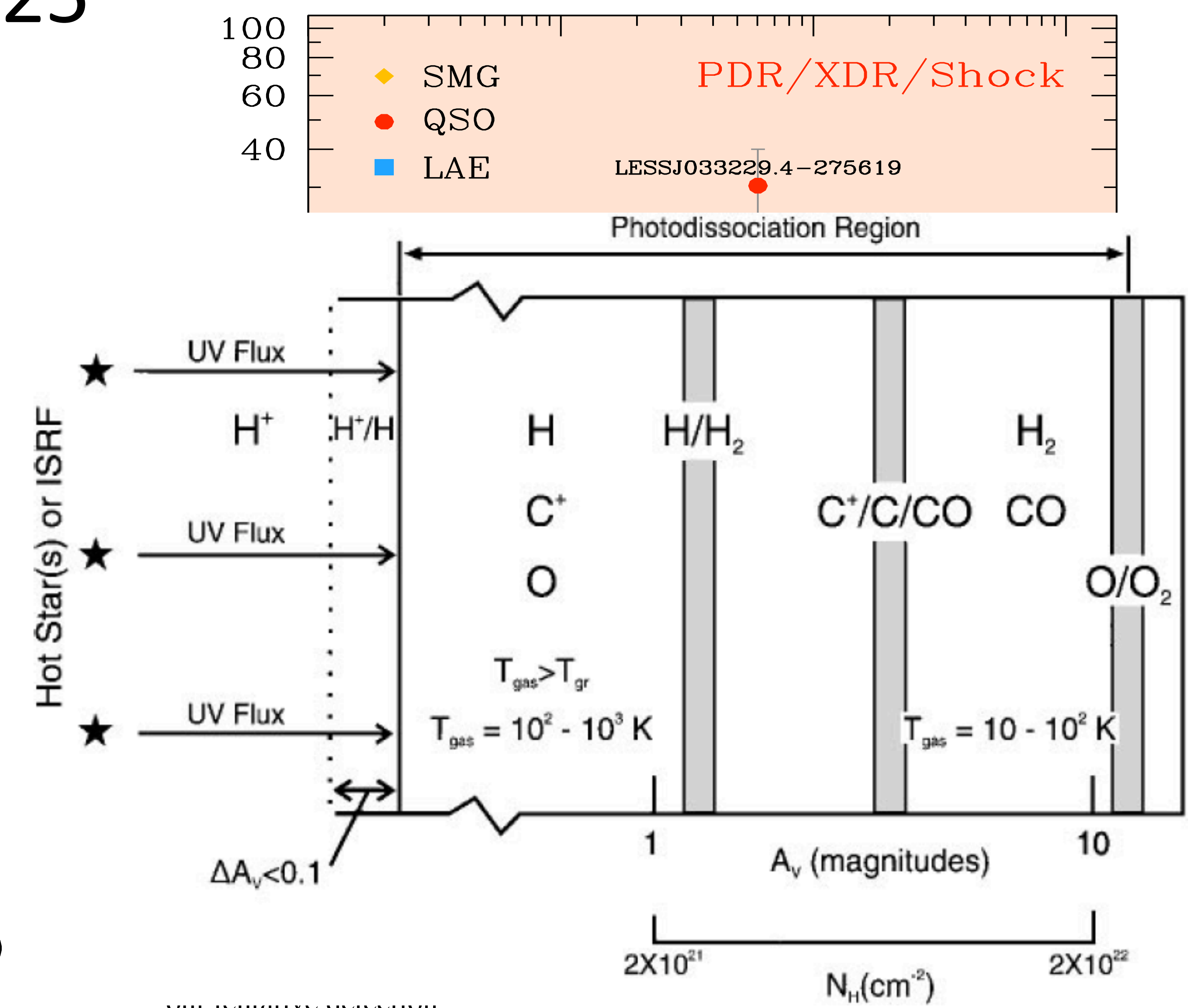

[NII] [CII] metallicity

(Nagao et al. A&A 542 2012)

ALESS 73.1, z=4.76

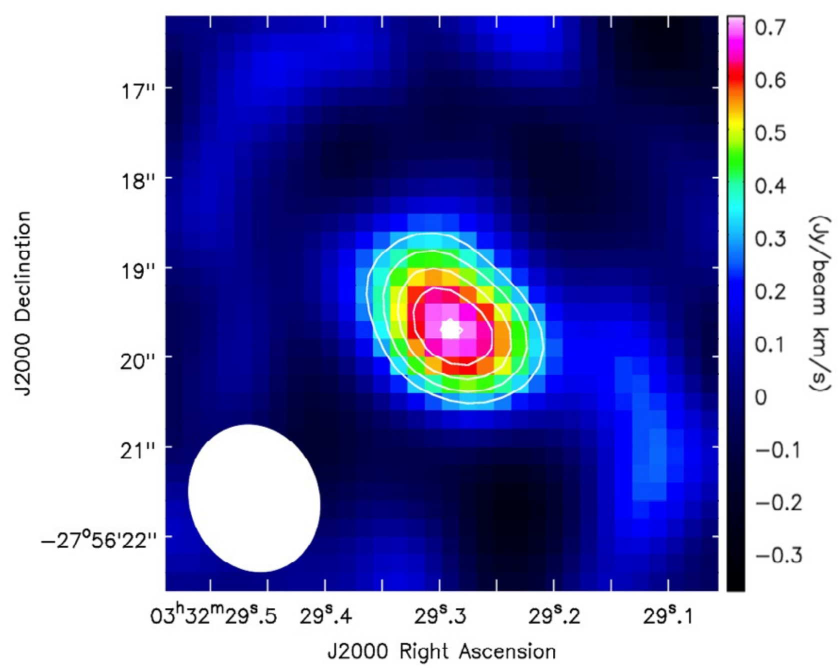

Fig. 1. Velocity-integrated [N II] map of LESS J0332 after the continuum subtraction, with the spatial sampling of 0.2 arcsec/pixel. The velocity range from -558 km s^{-1} to -154 km s^{-1} (with respect to the Lyα emission-line peak) is integrated. Contours at 3σ, 4σ, 5σ, 6σ, and 7σ levels are also given in the map. The shape of the synthesized beam is shown at the lower left-hand corner.

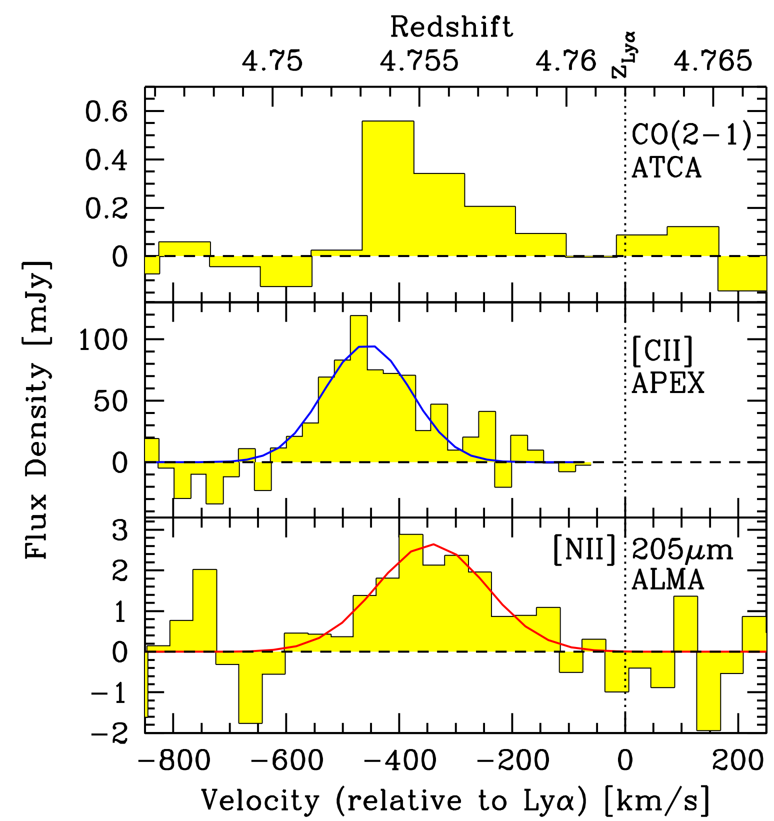

Fig. 2. *Top panel*: ATCA CO(2–1) spectrum of LESS J0332 adopting a 90 km s^{-1} binning (Coppin et al. 2010). *Middle panel*: APEX [C II] 158 μm spectrum with a 28 km s^{-1} binning (De Breuck

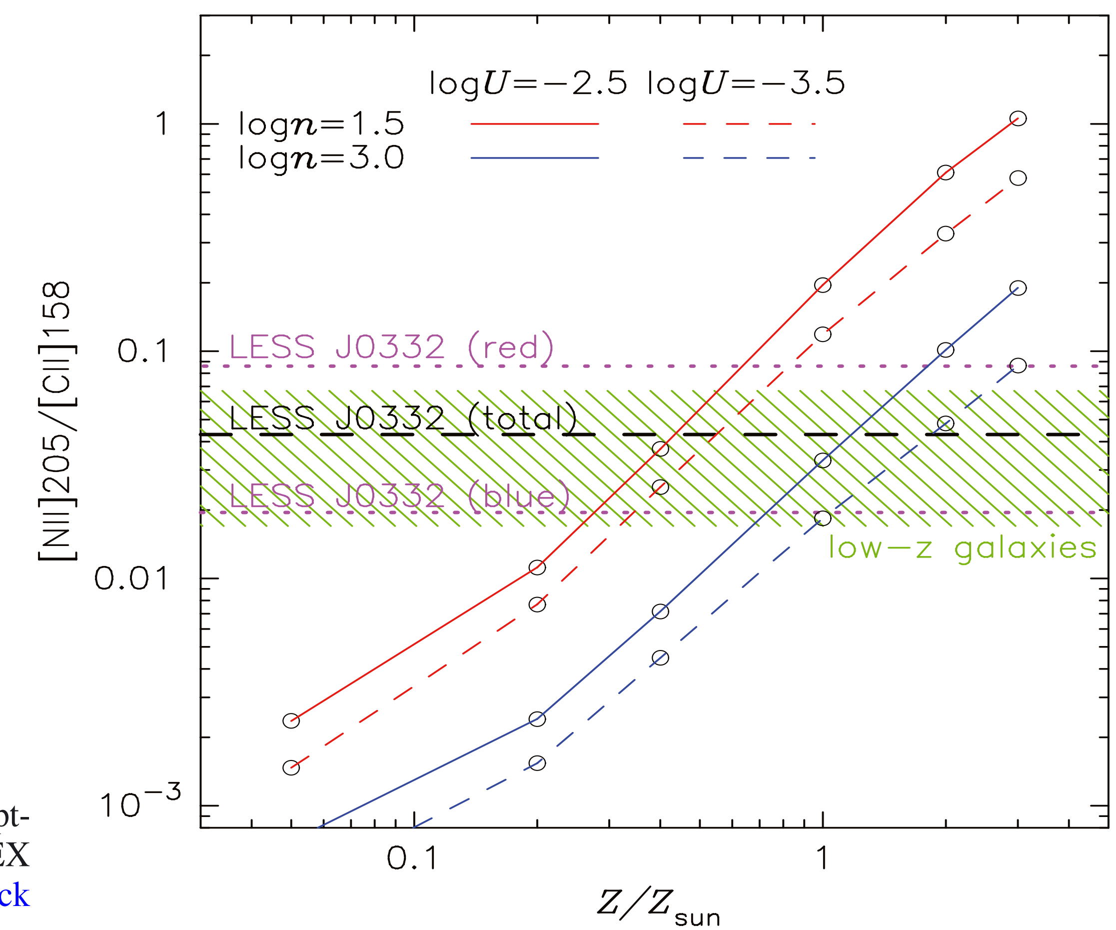

Summary

- [CII] is good
- Many lines is better

A [CII] and [OI] survey of z~1-2 star forming galaxies

Drew Brisbin, Carl Ferkinhoff, Thomas Nikola, Stephen Parshley, Gordon J. Stacey, Henrik Spoon, Steven Hailey-Dunsheath, Aprajita Verma

Presented by Drew Brisbin
ALMA postdoctoral fellow
Charlottesville, VA

August 7, 2014

Image: ESA

Local picture

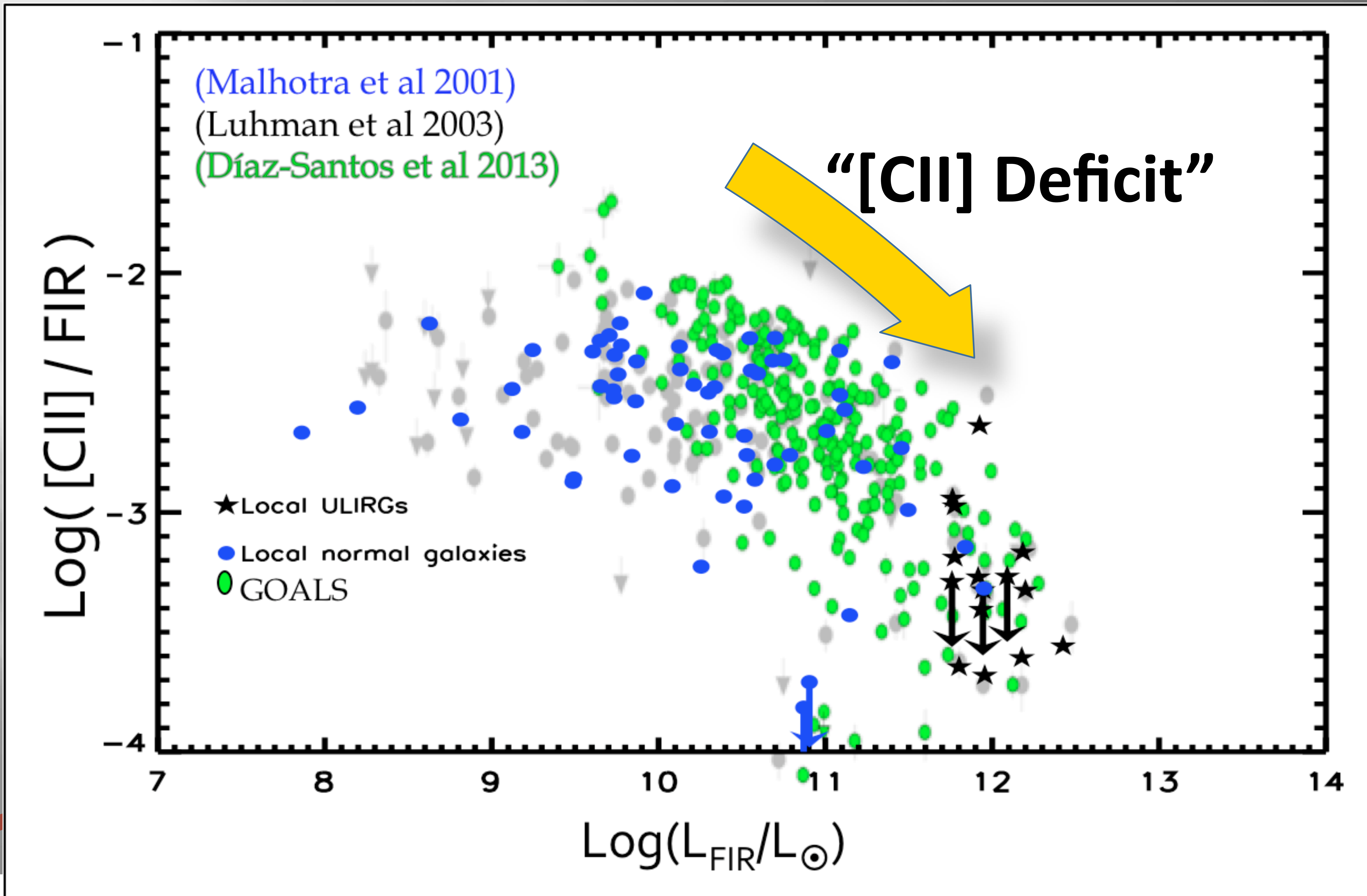

Nature of star formation

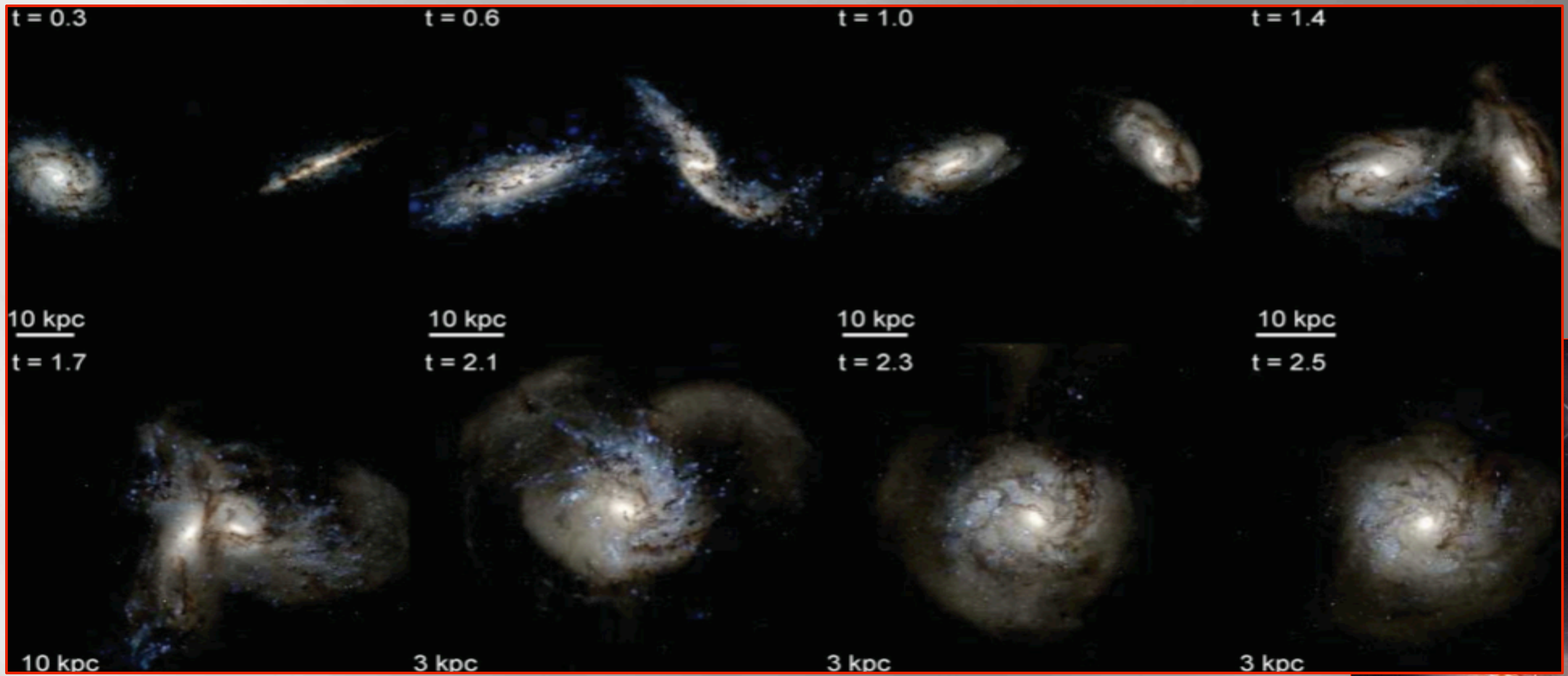

(Hopkins et al 2013)

major mergers

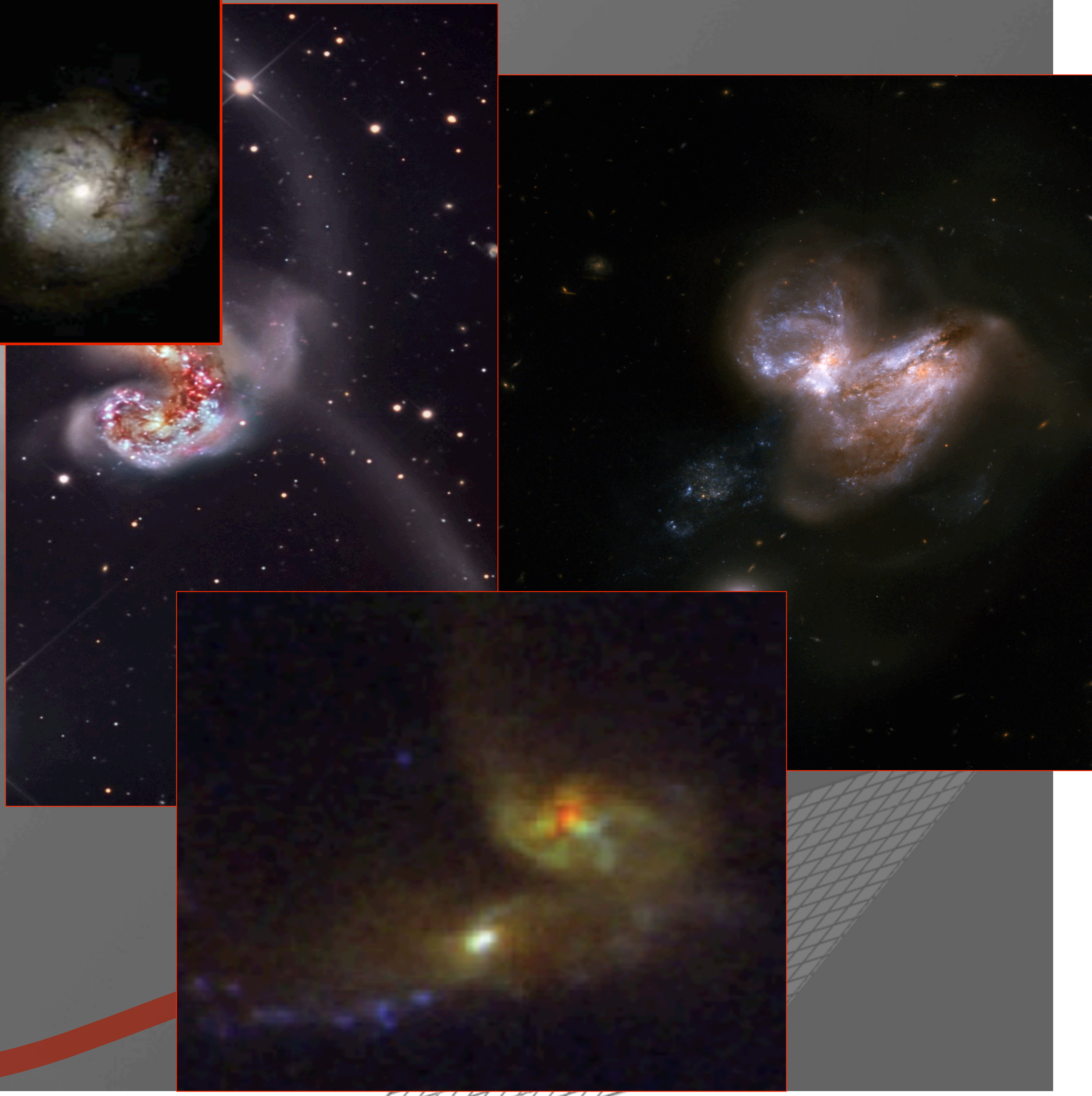

[CII]

- FUV reprocessed by dust to FIR
- Small fraction photo-ejects electrons and heats gas ➔[CII]

- Grain charge buildup
- Saturation of [CII]
  ➔ diminishing returns on [CII]

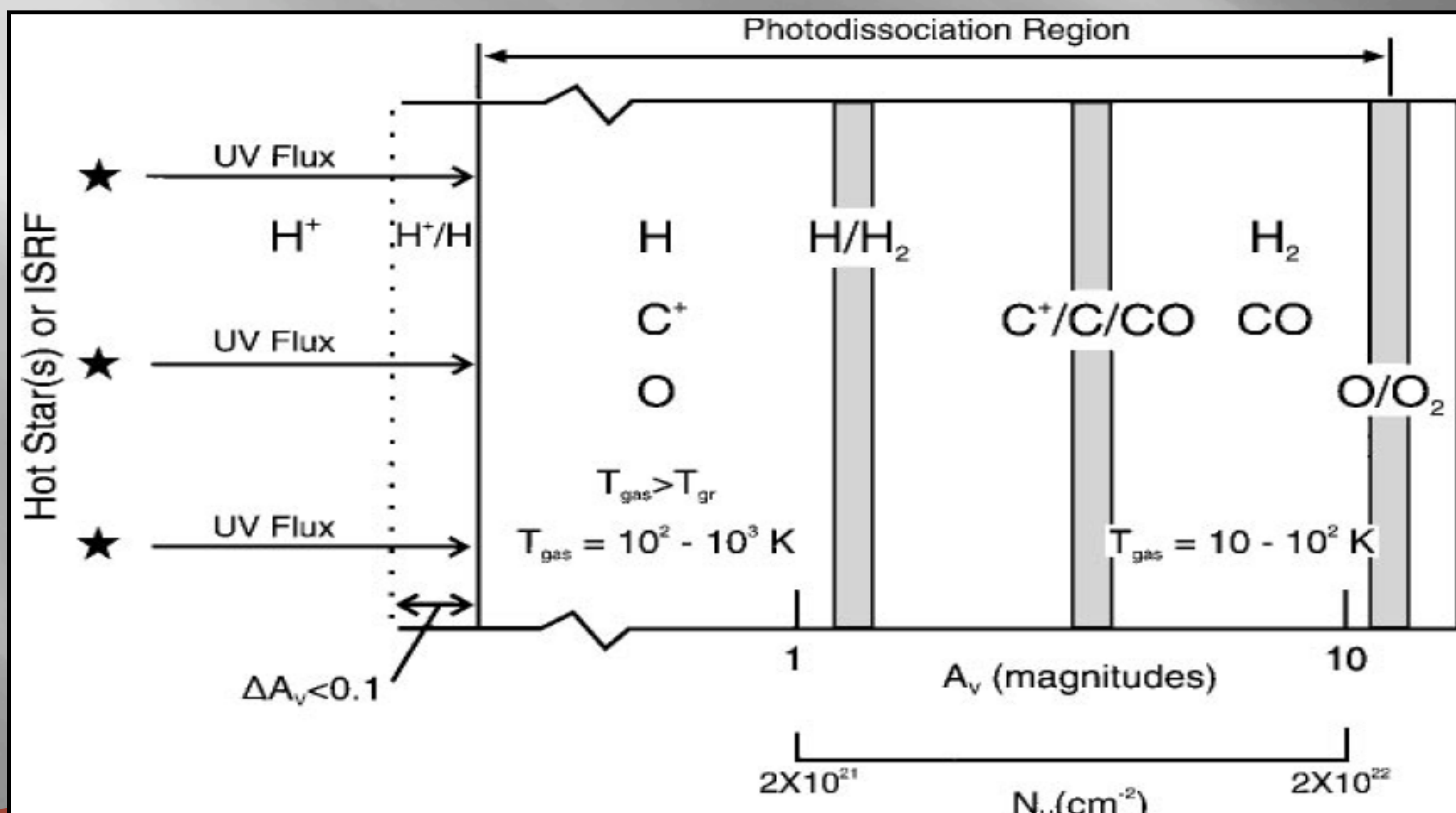

Hollenbach and Tielens 1997, ARAA 35, 179

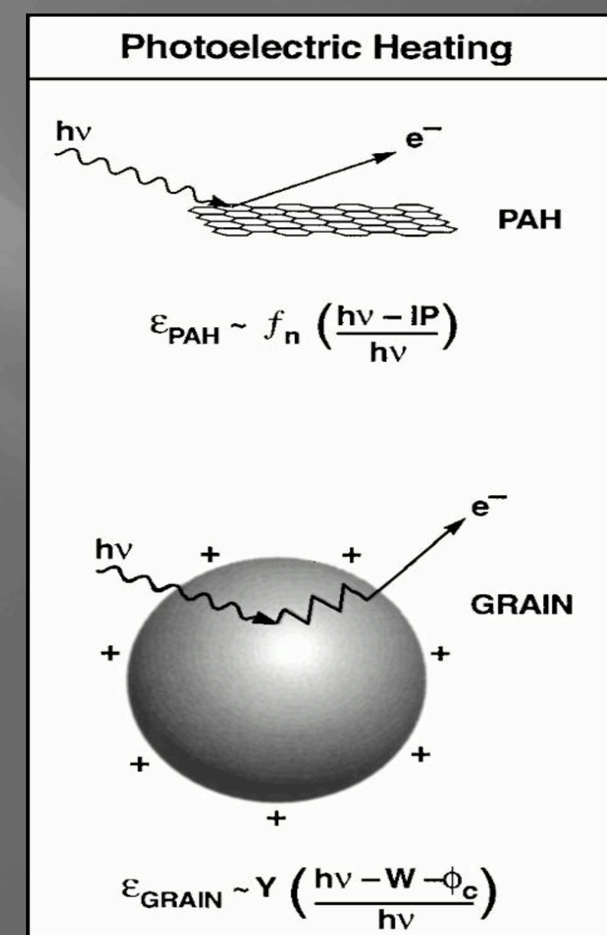

[CII]

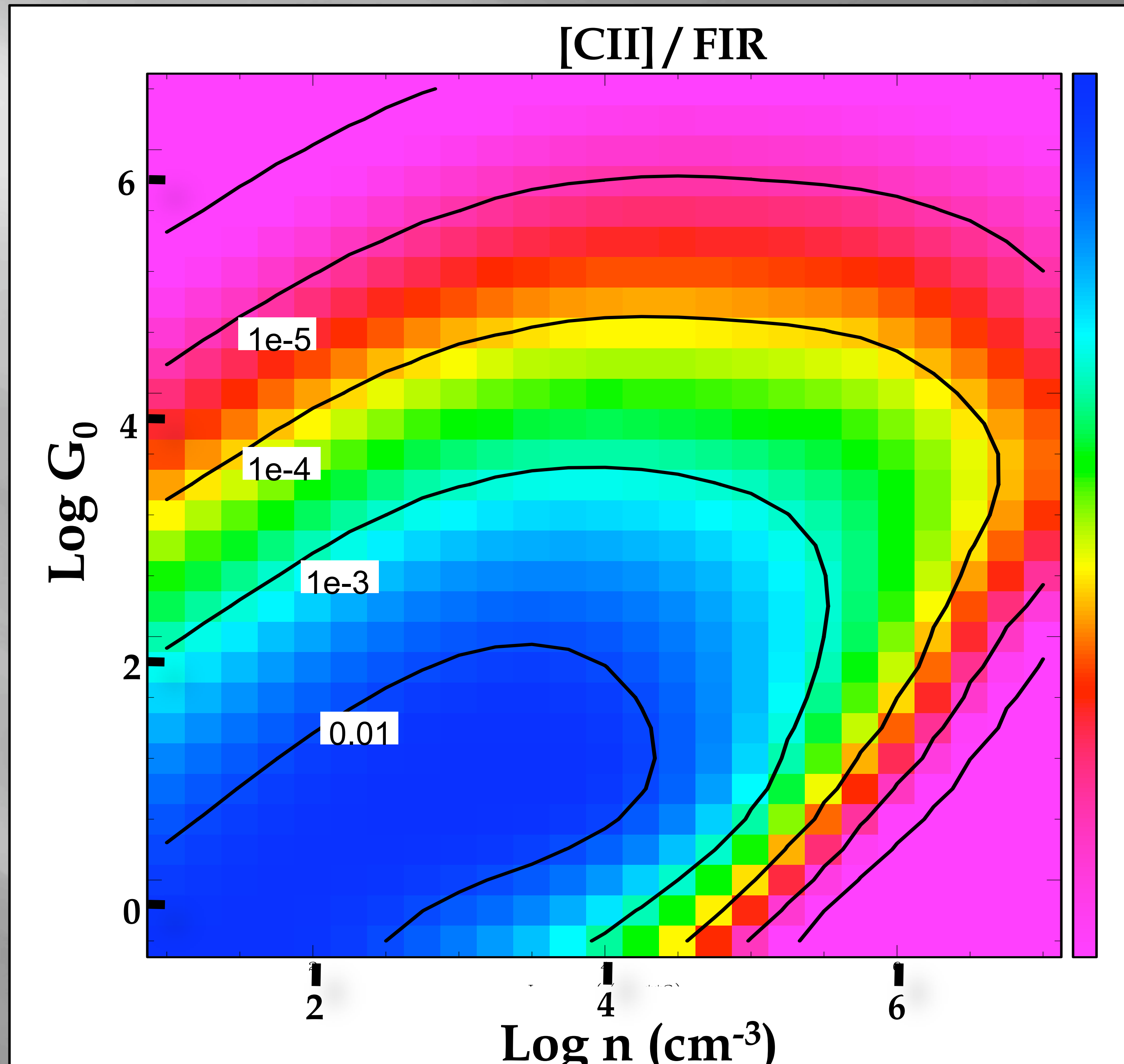

PDR Toolkit

Pound & Wolfire 2008, ADASS XVII, 394, 654

Kaufman et al. 2006, ApJ, 644, 283

Local picture

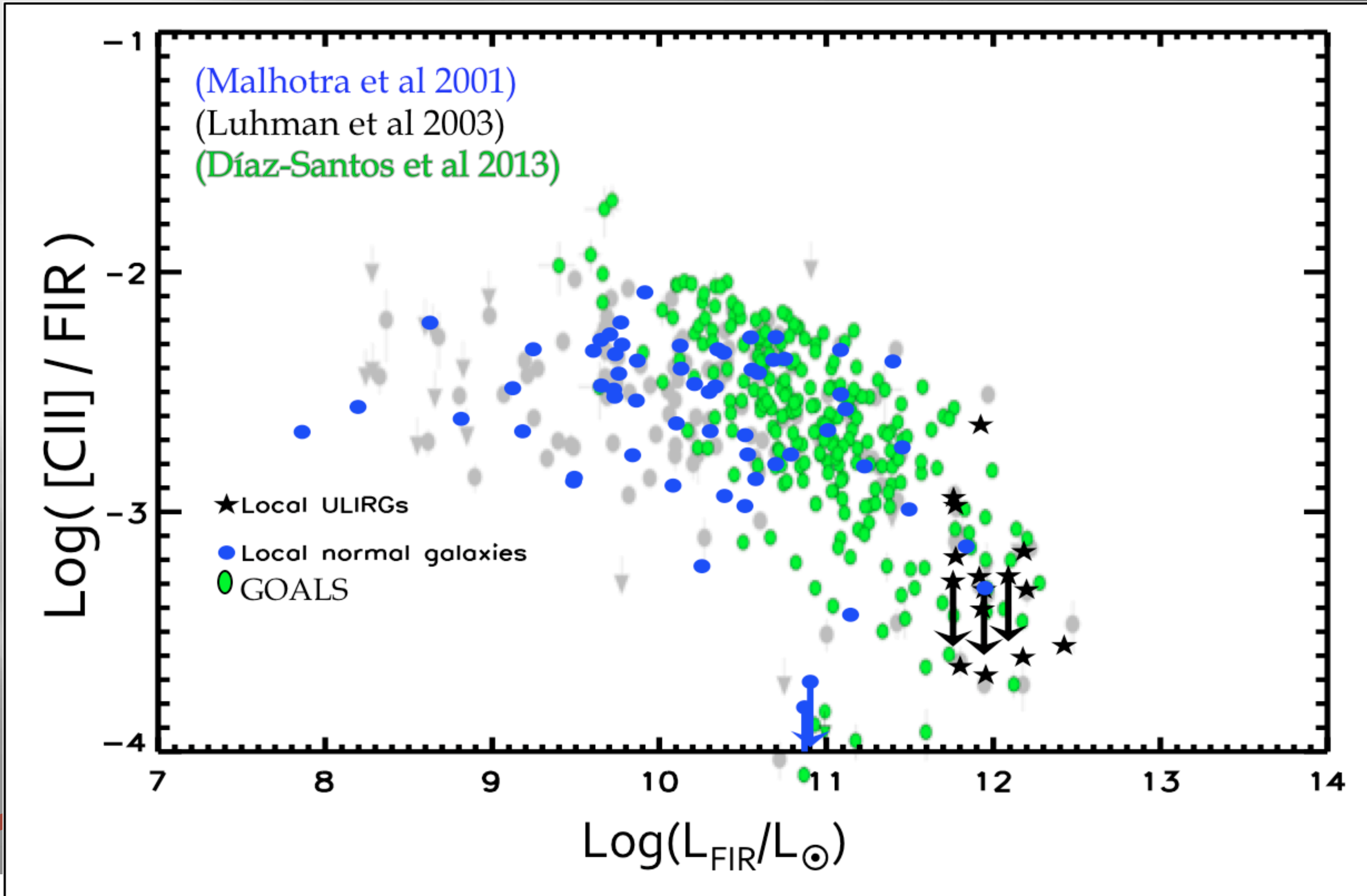

Big picture

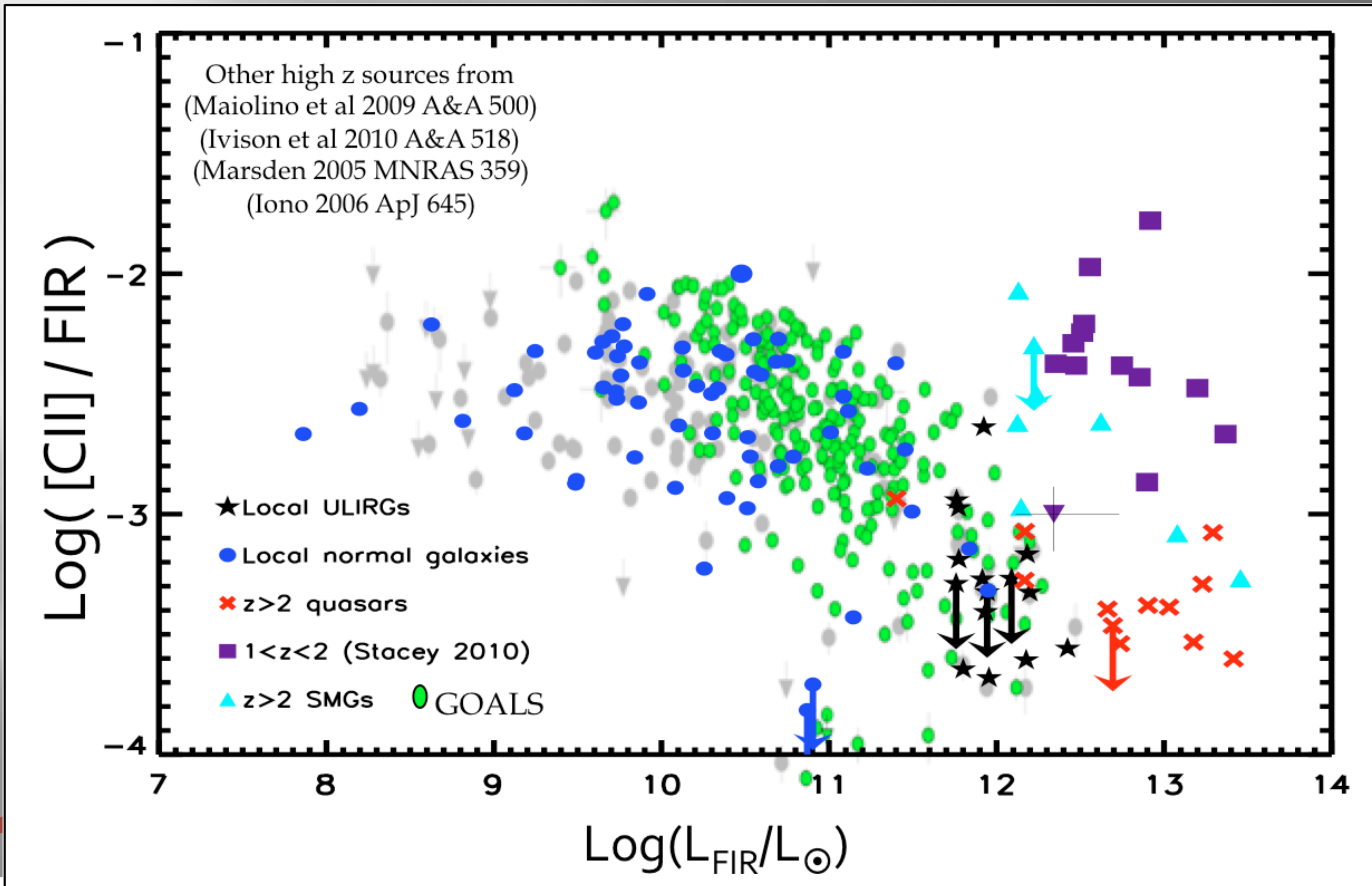

Other high z sources from
(Maiolino et al 2009 A&A 500)
(Ivison et al 2010 A&A 518)
(Marsden 2005 MNRAS 359)
(Iono 2006 ApJ 645)
Local ULIRGs
Local normal galaxies
z>2 quasars
1<z<2 (Stacey 2010)
z>2 SMGs
GOALS
Log([CII] / FIR)
Log(L_FIR/L_⊙)
−1
−2
−3
−4
7
8
9
10
11
12
13
14

Observations

- 8 luminous star forming galaxies with PAH detections
- z=1-2

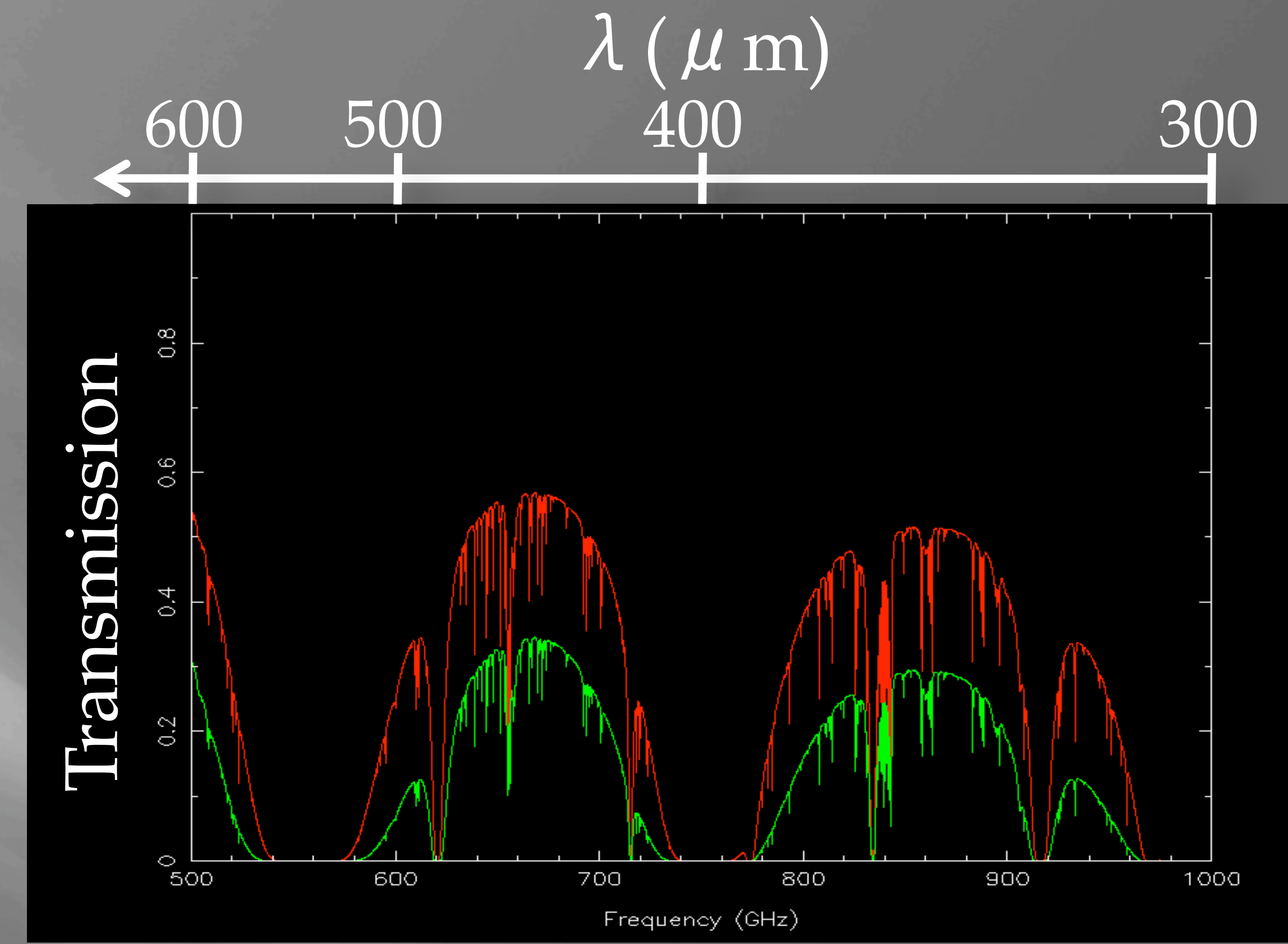

- Redshift (z) Early Universe Spectrometer (ZEUS)
  - Hailey-Dunsheath, S., PhD Dissertation, Cornell University, 2009.

- Caltech Submillimeter Observatory (CSO)

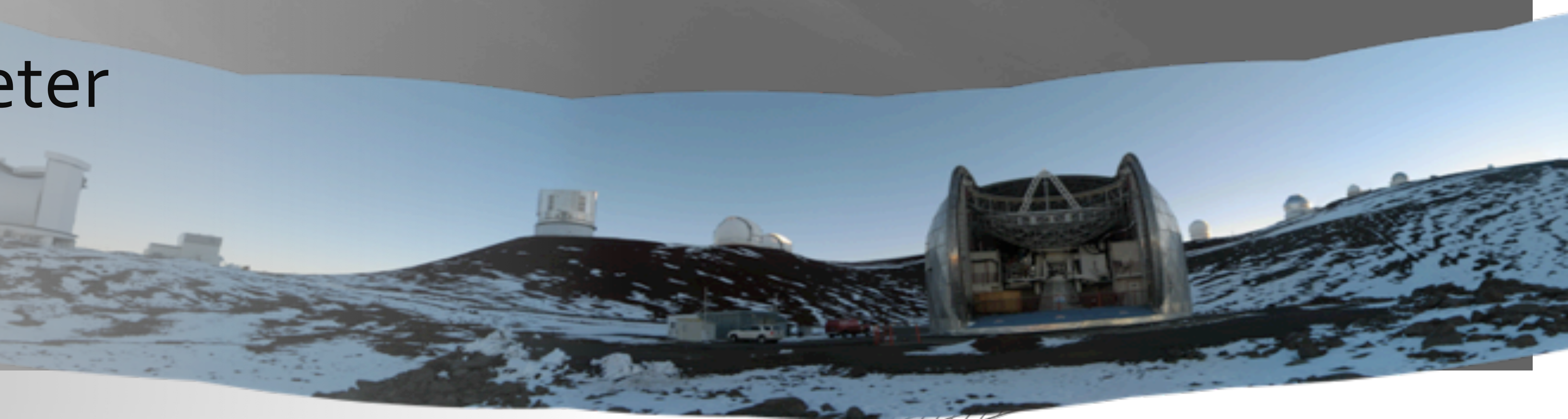

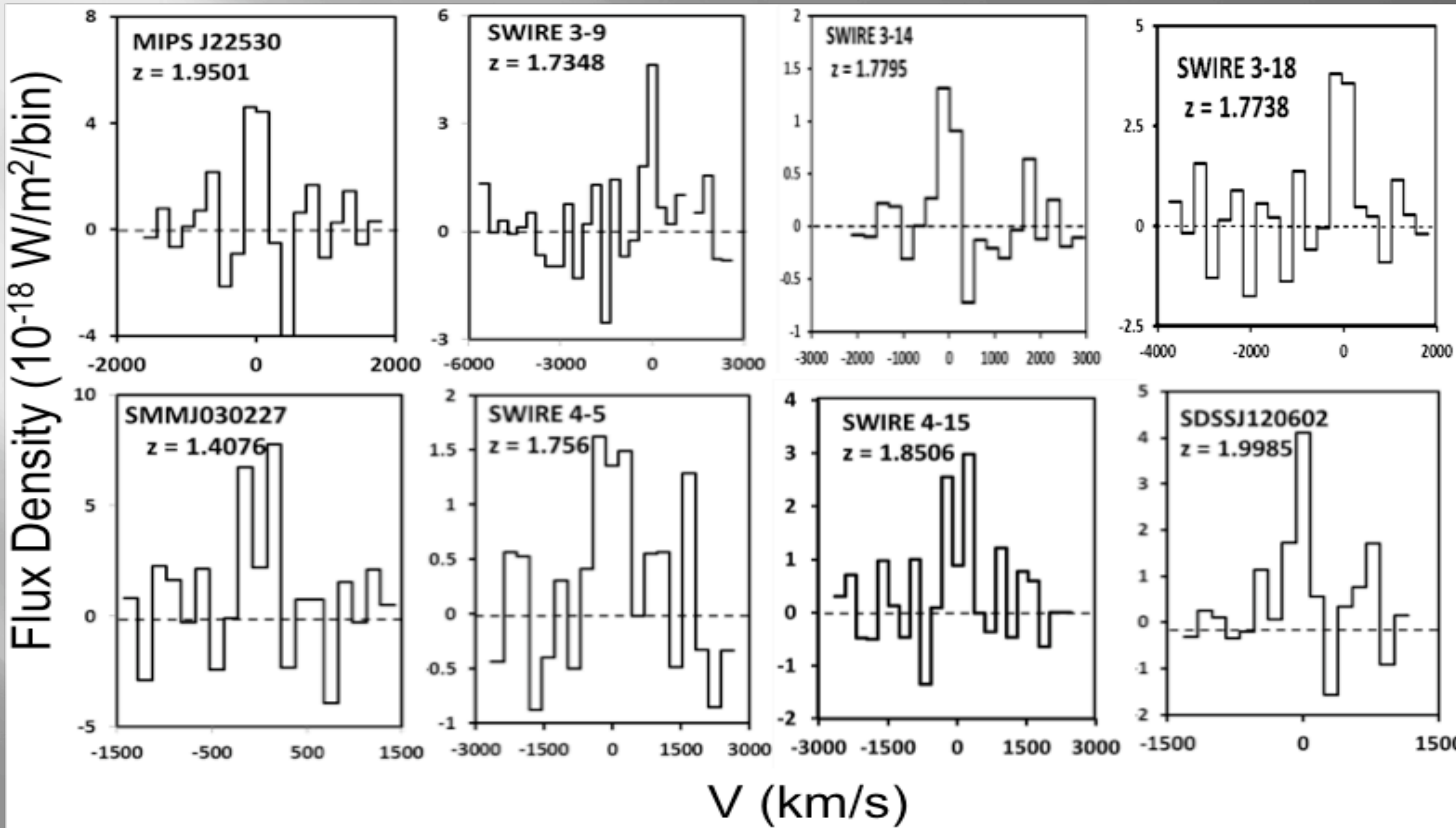

MIPS J22530
z = 1.9501
SWIRE 3-9
z = 1.7348
SWIRE 3-14
z = 1.7795
SWIRE 3-18
z = 1.7738
SMMJ030227
z = 1.4076
SWIRE 4-5
z = 1.756
SWIRE 4-15
z = 1.8506
SDSSJ120602
z = 1.9985
Flux Density (10^-18 W/m^2/bin)
V (km/s)

FIR Photometry from literature

- SCUBA
- Herschel (HerMES)

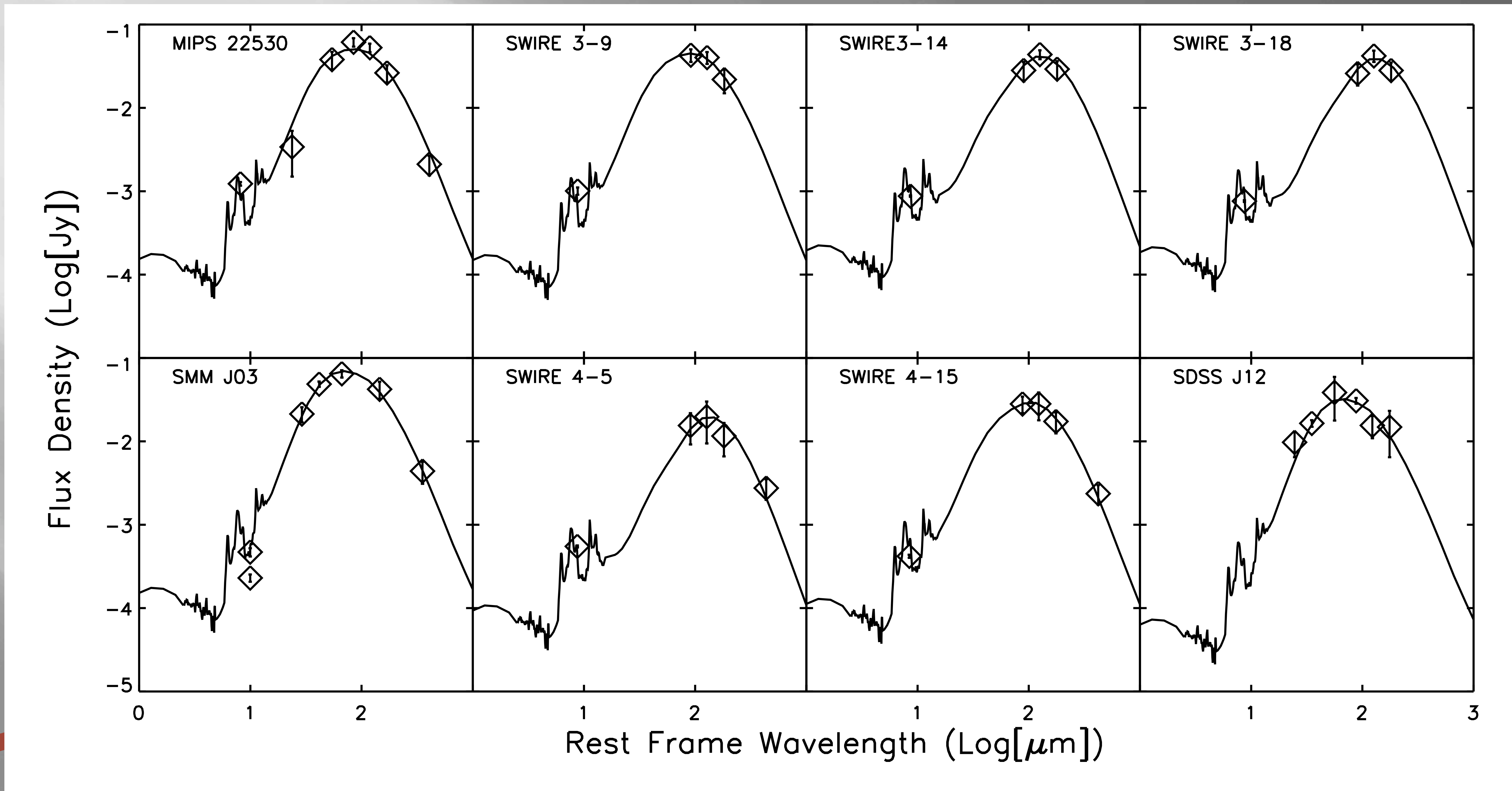

Current picture

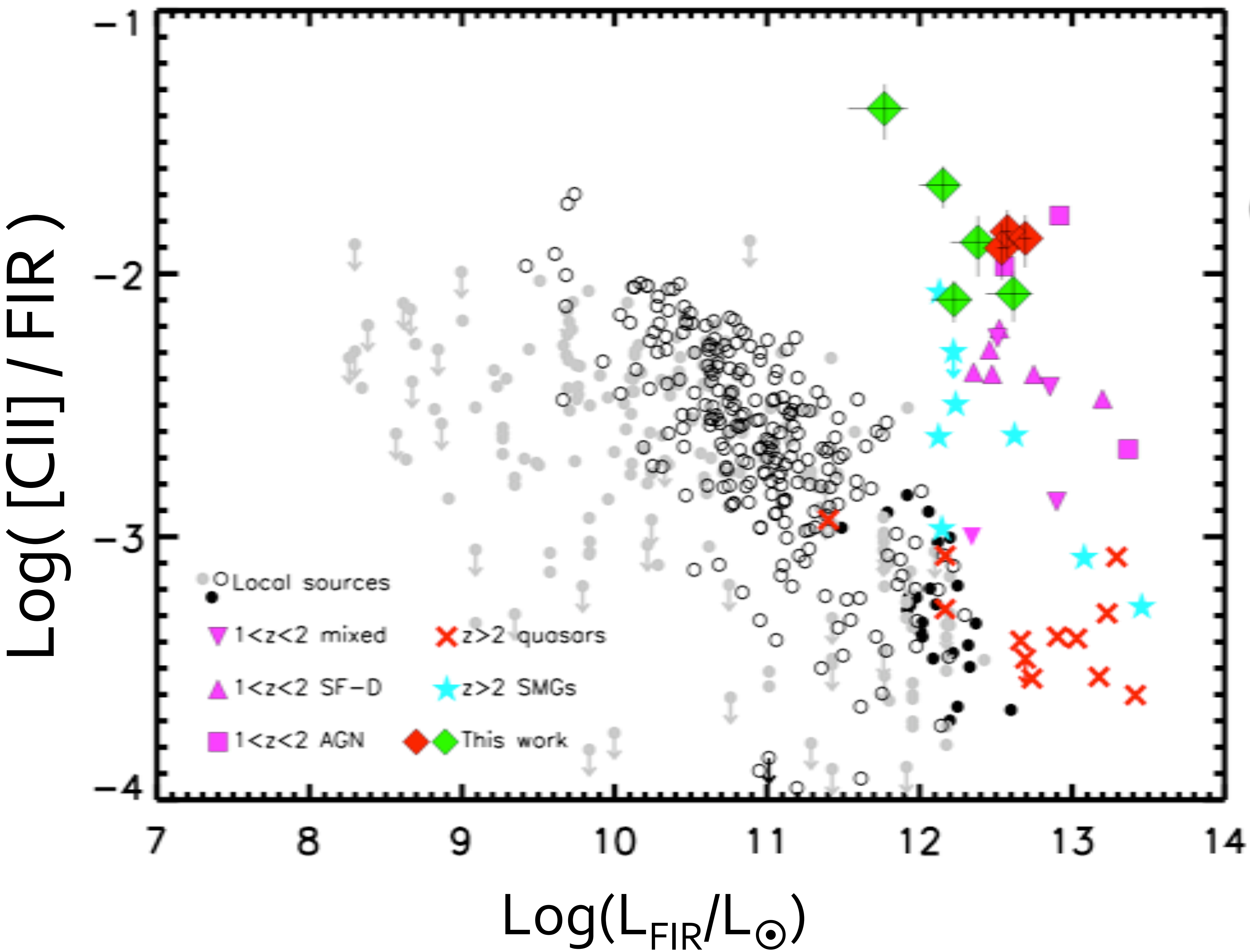

(Stacey 2010, Ferkinhoff 2014, Hailey-Dunsheath *in prep*)

(Brauher 2008)

(Armus 2009, Diaz-Santos 2013)

(Farrah 2013)

Other high z sources from
(Maiolino et al 2009 A&A 500)
(Ivison et al 2010 A&A 518)
(Marsden 2005 MNRAS 359)
(Iono 2006 ApJ 645)

Current picture

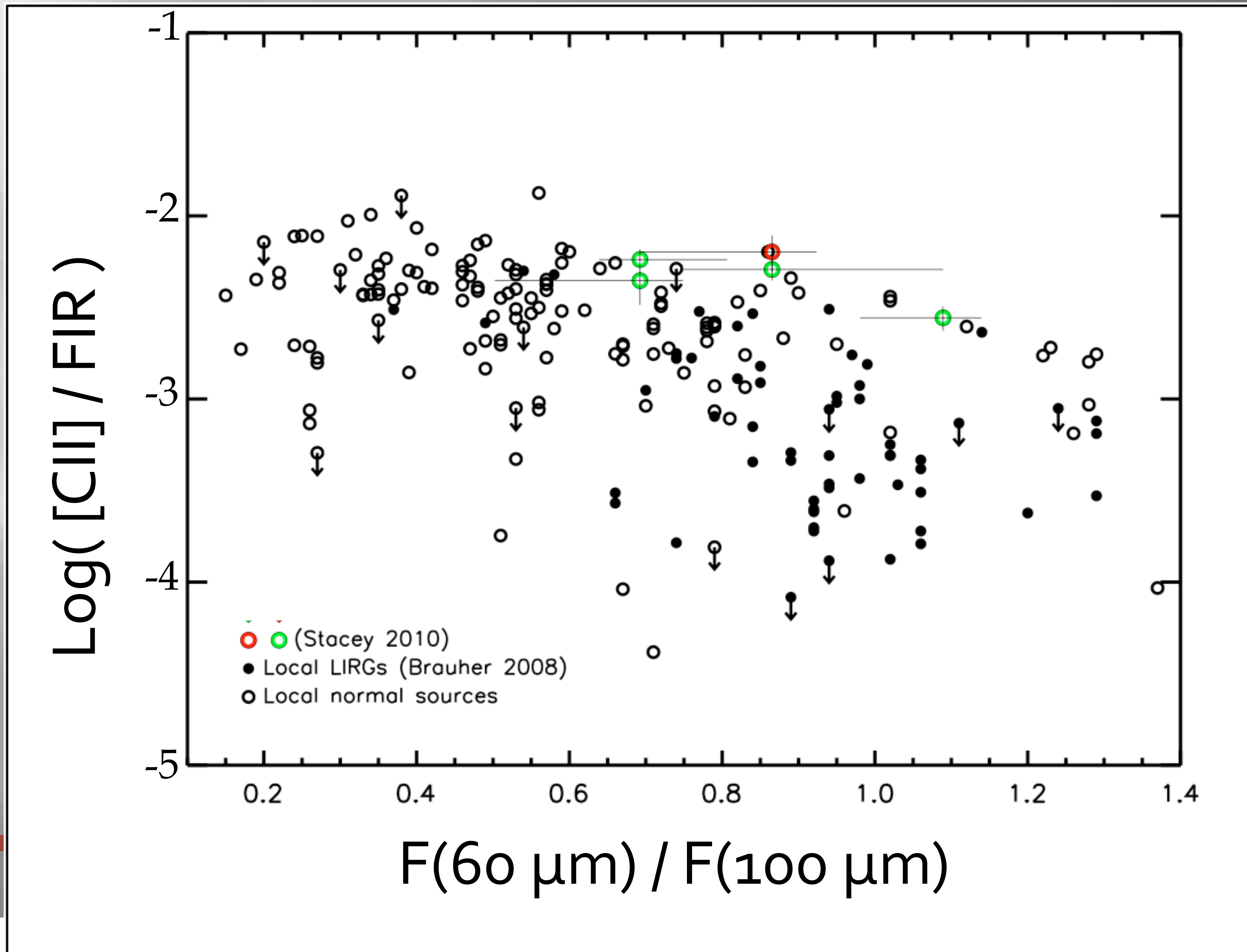

Current picture

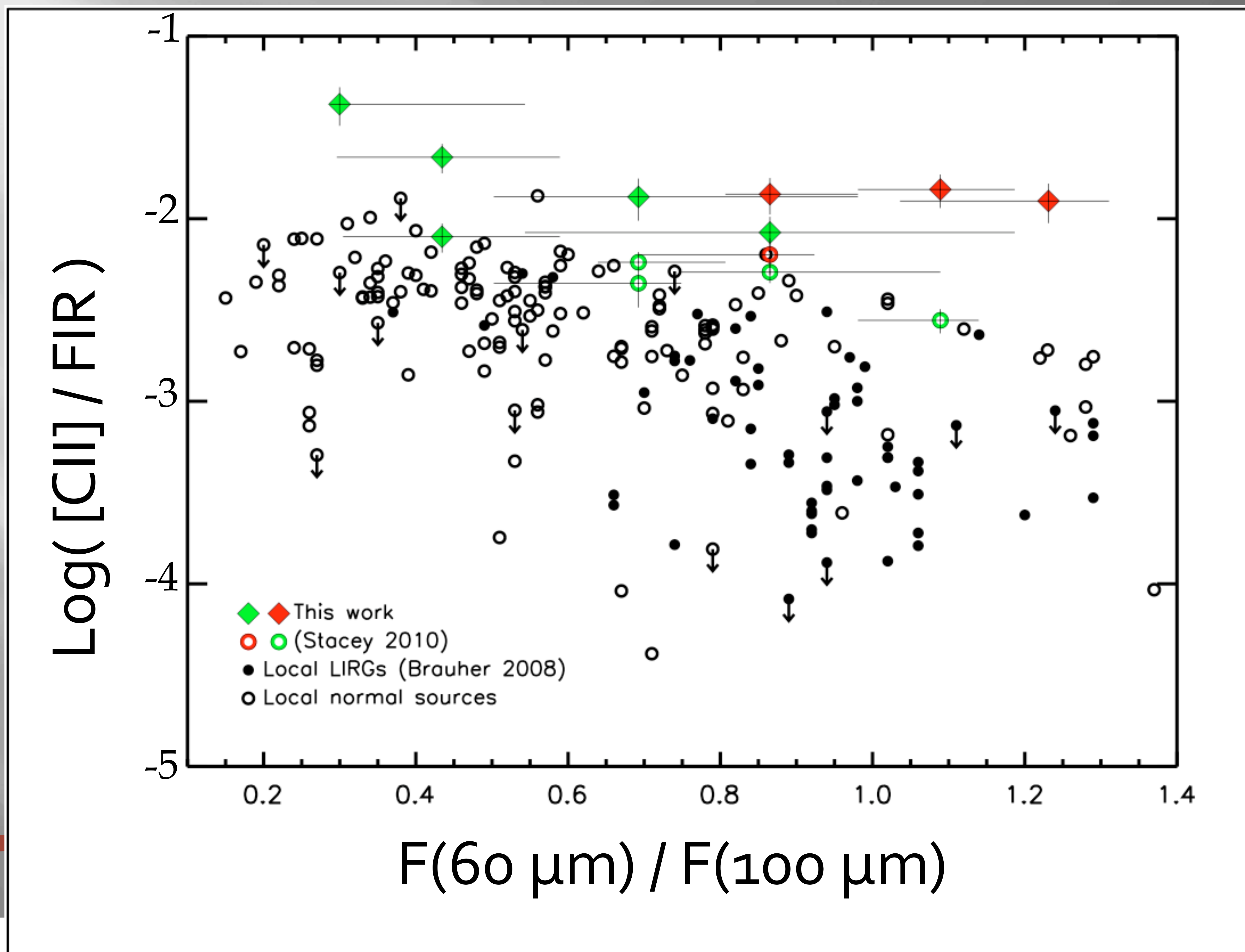

Current picture

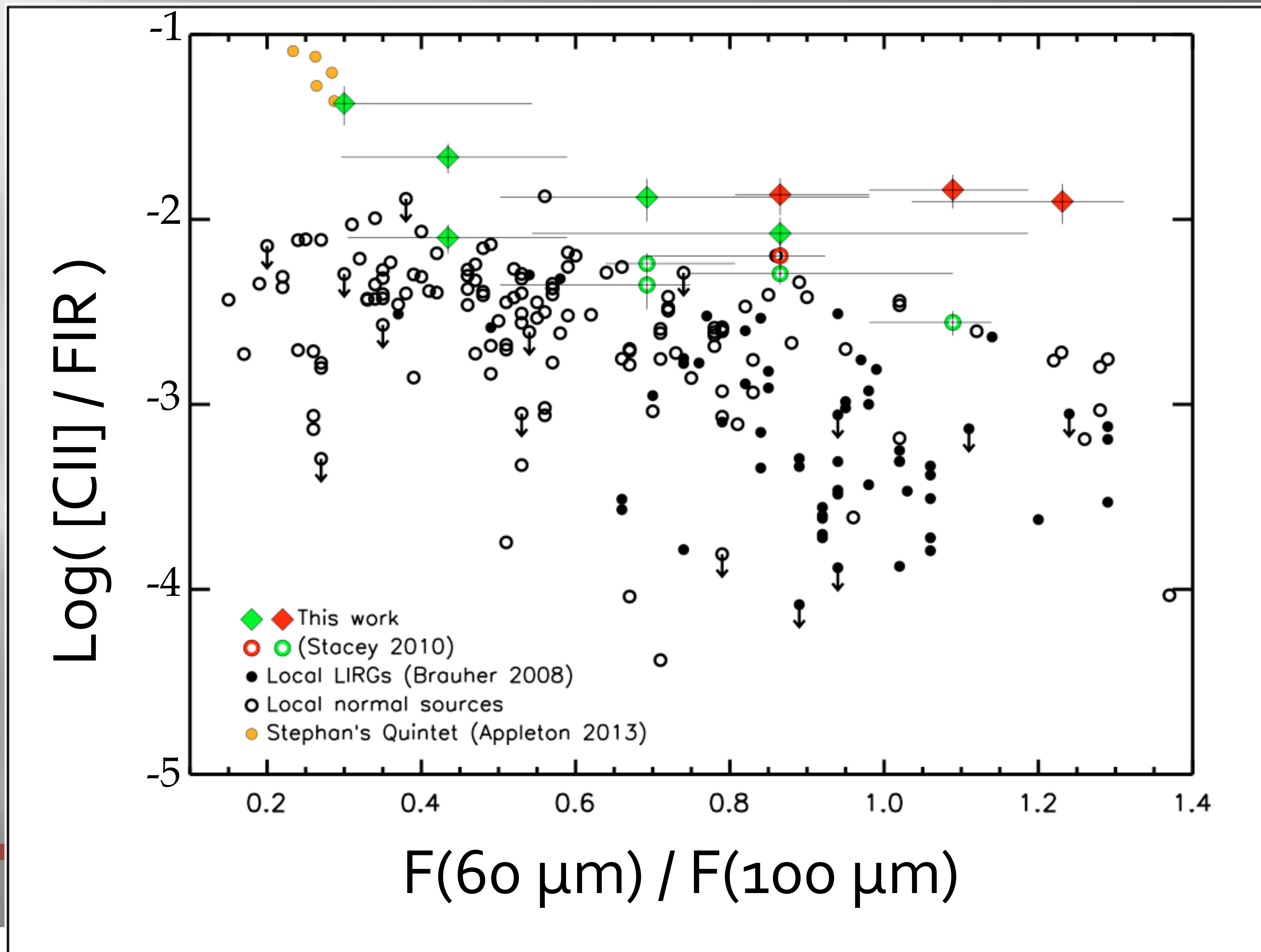

[OI] 63.2 μm

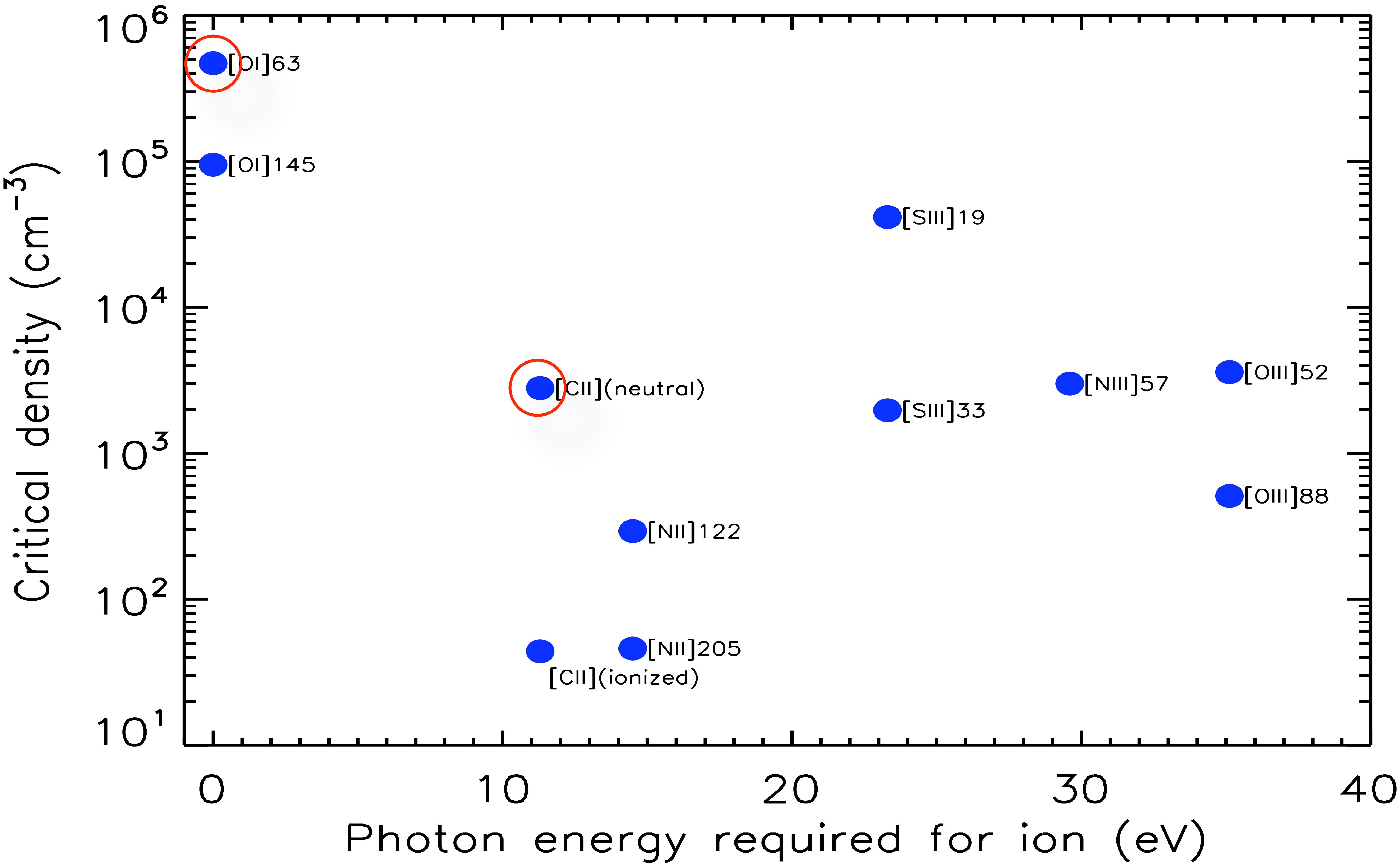

[OI]63
[OI]145
[SIII]19
[CII](neutral)
[SIII]33
[NIII]57
[OIII]52
[OIII]88
[NII]122
[NII]205
[CII](ionized)
Critical density (cm^{-3})
10^6
10^5
10^4
10^3
10^2
10^1
0
10
20
30
40
Photon energy required for ion (eV)

[OI] and [CII]

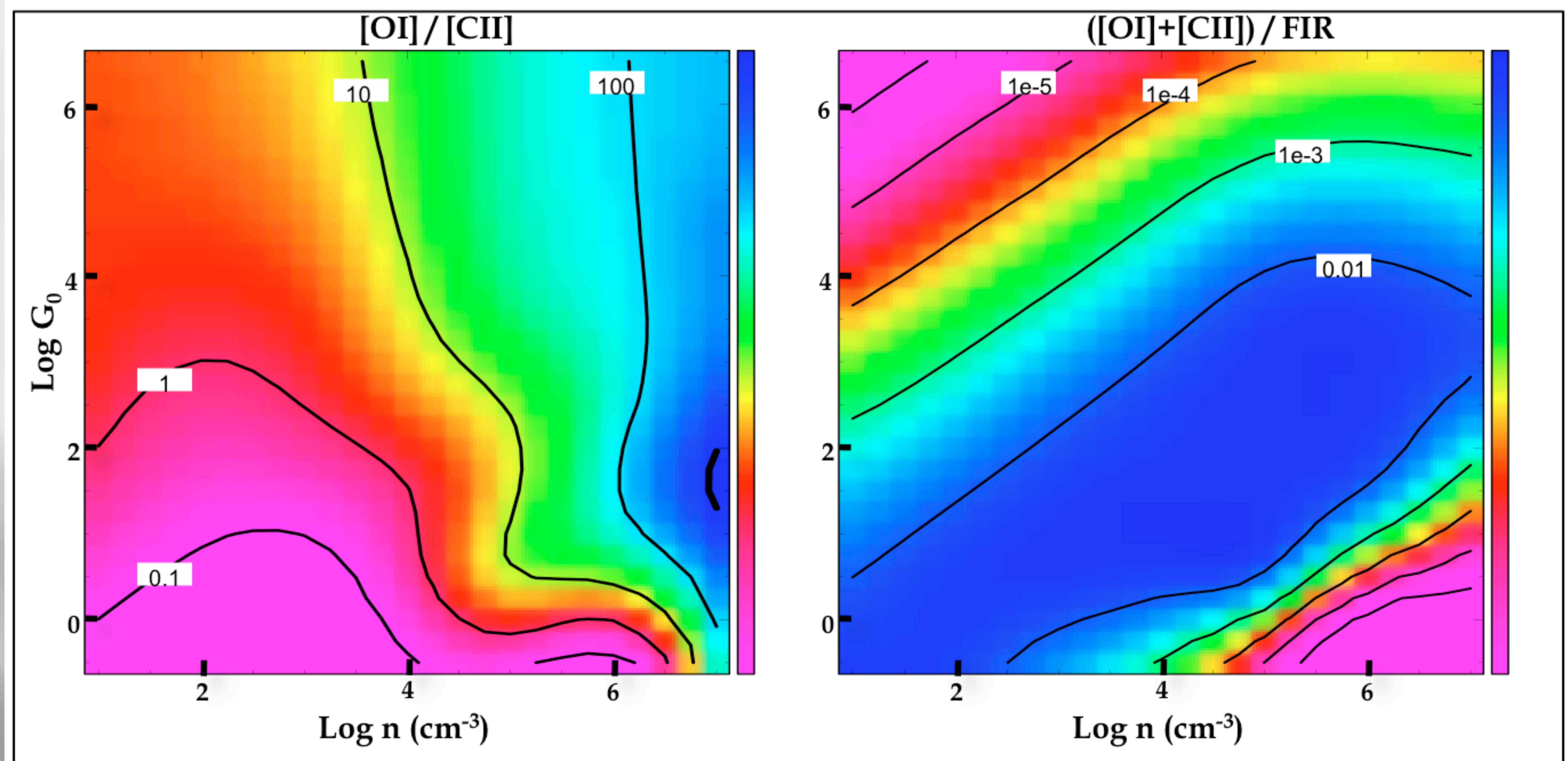

PDR Toolkit

Pound & Wolfire 2008, ADASS XVII, 394, 654

Kaufman et al. 2006, ApJ, 644, 283

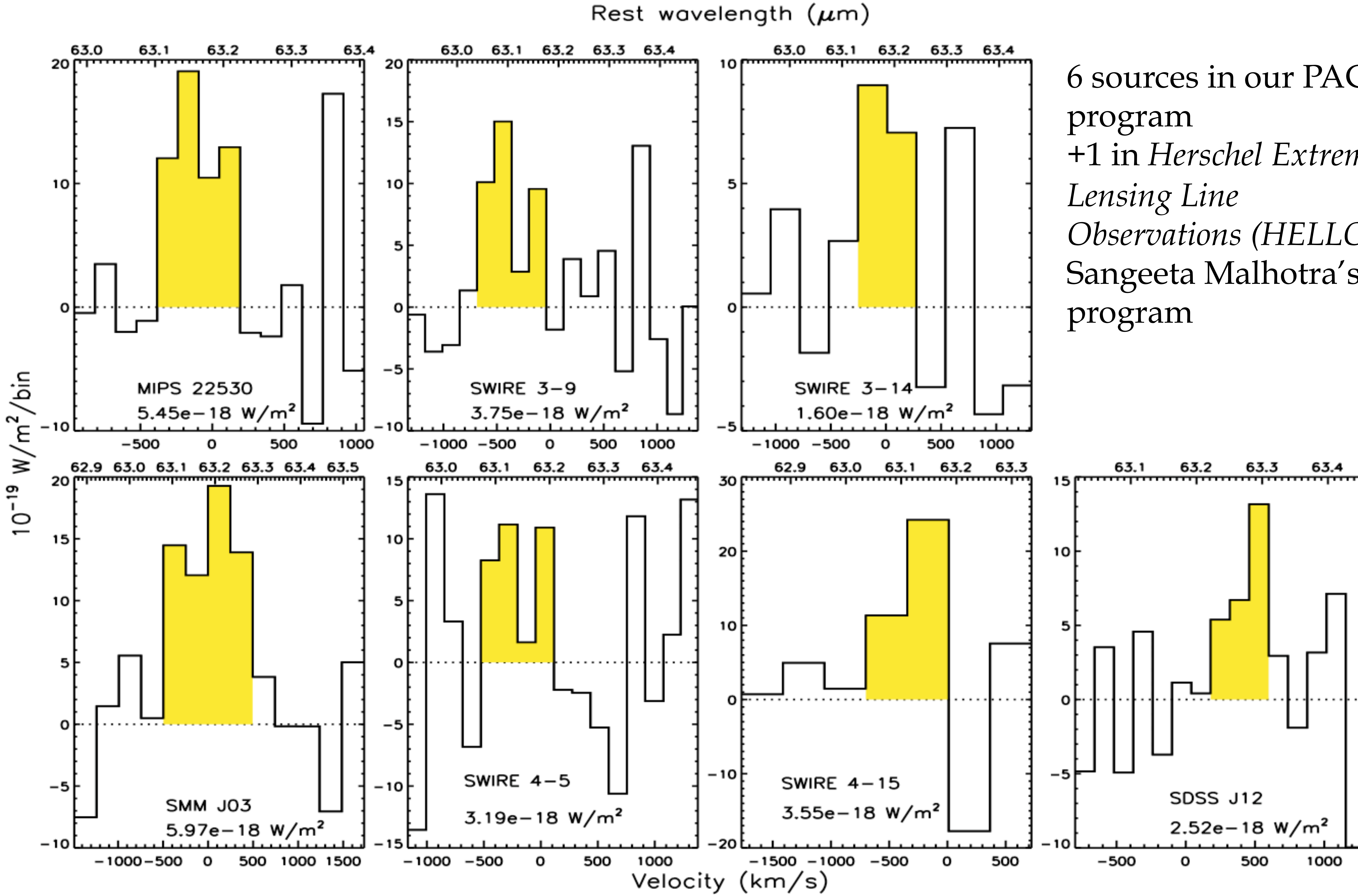

6 sources in our PACS program
+1 in *Herschel Extreme Lensing Line Observations (HELLO)* PI Sangeeta Malhotra's program

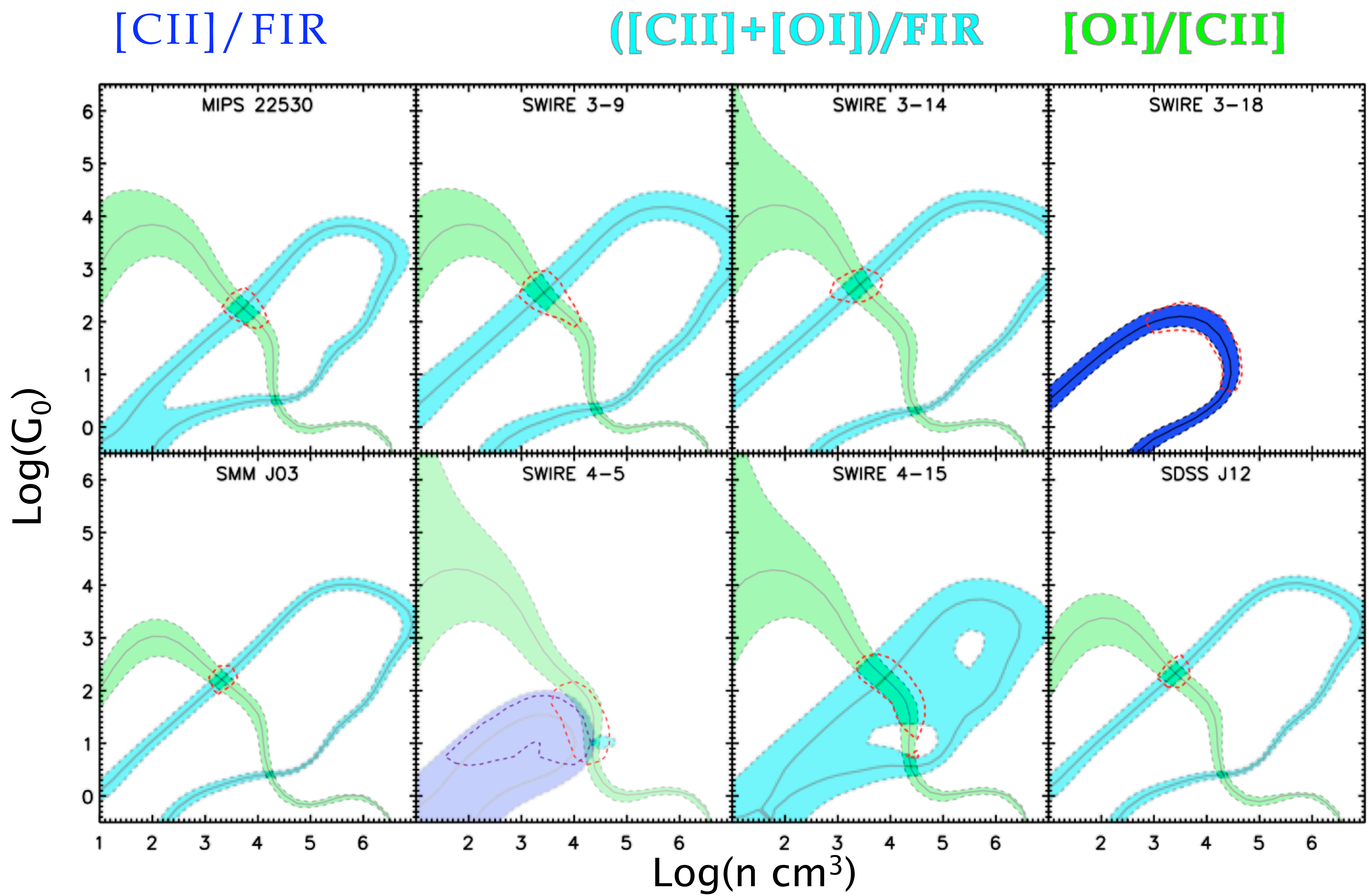
[CII]/FIR
([CII]+[OI])/FIR
[OI]/[CII]
MIPS 22530
SWIRE 3-9
SWIRE 3-14
SWIRE 3-18
SMM J03
SWIRE 4-5
SWIRE 4-15
SDSS J12
Log(G$_0$)
Log(n cm^3)

[OI] and [CII]

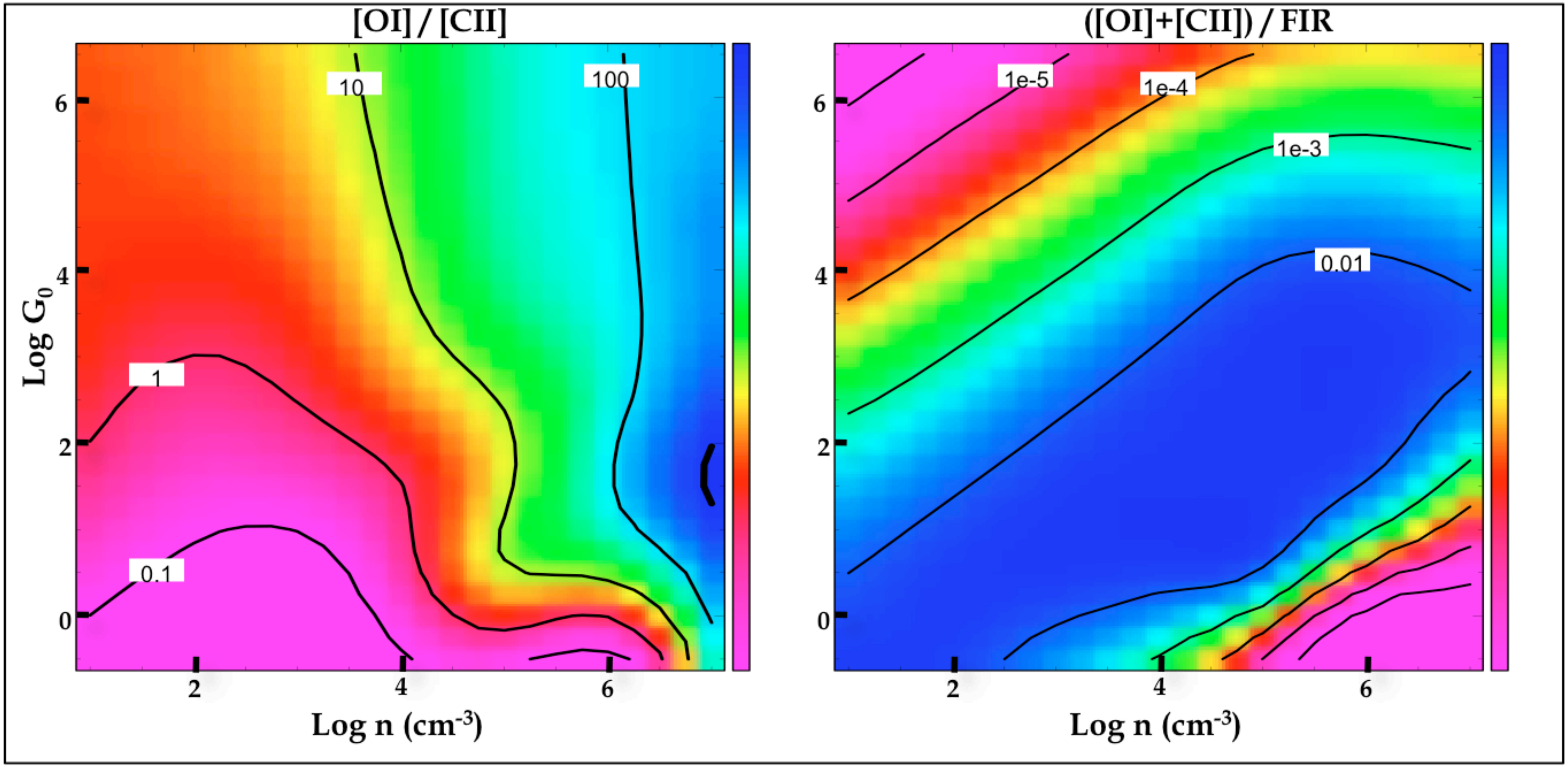

PDR Toolkit

Pound & Wolfire 2008, ADASS XVII, 394, 654

Kaufman et al. 2006, ApJ, 644, 283

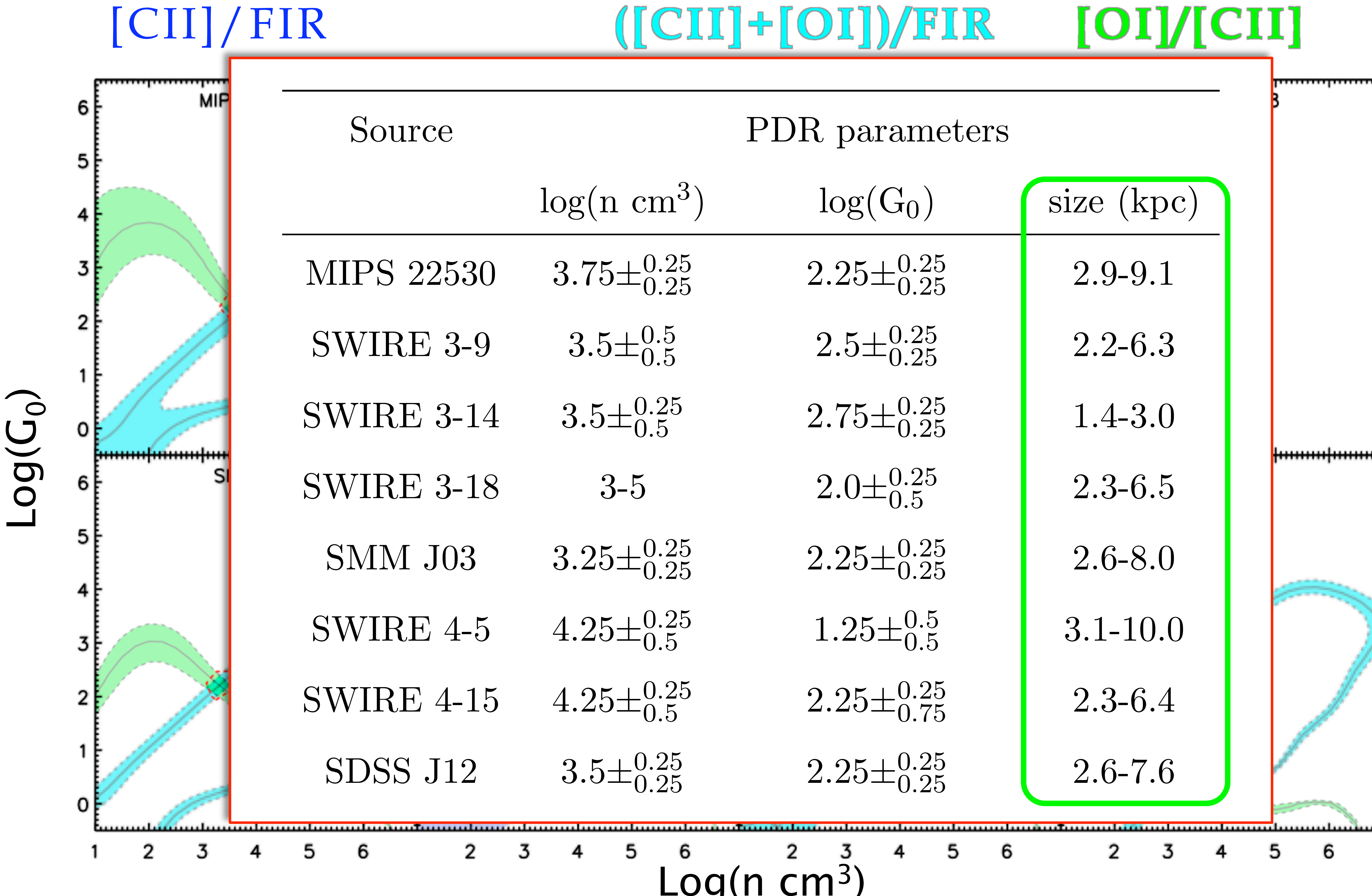

Source	PDR parameters		
	log(n cm^3)	log(G$_0$)	size (kpc)
MIPS 22530	$3.75\pm^{0.25}_{0.25}$	$2.25\pm^{0.25}_{0.25}$	2.9-9.1
SWIRE 3-9	$3.5\pm^{0.5}_{0.5}$	$2.5\pm^{0.25}_{0.25}$	2.2-6.3
SWIRE 3-14	$3.5\pm^{0.25}_{0.5}$	$2.75\pm^{0.25}_{0.25}$	1.4-3.0
SWIRE 3-18	3-5	$2.0\pm^{0.25}_{0.5}$	2.3-6.5
SMM J03	$3.25\pm^{0.25}_{0.25}$	$2.25\pm^{0.25}_{0.25}$	2.6-8.0
SWIRE 4-5	$4.25\pm^{0.25}_{0.5}$	$1.25\pm^{0.5}_{0.5}$	3.1-10.0
SWIRE 4-15	$4.25\pm^{0.25}_{0.5}$	$2.25\pm^{0.25}_{0.75}$	2.3-6.4
SDSS J12	$3.5\pm^{0.25}_{0.25}$	$2.25\pm^{0.25}_{0.25}$	2.6-7.6

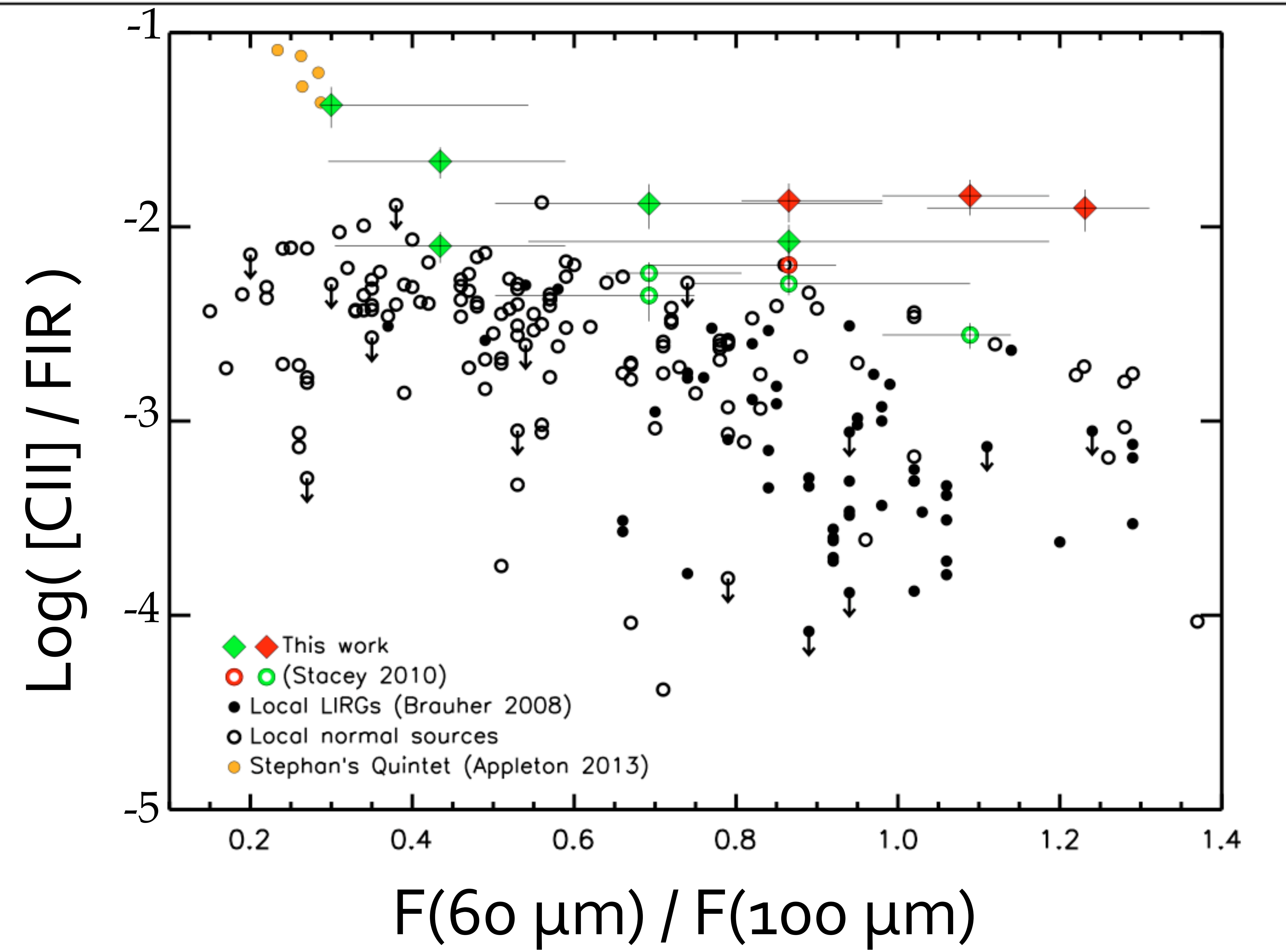

Log([CII] / FIR)
-1
-2
-3
-4
-5
0.2
0.4
0.6
0.8
1.0
1.2
1.4
F(60 μm) / F(100 μm)
This work
(Stacey 2010)
Local LIRGs (Brauher 2008)
Local normal sources
Stephan's Quintet (Appleton 2013)

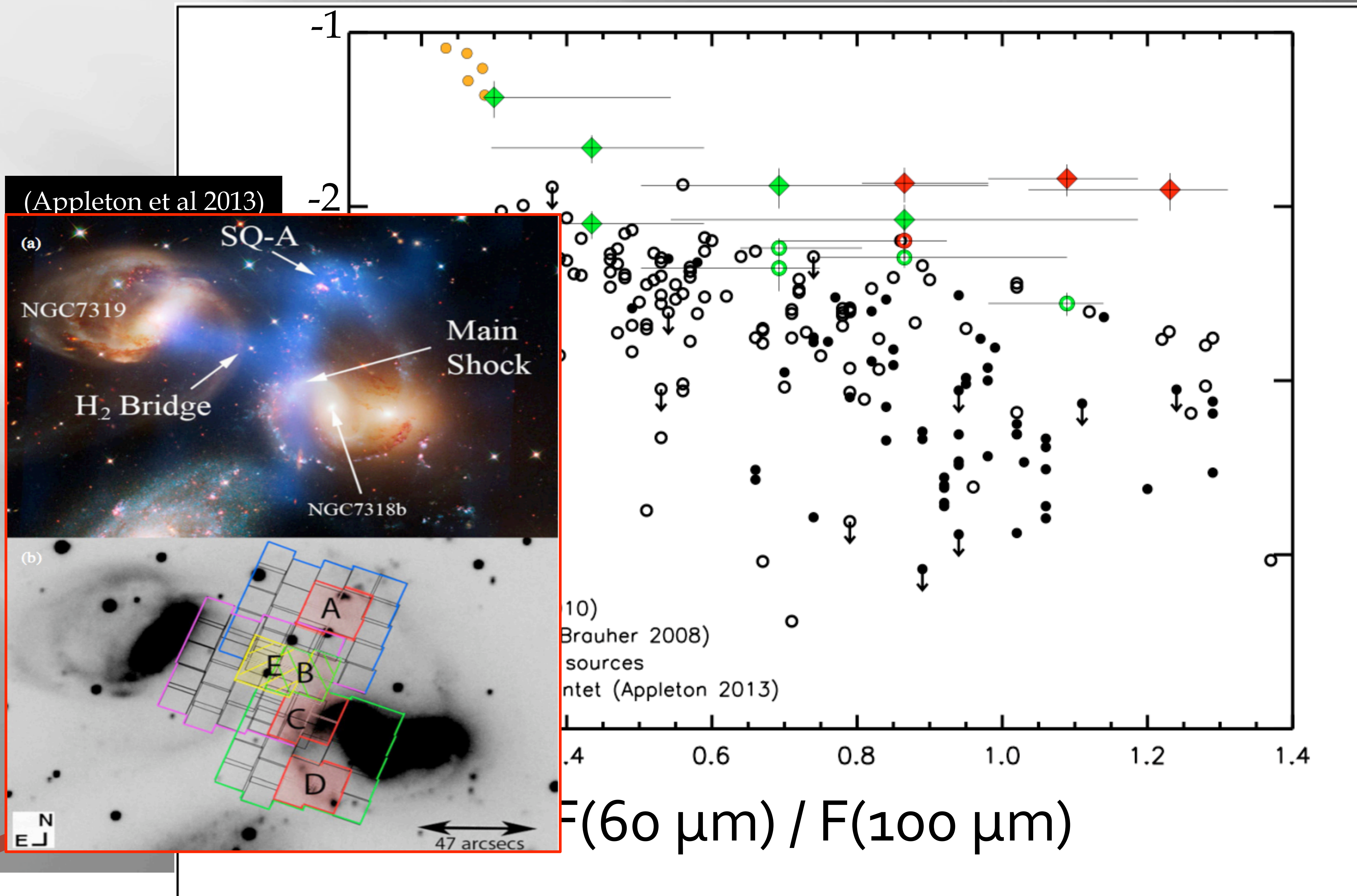

F(60 μm) / F(100 μm)

Summary

- ‘CII deficit’ ~ indicates mode of star formation
  - [CII]/FIR ~ merger fraction?
- High z ULIRGS - high [CII]/FIR ratios
- PDR paradigm
  - Modest SF extended over several kpc scale
- Individual pictures emerging
  - Shocks may be involved

[OI]145 / FIR

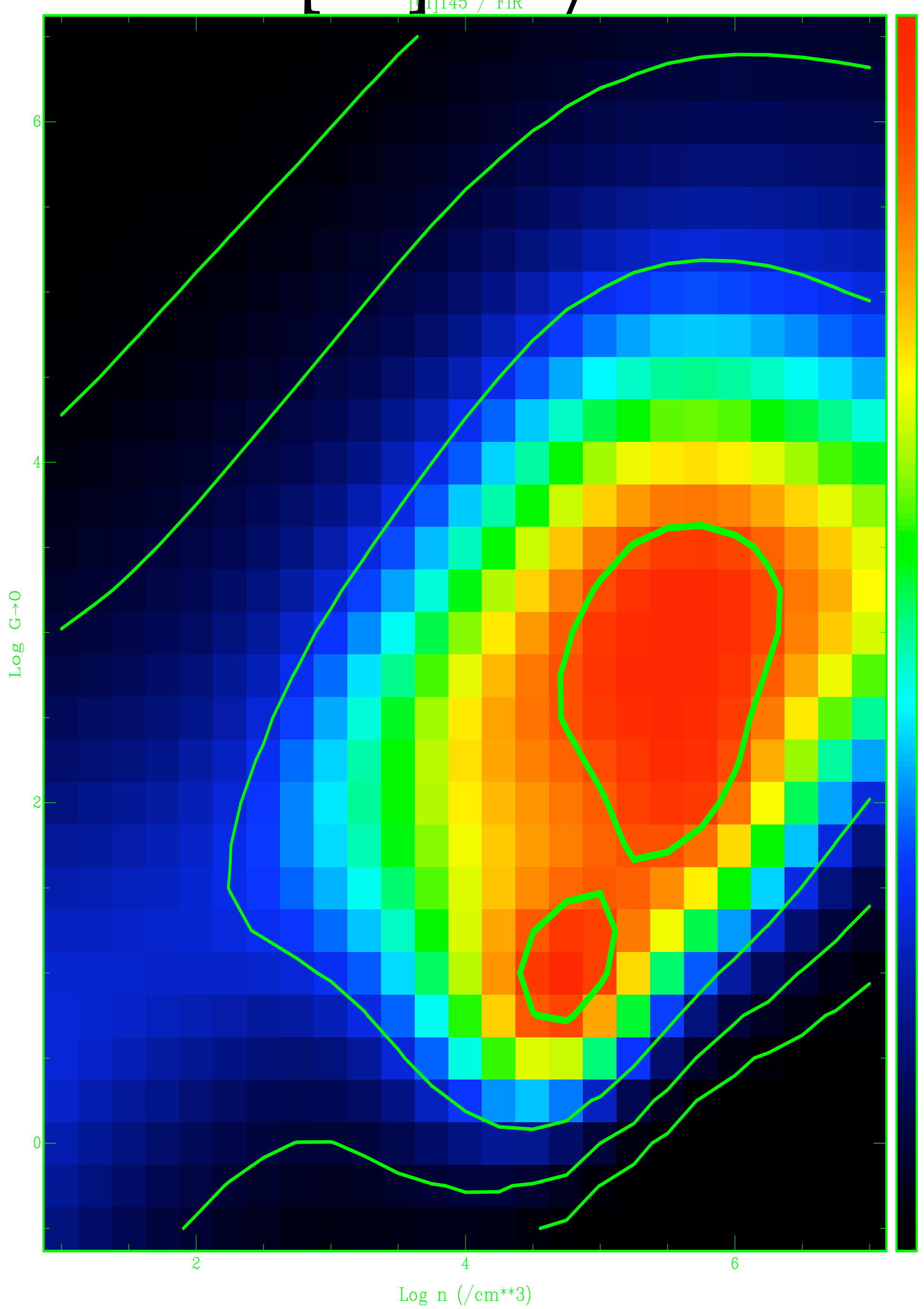

[OI]145 / [OI] 63

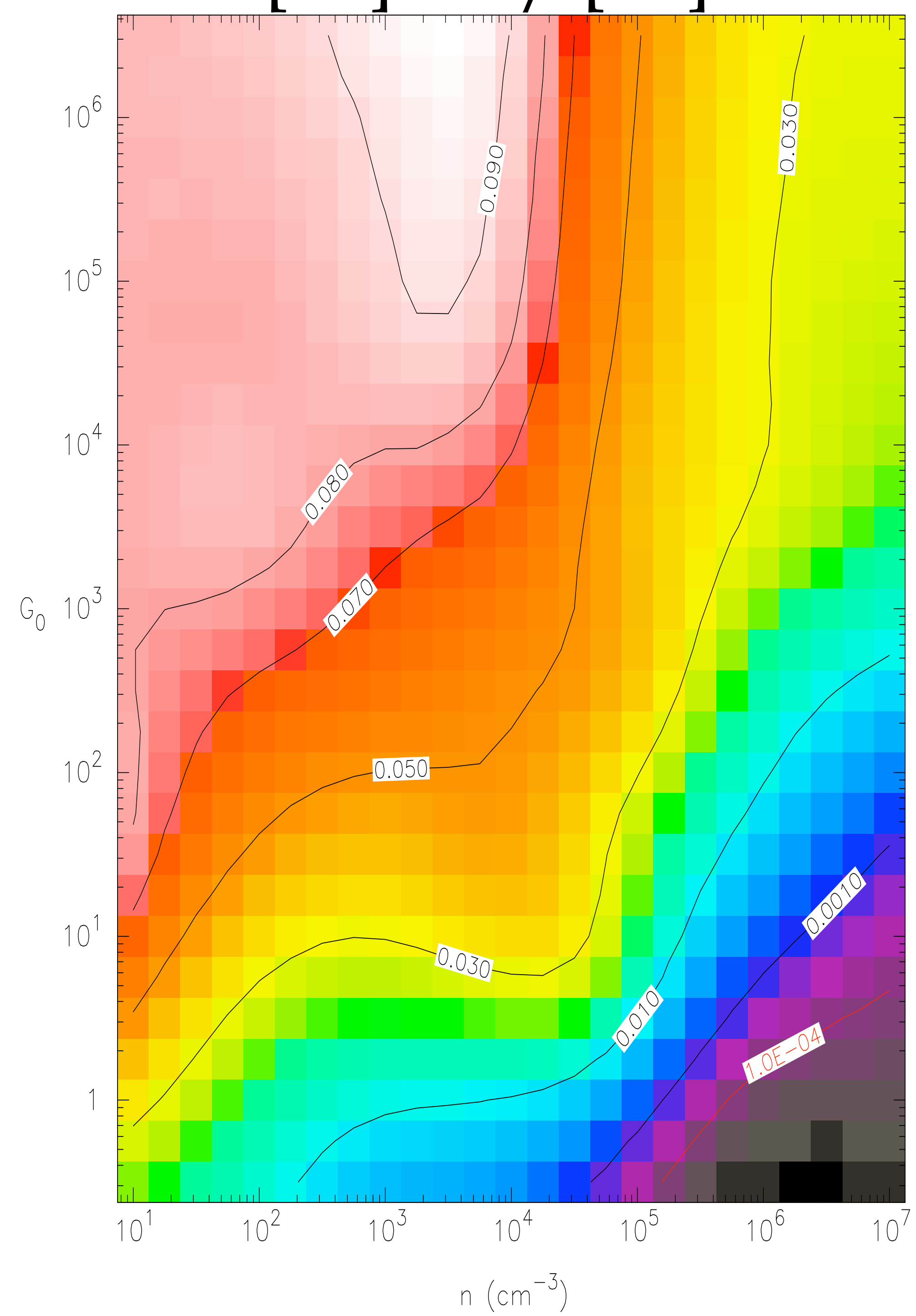

[CI] 609

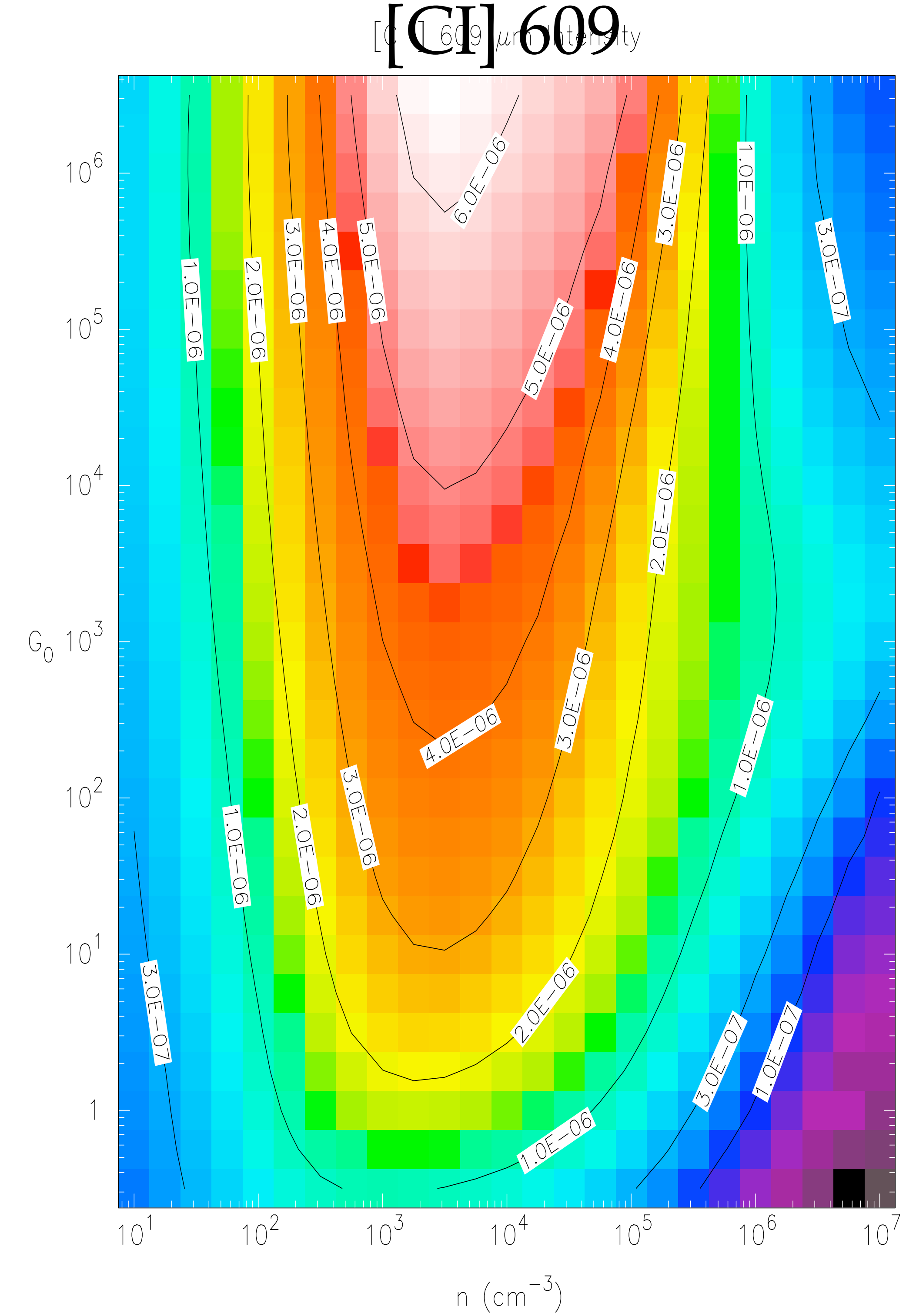

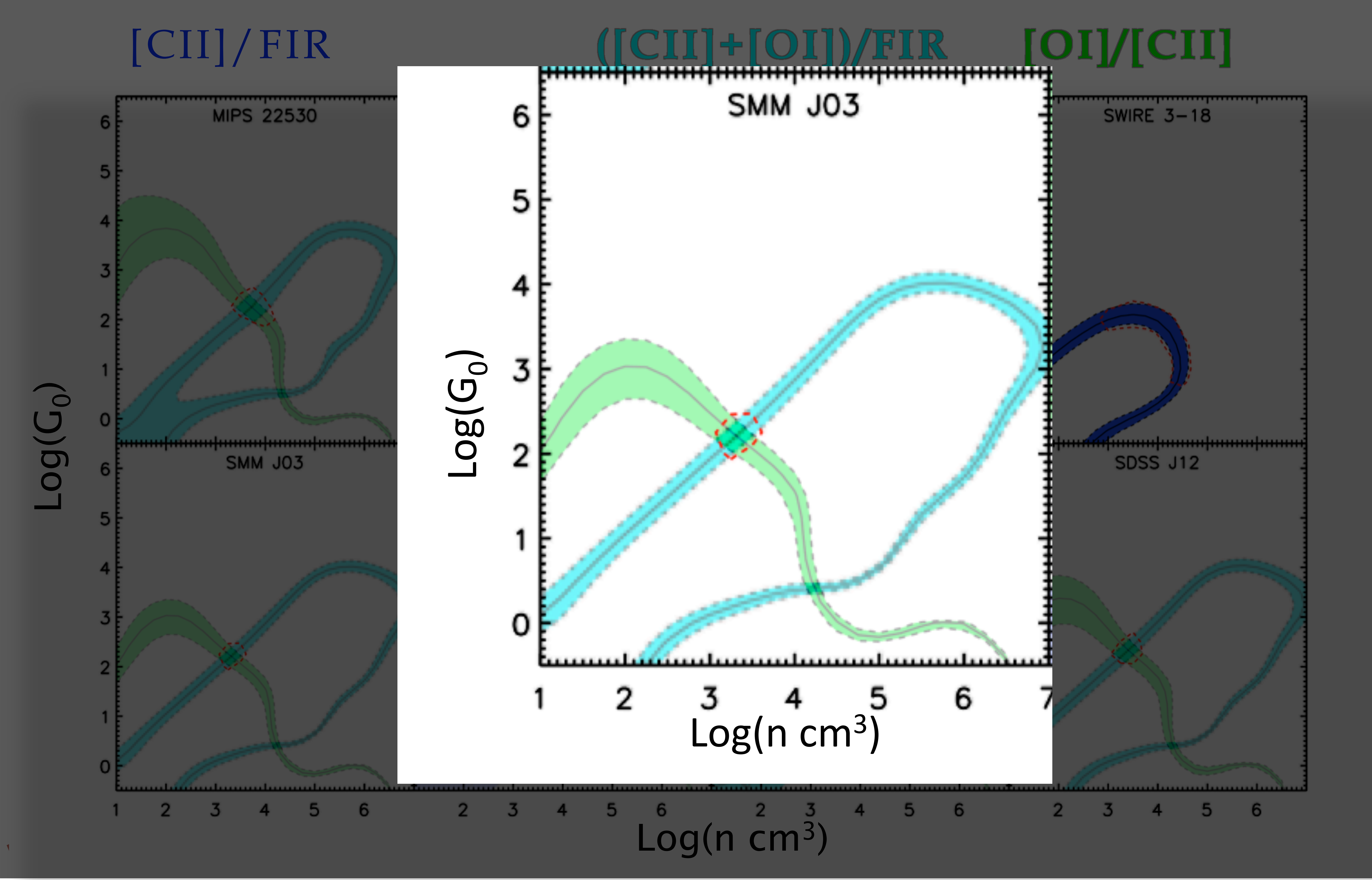

[CII]/FIR
([CII]+[OI])/FIR
[OI]/[CII]
MIPS 22530
SMM J03
SWIRE 3-18
SDSS J12
Log(G$_0$)
Log(n cm^3)

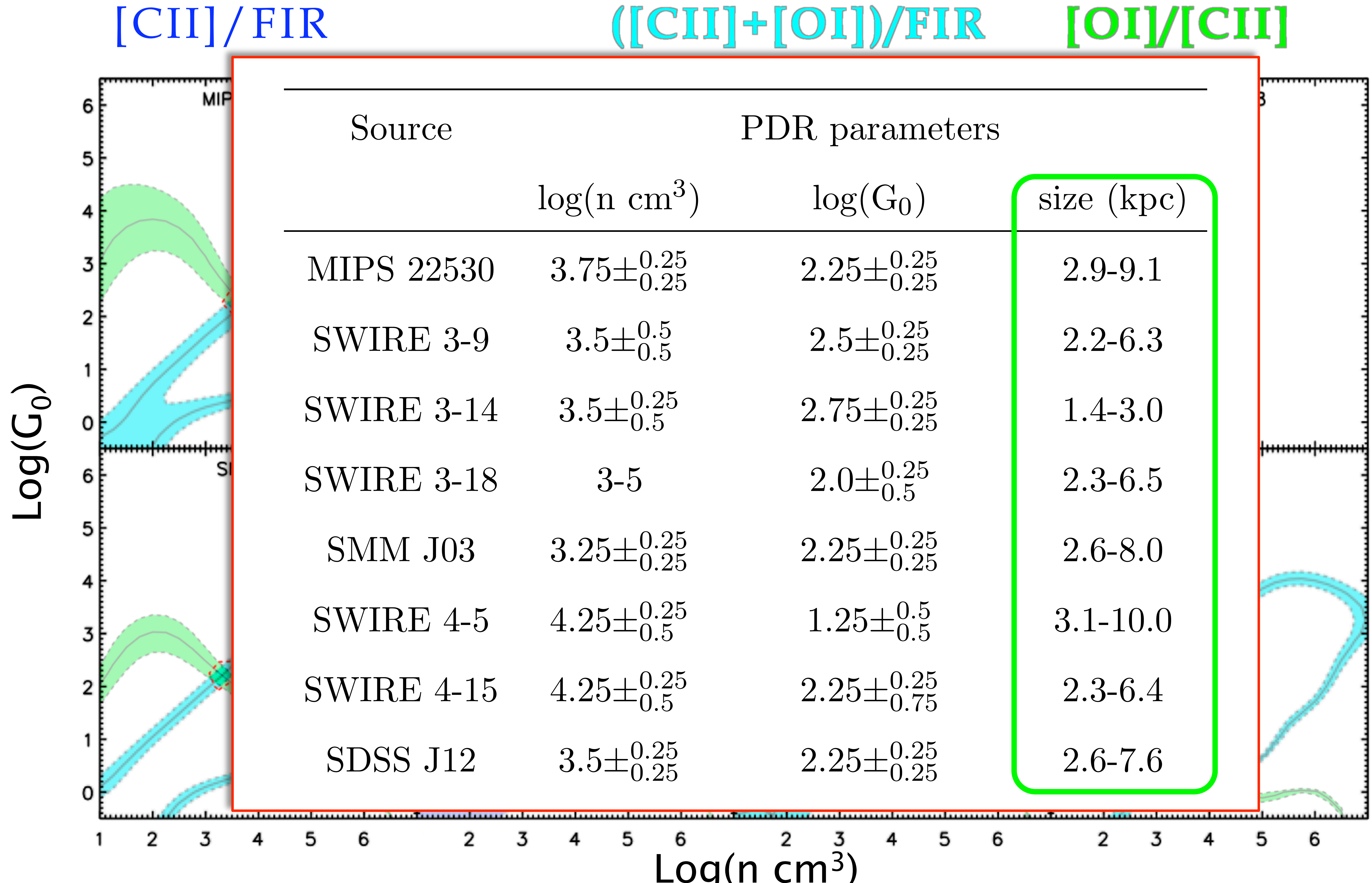

Source	PDR parameters		
	log(n cm^3)	log(G$_0$)	size (kpc)
MIPS 22530	$3.75\pm^{0.25}_{0.25}$	$2.25\pm^{0.25}_{0.25}$	2.9-9.1
SWIRE 3-9	$3.5\pm^{0.5}_{0.5}$	$2.5\pm^{0.25}_{0.25}$	2.2-6.3
SWIRE 3-14	$3.5\pm^{0.25}_{0.5}$	$2.75\pm^{0.25}_{0.25}$	1.4-3.0
SWIRE 3-18	3-5	$2.0\pm^{0.25}_{0.5}$	2.3-6.5
SMM J03	$3.25\pm^{0.25}_{0.25}$	$2.25\pm^{0.25}_{0.25}$	2.6-8.0
SWIRE 4-5	$4.25\pm^{0.25}_{0.5}$	$1.25\pm^{0.5}_{0.5}$	3.1-10.0
SWIRE 4-15	$4.25\pm^{0.25}_{0.5}$	$2.25\pm^{0.25}_{0.75}$	2.3-6.4
SDSS J12	$3.5\pm^{0.25}_{0.25}$	$2.25\pm^{0.25}_{0.25}$	2.6-7.6

General Source Characteristics

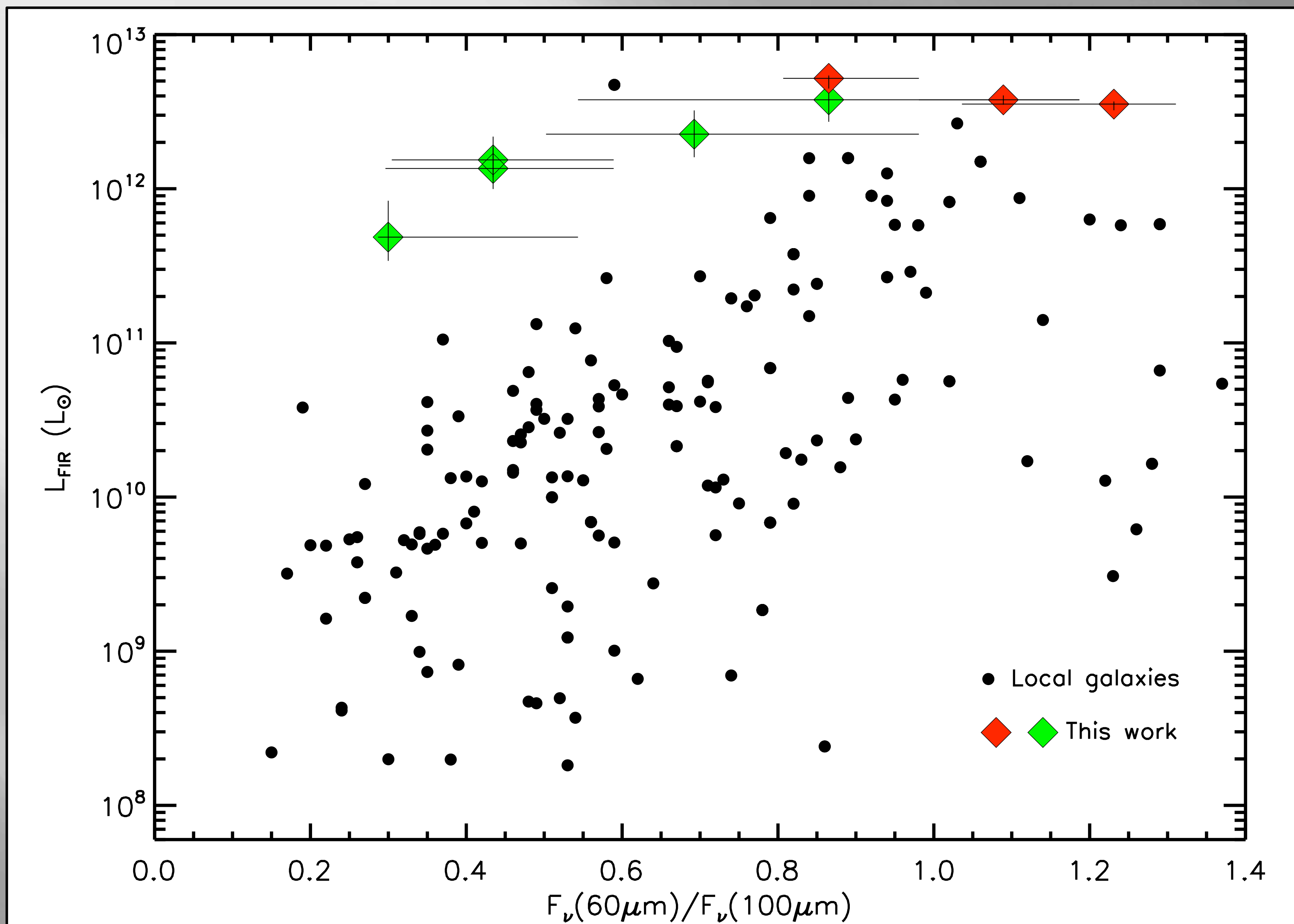

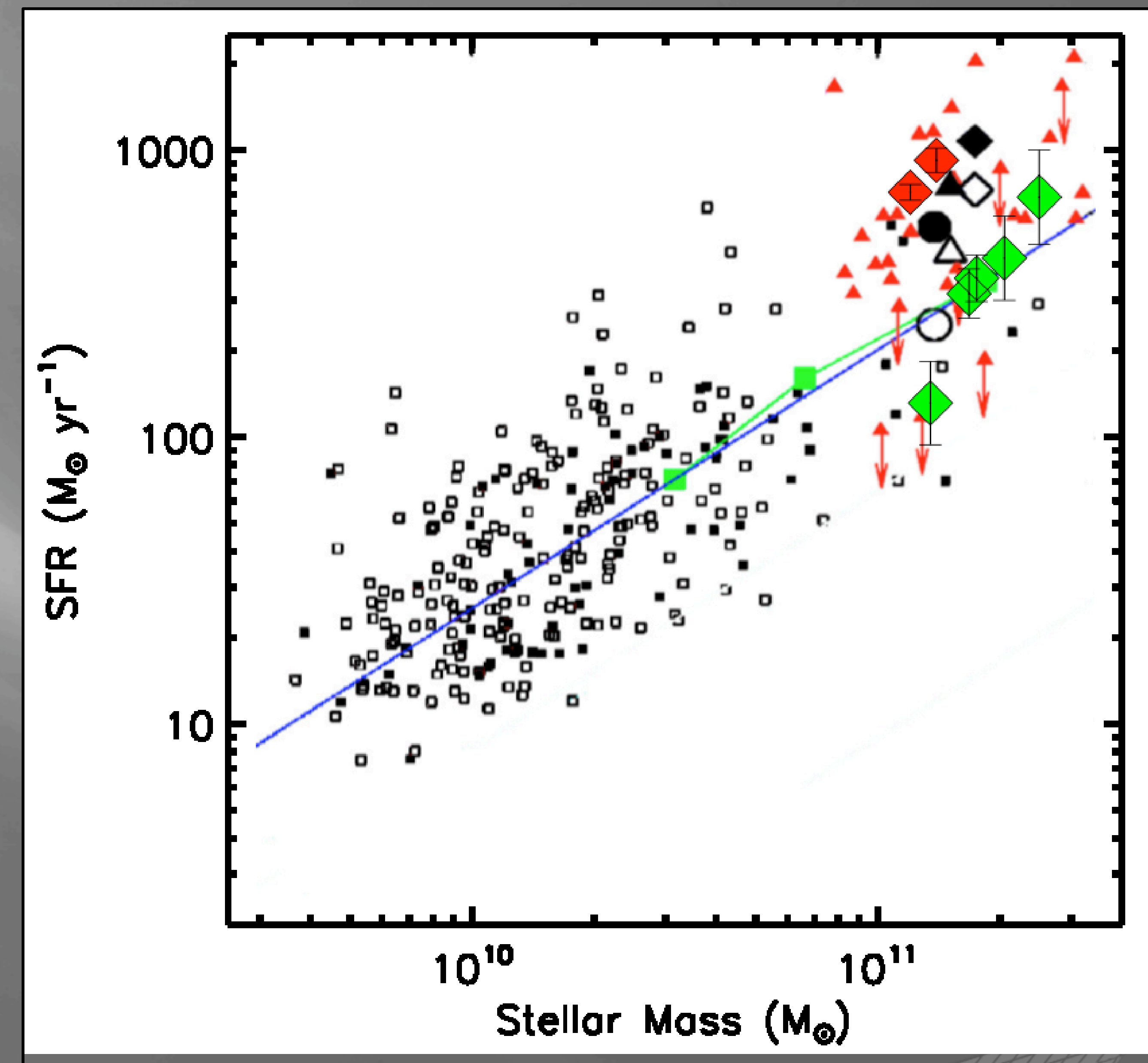

[OI] trends

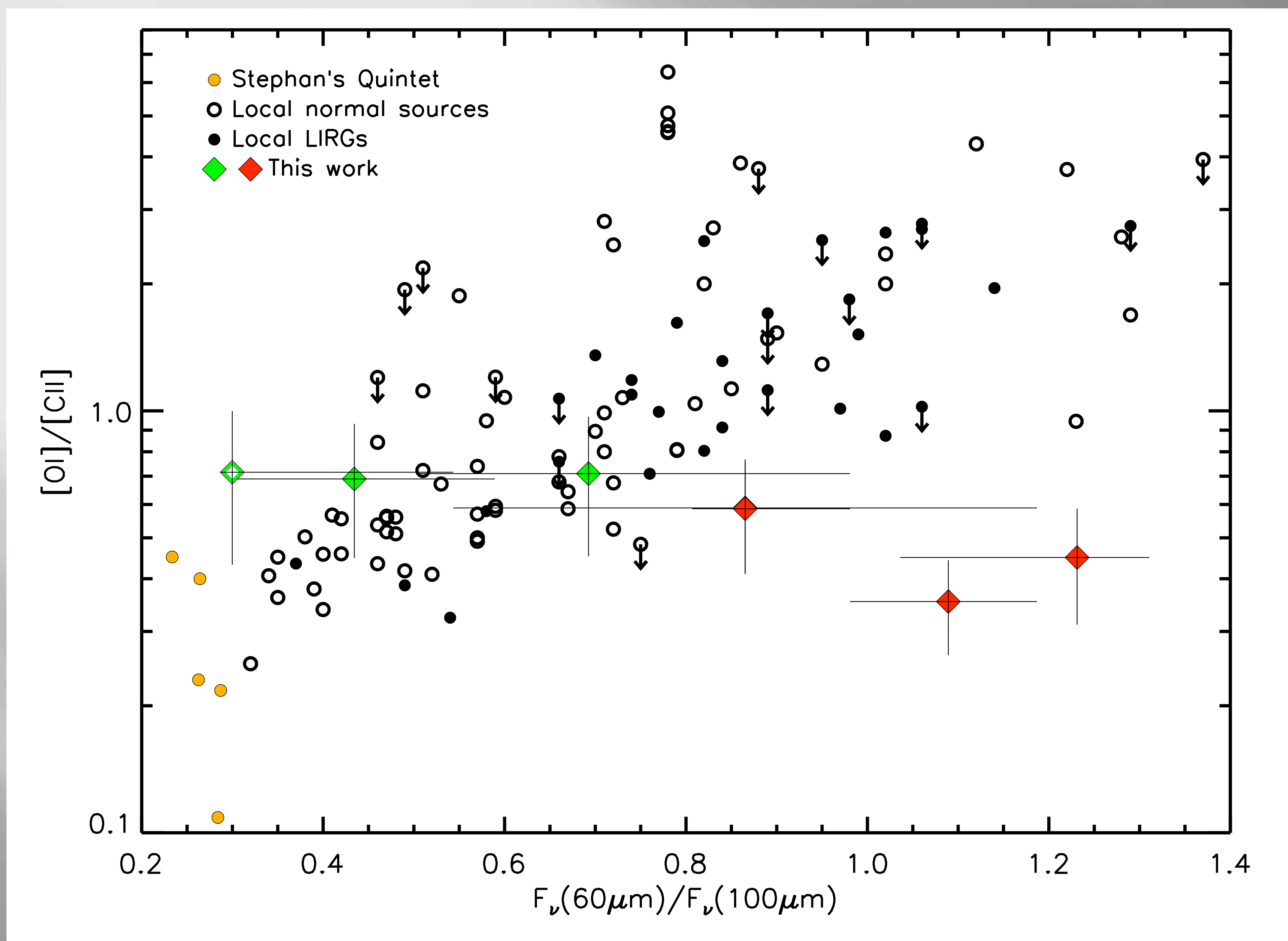
Stephan's Quintet
Local normal sources
Local LIRGs
This work
[OI]/[CII]
Fν(60μm)/Fν(100μm)
0.1
1.0
0.2
0.4
0.6
0.8
1.0
1.2
1.4

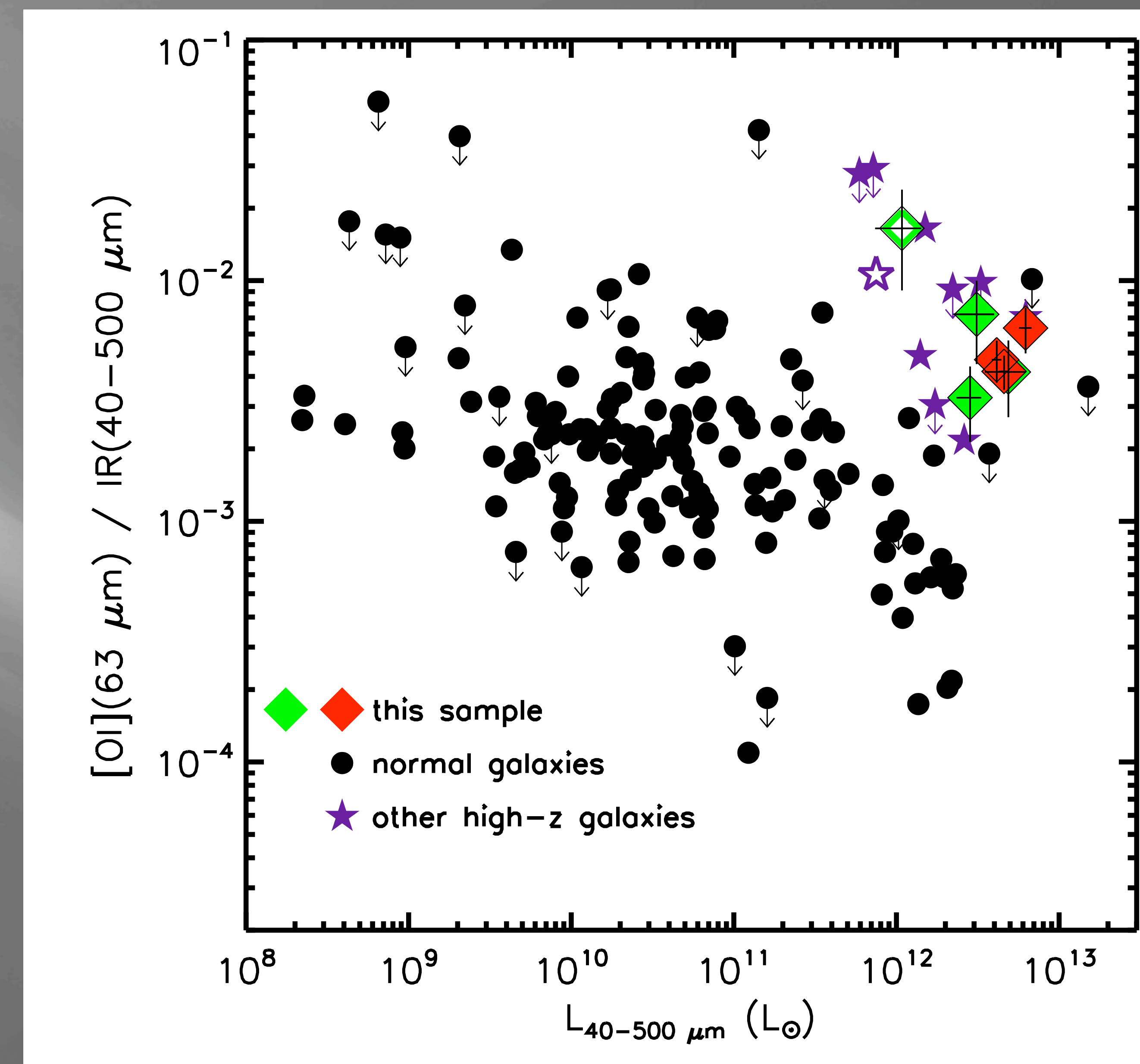
this sample
normal galaxies
other high-z galaxies
[OI](63 μm) / IR(40–500 μm)
L40–500 μm (L⊙)
10^-1
10^-2
10^-3
10^-4
10^8
10^9
10^10
10^11
10^12
10^13

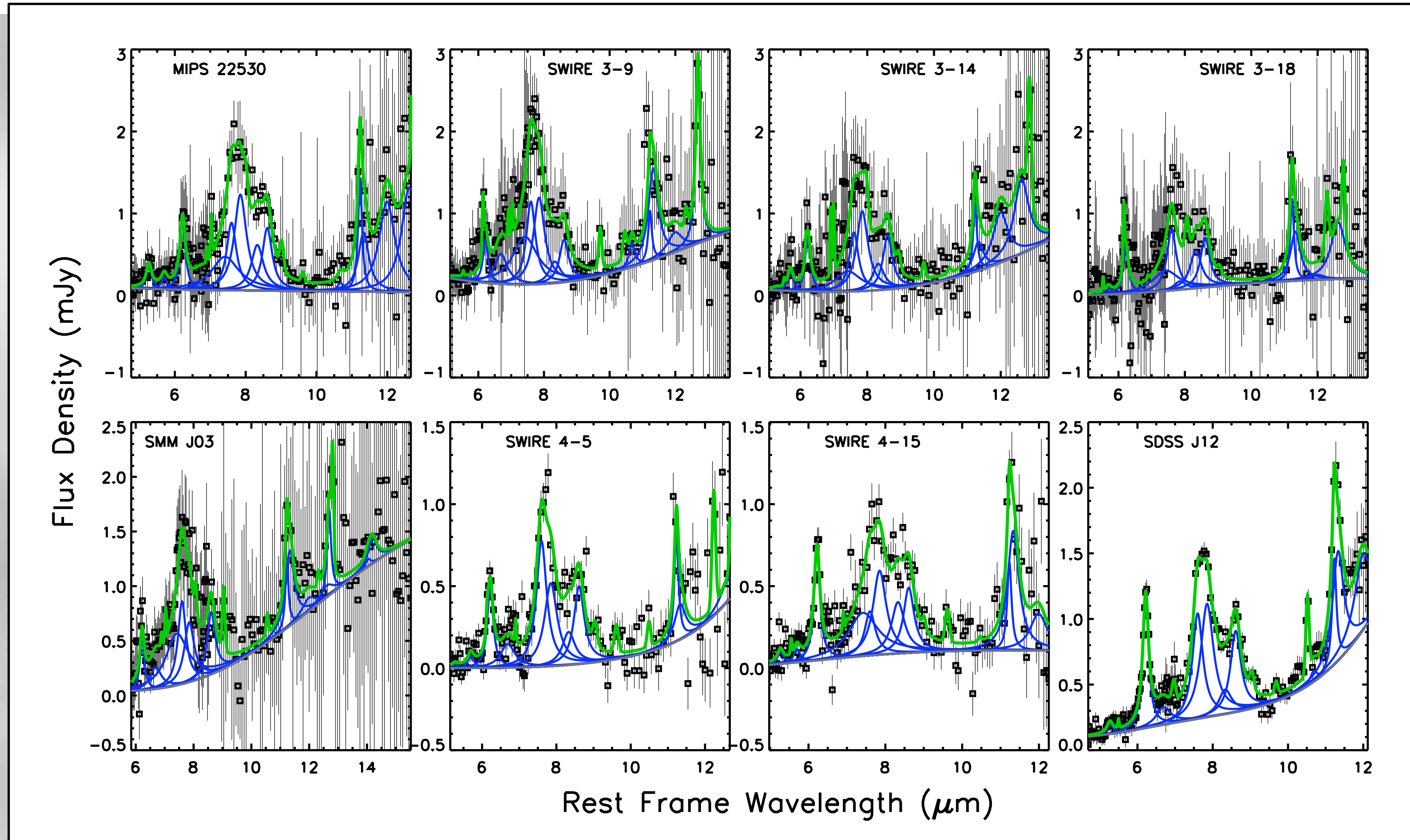

MIPS 22530
SWIRE 3-9
SWIRE 3-14
SWIRE 3-18
SMM J03
SWIRE 4-5
SWIRE 4-15
SDSS J12
Flux Density (mJy)
Rest Frame Wavelength (μm)

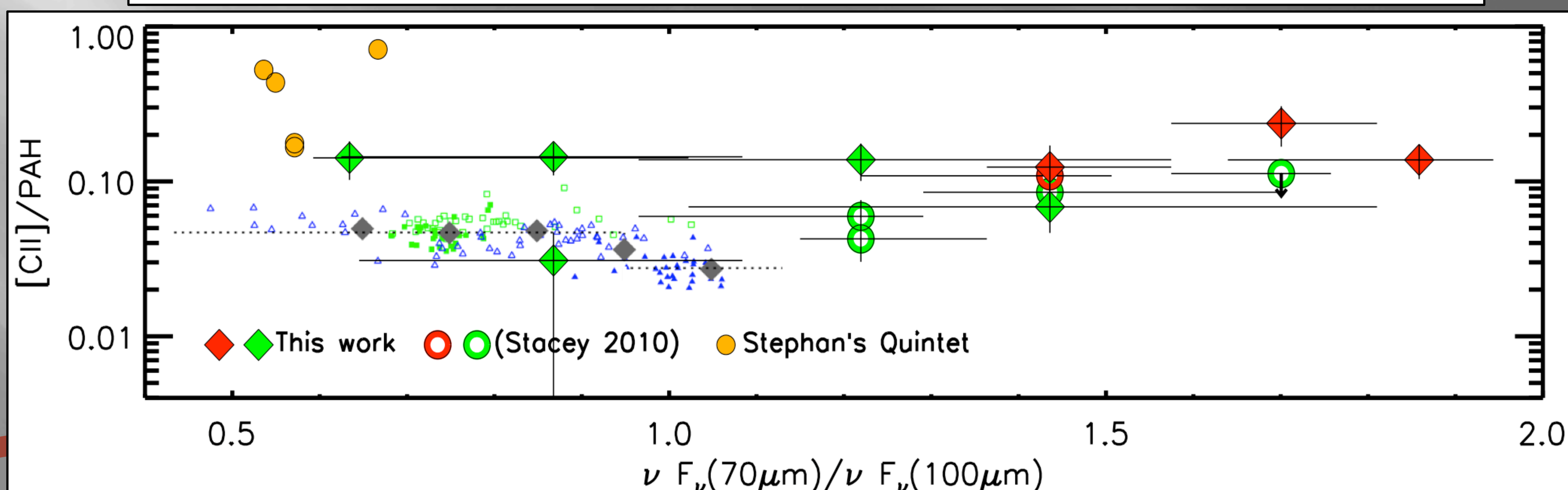

[CII]/PAH
This work
(Stacey 2010)
Stephan's Quintet
ν Fν(70μm)/ν Fν(100μm)

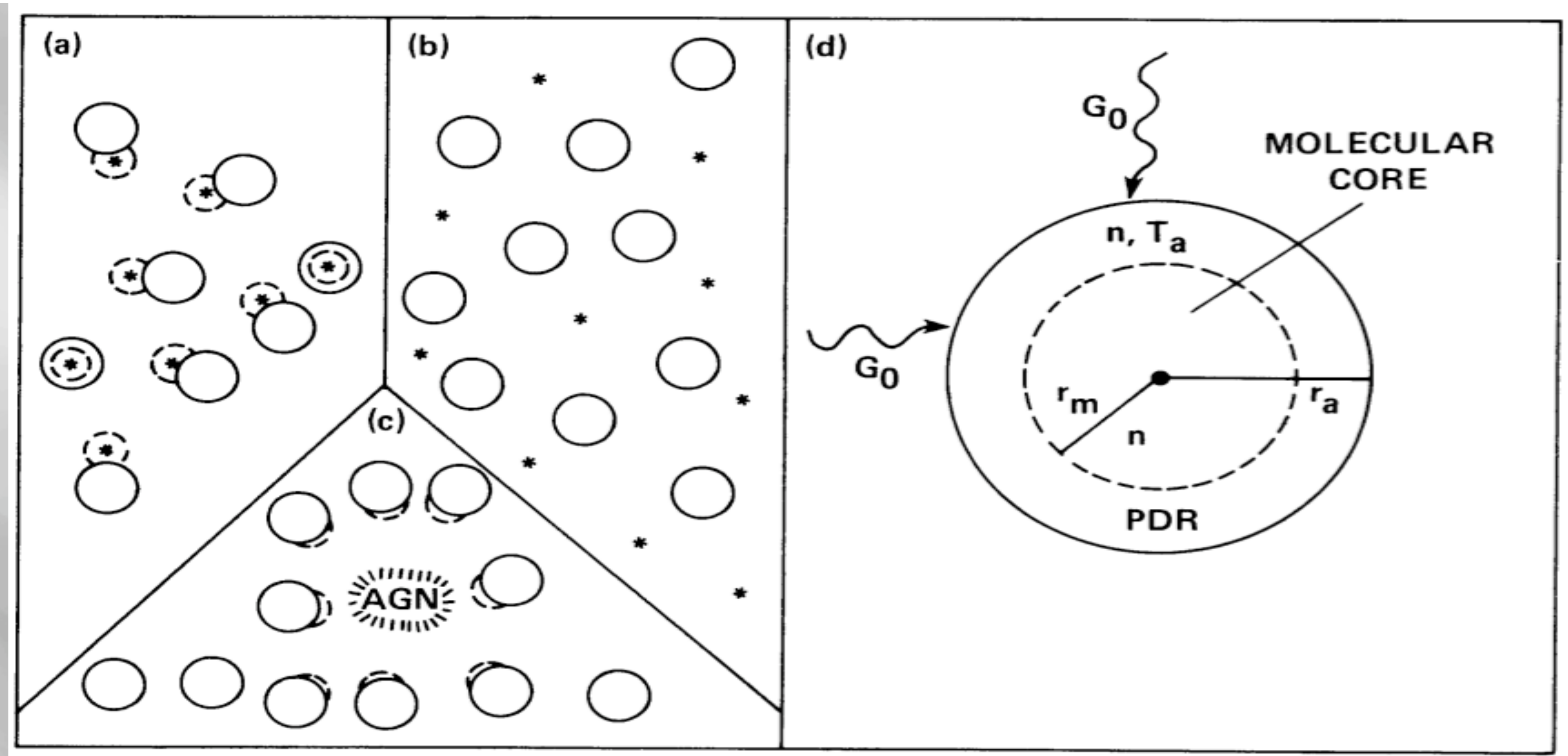

(Wolfire, Tielens, and Hollenbach, 1990)

$$G_0 \propto \frac{L_{IR}\lambda}{R^3}(1 - e^{-R/\lambda})$$

$$\lambda >> R$$

$$G_0 \sim \frac{L_{IR}\lambda}{R^3}$$

$$\lambda << R$$

$$G_0 \sim \frac{L_{IR}}{R^2}$$

Current picture

- Super extended, modest UV SF?

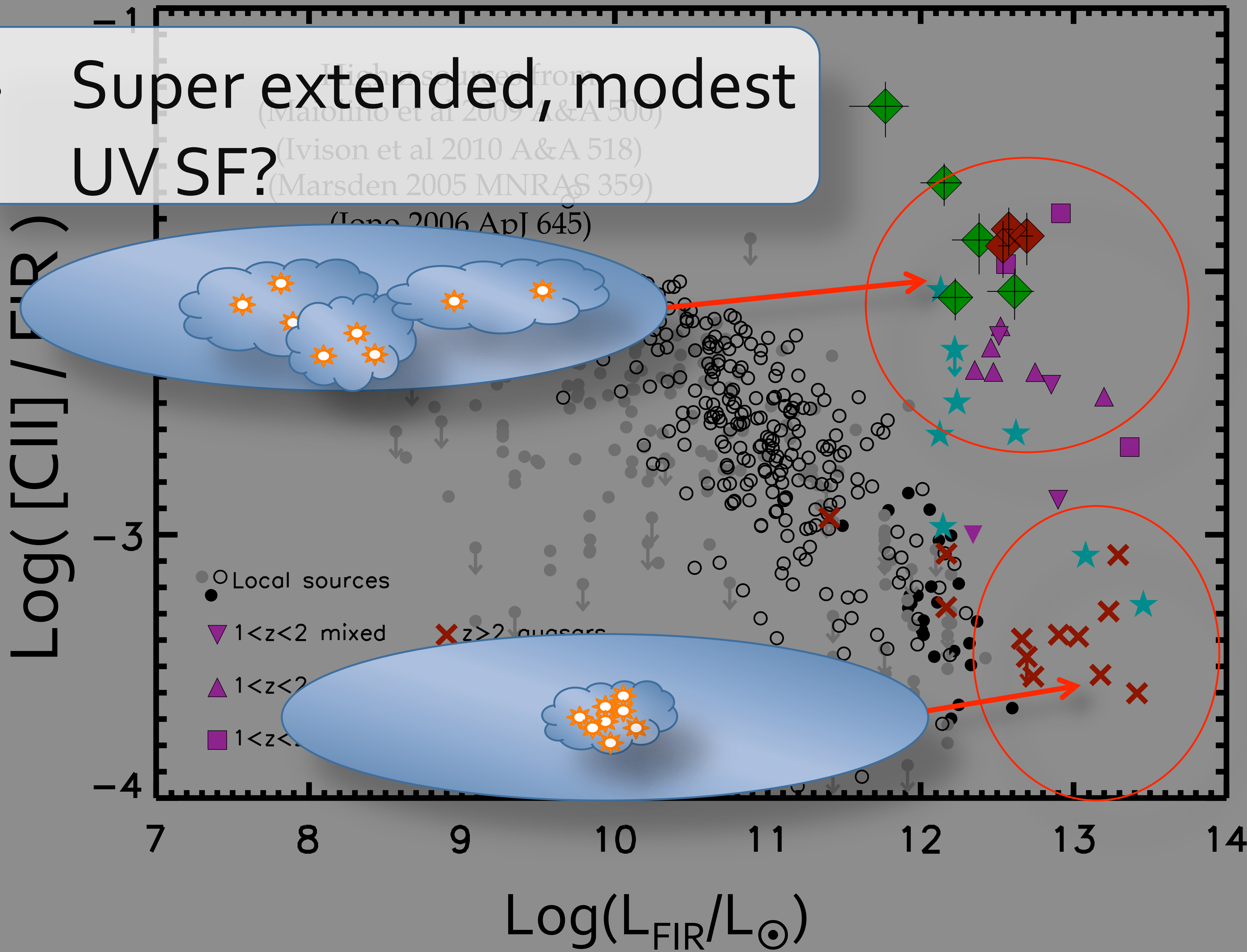

(Stacey 2010, Ferkinhoff 2014, Hailey-Dunsheath *in prep*)

(Brauher 2008)

(Armus 2009, Diaz-Santos 2013)

(Farrah 2013)

Other high z sources from
(Maiolino et al 2009 A&A 500)
(Ivison et al 2010 A&A 518)
(Marsden 2005 MNRAS 359)
(Iono 2006 ApJ 645)